Survey of Video Diffusion Models: Foundations, Implementations, and Applications

Anonymous authors
Paper under double-blind review

Abstract

Recent advances in diffusion models have revolutionized video generation, offering superior temporal consistency and visual quality compared to traditional generative adversarial networks-based approaches. While this emerging field shows tremendous promise in applications, it faces significant challenges in motion consistency, computational efficiency, and ethical considerations. This survey provides a comprehensive review of diffusion-based video generation, examining its evolution, technical foundations, and practical applications. We present a systematic taxonomy of current methodologies, analyze architectural innovations and optimization strategies, and investigate applications across low-level vision tasks such as denoising and super-resolution. Additionally, we explore the synergies between diffusion-based video generation and related domains, including video representation learning, question answering, and retrieval. Compared to the existing surveys (Lei et al., 2024a;b; Melnik et al., 2024; Cao et al., 2023; Xing et al., 2024c) which focus on specific aspects of video generation, such as human video synthesis (Lei et al., 2024a) or long-form content generation (Lei et al., 2024b), our work provides a broader, more updated, and more fine-grained perspective on diffusion-based approaches with a special section for evaluation metrics, industry solutions, and training engineering techniques in video generation. This survey serves as a foundational resource for researchers and practitioners working at the intersection of diffusion models and video generation, providing insights into both the theoretical frameworks and practical implementations that drive this rapidly evolving field.

Contents

1 Introduction **3**

2 Foundation **5**

2.1 Video generative paradigm 5

2.1.1 GAN video models 5

2.1.2 Auto-regressive video models 5

2.1.3 Video diffusion models 6

2.1.4 Auto-regressive video diffusion models 6

2.2 Learning foundation 7

2.2.1 Denoising diffusion probabilistic models (DDPM) 7

2.2.2 Denoising diffusion implicit models (DDIM) 7

2.2.3 Elucidated diffusion models (EDM) 8

2.2.4 Flow matching and rectified flow 8

2.2.5 Learning from feedback and reward models . . . 9
2.2.6 One-shot and few-shot learning . . . 10
2.2.7 Training-free methods . . . 10
2.2.8 Token learning . . . 10
2.3 Guidance . . . 11
2.3.1 Classifier guidance . . . 11
2.3.2 Classifier-free guidance . . . 12
2.4 Diffusion model frameworks . . . 13
2.4.1 Pixel diffusion and latent diffusion . . . 13
2.4.2 Optical-flow-based diffusion models . . . 14
2.4.3 Noise scheduling . . . 15
2.4.4 Agent-based diffusion models . . . 15
2.5 Architecture . . . 15
2.5.1 UNet . . . 15
2.5.2 Diffusion transformers . . . 17
2.5.3 VAE for latent space compression . . . 18
2.5.4 Text encoder . . . 19

3 Implementation **20**
3.1 Datasets . . . 20
3.2 Training engineering . . . 20
3.3 Evaluation metrics and benchmarking findings . . . 22
3.4 Industry solutions . . . 24

4 Applications **25**
4.1 Conditions . . . 25
4.1.1 Image condition . . . 26
4.1.2 Spatial condition . . . 28
4.1.3 Camera parameter condition . . . 29
4.1.4 Audio condition . . . 30
4.1.5 High-level video condition . . . 32
4.1.6 Other conditions . . . 34
4.2 Enhancement . . . 35
4.2.1 Video denoising and deblurring . . . 35
4.2.2 Video inpainting . . . 35
4.2.3 Video interpolation and extrapolation/prediction . . . 37
4.2.4 Video super-resolution . . . 38

4.2.5 Combining multiple video enhancement tasks . . . 40
4.2.6 Summary . . . 40
4.3 Personalization . . . 40
4.4 Consistency . . . 42
4.5 Long video . . . 44
4.6 3D-aware video diffusion . . . 45
4.6.1 Training on 3D dataset . . . 46
4.6.2 Architecture for 3D diffusion models . . . 47
4.6.3 Camera conditioning . . . 47
4.6.4 Inference-time tricks . . . 48

5 Benefits to other domains 48
5.1 Video representation learning . . . 48
5.2 Video retrieval . . . 49
5.3 Video QA and captioning . . . 49
5.4 3D and 4D generation . . . 50
5.4.1 Video diffusion for 3D generation . . . 50
5.4.2 Video diffusion for 4D generation . . . 51

6 Conclusion and outlook 52

1 Introduction

Video generation (Ren et al., 2024; Zheng et al., 2024c; Davtyan & Favaro, 2022) has emerged as a critical and transformative technology in recent years. The ability to generate high-quality, realistic videos has numerous applications, from entertainment and advertising (Wang & Shi, 2023) to virtual reality (Hu et al., 2021) and autonomous systems (Zhou et al., 2024c), further enabling enhanced user experiences, cost-effective content creation, and new avenues for creative expression.

In the past few years, video generation (Clark et al., 2019; Aldausari et al., 2022; Hong et al., 2022) has experienced remarkable progress, particularly with the adoption of Generative Adversarial Networks (GANs, (Goodfellow et al., 2014)). Researchers have implemented various strategies to improve the temporal coherence (Chai et al., 2023), realism, and diversity of generated videos. Despite these advancements, GAN-based methods often face challenges in training stability and achieving high-quality outputs consistently. The introduction of diffusion models (Ho et al., 2020; Nichol & Dhariwal, 2021; Sohl-Dickstein et al., 2015) has revolutionized this area by offering a probabilistic framework that overcomes many limitations of GANs. Diffusion-based models (Kwak et al., 2024; Chai et al., 2023; Wang & Yang, 2024; Ho et al., 2022c) have demonstrated superior performance in generating temporally consistent and visually compelling videos, motivating further research in the domain.

However, diffusion-based video generation presents several fundamental challenges. A primary concern lies in ensuring motion consistency across frames, a critical factor for producing temporally consistent and realistic videos. Moreover, generated videos must adhere to physical rules, such as accurate object dynamics and environmental interactions, to maintain realism. Long video generation poses another challenge, requiring models to handle complex temporal dependencies over extended sequences. Furthermore, the computational demands of training diffusion-based models are substantial, often leading to inefficiencies that limit scalability.

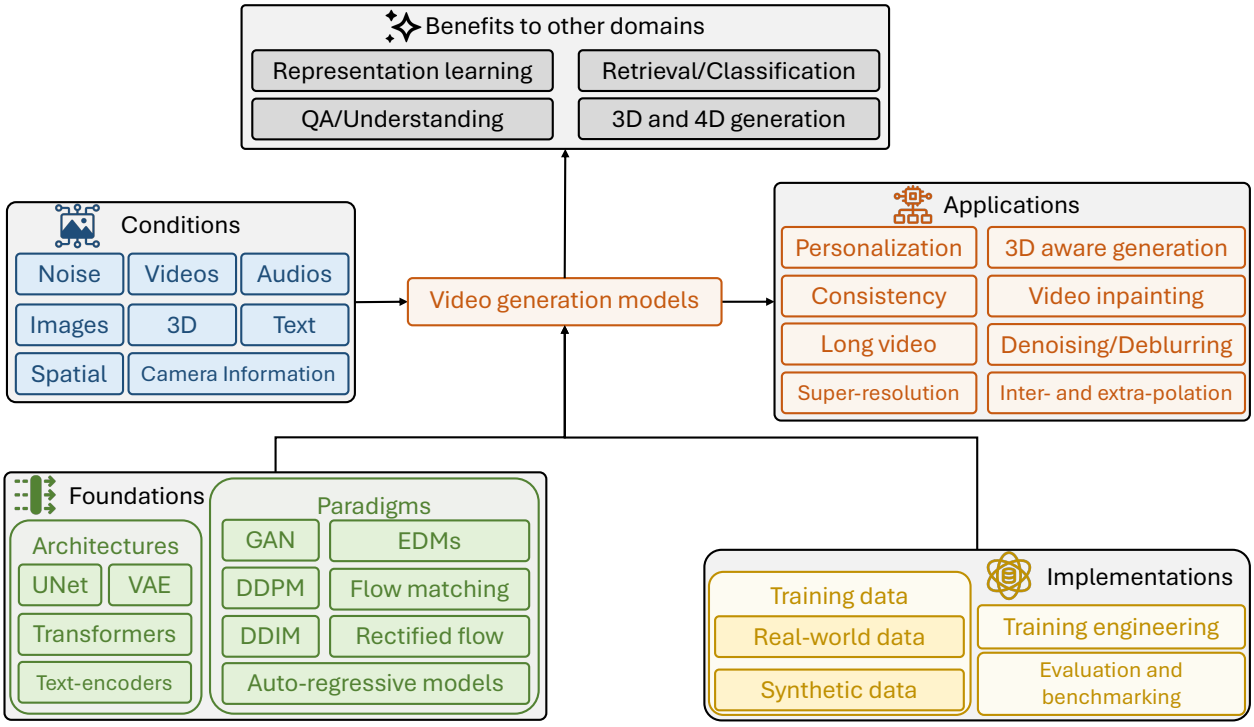

Figure 1: Overview of video generation methods. Generally, the input conditions can be noises, images, videos, audios, texts, and 3D point clouds. The architectures (UNet, VAE, and/or Transformers) are trained using GAN or diffusion models with training data of real-world data or synthetic data with different paradigms. The applications are in several folds, *e.g.*, video personalization, consistency-aware generation, and long video generalization. On the other side, video generation models can also benefit other video tasks, such as, video retrieval, understanding, and representation learning.

Similarly, inference acceleration remains a severe issue, as generating high-quality videos in real-time is critical for many applications. Beyond these technical challenges, ethical considerations also play a pivotal role, including mitigating biases in generated content and preventing the creation of harmful or misleading visual outputs.

In response to the rapid advancements and emerging challenges of diffusion-based video generation, this survey provides a systematic analysis of current methodologies, recent advances, and future directions in the field.

Our contributions. This survey presents a comprehensive analysis of diffusion-based video generation, focusing on both technical foundations and practical applications. While existing surveys (Lei et al., 2024a;b; Melnik et al., 2024; Cao et al., 2023; Xing et al., 2024c) have addressed specific aspects of video generation, such as human video synthesis (Lei et al., 2024a) or long-form content generation (Lei et al., 2024b), our work provides a broader, more updated, and more fine-grained perspective on diffusion-based approaches. Compared to related surveys (Xing et al., 2024c; Melnik et al., 2024), we offer more extensive coverage of diffusion models and their applications with a detailed overview of datasets, evaluation metrics, industry solutions, and training engineering techniques for video generation. The main contributions of this paper are as follows:

- To the best of our knowledge, this is the most comprehensive survey on diffusion-based video generation, including model paradigms, learning foundation, implementation details, applications, and relations to other domains.

- Compared to related surveys, our survey covers a broader scope of diffusion models and their applications with a detailed overview of datasets, evaluation metrics, industry solutions, and training engineering techniques for video generation.

The rest of the survey is organized as follows: Section 2 lays the groundwork by exploring foundational concepts, including video generation paradigms such as GAN-based models, auto-regressive models, and diffusion models. Section 3 focuses on implementation, addressing practical aspects such as datasets, training engineering techniques, and evaluation metrics, along with benchmarking findings to highlight model performance. Section 4 covers diverse applications, including conditional generation tasks, enhancement methods such as video denoising, inpainting, interpolation, extrapolation, and super-resolution, as well as personalization, consistency, long-video generation, and emerging 3D-aware diffusion models. Finally, Section 5 discusses the benefits of diffusion-based video generation to other domains, such as video representation learning, retrieval, QA, and 3D and 4D generation, emphasizing its broader impact in advancing related fields. This structure provides a comprehensive and cohesive understanding of diffusion-based video generation, from foundational principles to advanced applications.

2 Foundation

2.1 Video generative paradigm

2.1.1 GAN video models

GANs consist of a generator and a discriminator. The generator aims to produce realistic samples, while the discriminator seeks to differentiate between the generated samples and the ground truth samples. For video generation, GANs have been extended to model temporal consistency and generate realistic video frames. For example, TGAN (Saito et al., 2017) uses two generators, with a temporal generator creating motion features and an image generator producing video frames. TGAN-v2 (Saito et al., 2020) improves efficiency by generating videos at multiple temporal resolutions using a cascade of generator modules. MoCoGAN (Tulyakov et al., 2018) separates latent space into motion and content parts, predicting motion vectors auto-regressively, while DVD-GAN (Clark et al., 2019) generates all frames in parallel and conditions on class labels. MoCoGAN-HD (Tian et al., 2020) disentangles content and motion differently, with a motion generator predicting a latent motion trajectory. DIGAN (Yu et al., 2021) further leverages implicit neural representations to efficiently generate longer video sequences with a motion discriminator focused on frame pairs rather than entire sequences. StyleGAN2 (Karras et al., 2020) introduced a highly expressive and controllable latent space for photorealistic image synthesis, laying a foundational framework for video synthesis through sparse motion cues and efficient control mechanisms. Building on this, StyleGAN-V (Skorokhodov et al., 2022) advanced the field by modelling videos as continuous-time signals, improving temporal coherence while supporting high-resolution and long-duration generation. Extending these developments, StyleInv (Wang et al., 2023i)) proposed a non-autoregressive GAN inversion network, achieving smoother motion transitions and enabling style transfer through fine-tuning. AniFaceGAN (Wu et al., 2022c) adapted StyleGAN2 into an animatable 3D-aware GAN, enabling multiview-consistent face animation generation, particularly for face-centric applications. Recently, SIDGAN (Muaz et al., 2023) tackled high-resolution dubbed video generation by introducing shift-invariant learning and a pyramid-based decoder, enabling accurate lip-syncing and high-quality textures even under challenging conditions. Further advancing lip-sync technology, StyleLipSync (Ki & Min, 2023) leveraged pre-trained StyleGAN to generate temporally consistent lip-synced videos with pose-aware masking and moving-average-based latent smoothing, enabling high-fidelity results for arbitrary identities. Details about the GAN application on video generation can be found (Aldausari et al., 2022).

2.1.2 Auto-regressive video models

Auto-Regressive models generate data by modelling the conditional distribution of each data point given its preceding data points. In the context of video generation, Auto-Rregressive models generate realistic and coherent videos by predicting each frame based on previously generated frames. Generally, three strategies

have been employed. The first is pixel-level auto-regression. Traditional representative methods, such as Video Pixel Networks (VPN) (Kalchbrenner et al., 2017), used LSTMs to capture temporal dependencies and PixelCNN (Reed et al., 2017) to model spatial and color dependencies within each frame. The second is frame-level auto-regression. (Huang et al., 2022a) proposed auto-regressive GAN to predict frames based on a single still frame. The third is latent-level auto-regression, which significantly saves processing time due to reduced data redundancy and achieves a good time quality trade-off (Rakhimov et al., 2020; Seo et al., 2022; Yan et al., 2021; Ge et al., 2022; Hong et al., 2023a).

2.1.3 Video diffusion models

GAN-based and Auto-Regressive models often face challenges in maintaining temporal consistency and computational efficiency when generating videos. While GANs struggle with maintaining temporal consistency and often produce unstable or inconsistent frames, diffusion models excel at generating smooth, coherent sequences, particularly for long videos, because their iterative denoising process ensures frame-to-frame consistency. Also, despite Auto-Regressive model can handle both continuous and discrete data, it normally requires high computational cost. In terms of frame quality, diffusion models generate more detailed and higher-resolution outputs compared to GANs, which are prone to artifacts from adversarial training, and autoregressive models, which face resolution limitations due to the compounding of errors in sequential prediction[cite]. Diffusion models also offer superior controllability and local editing capabilities because they can refine specific parts of the video during the denoising process without affecting other regions while GANs and autoregressive methods generate frames in a more holistic or sequential manner[cite].

Diffusion models offer a more efficient solution by framing video generation as a denoising process. Early models, such as the Video Diffusion Model (VDM) (Ho et al., 2022c), adapted the U-Net architecture to 3D for spatio-temporal video generation but faced high computational costs and limited resolution.

Later, Imagen-Video (Ho et al., 2022a) uses a cascaded diffusion process (Ho et al., 2022b) to generate high-resolution videos. It introduces temporal attention layers between spatial layers to capture motion information effectively. Make-a-Video (Singer et al., 2022) is another powerful competitor in text-video synthesis by conditioning on the CLIP semantic space. It generates keyframes based on text input and uses a cascade of interpolation and upsampling diffusion models to ensure high consistency and fidelity. However, both of these pioneering models come with high computational costs. To address this, MagicVideo (Zhou et al., 2022) introduced low-dimensional latent embedding space in their diffusion process by a pretrained variational-auto-encoder (VAE), significantly reducing computational demands. Video LDM (Blattmann et al., 2023b) also extended the adaptation of the Latent Diffusion Models (Rombach et al., 2022) to text-to-video generation tasks by adding temporal attention layers to a pre-trained text-to-image diffusion model and fine-tune them on labeled video data. Their model is capable of generating long-driving car video sequences auto-regressively and producing videos of personalized characters. Recently, CCEdit (Feng et al., 2024a) leverages diffusion models with a trident network architecture that decouples structure and appearance control, ensuring precise and creative editing capabilities.

2.1.4 Auto-regressive video diffusion models

Some recent works further exploit auto-regressive framework in the context of video generation with diffusion models (Weng et al., 2024; Jin et al., 2024; Xie et al., 2024a). ART • V (Weng et al., 2024) first utilized autoregressive diffusion to generate frames sequentially, employing masked diffusion to enhance coherence and reduce inconsistencies. Subsequently, Pyramidal Flow Matching (Jin et al., 2024) introduced spatial and temporal pyramids to optimize autoregressive generation, reducing computational costs and improving scalability. Progressive Autoregressive Video Diffusion Models (Xie et al., 2024a) refined this by using a progressive noise schedule, enabling smoother transitions in long videos. CausVid (Yin et al., 2024) advanced the field by converting bidirectional diffusion models into causal autoregressive generators through asymmetric distillation, achieving real-time frame-by-frame generation with low latency and reduced error accumulation.

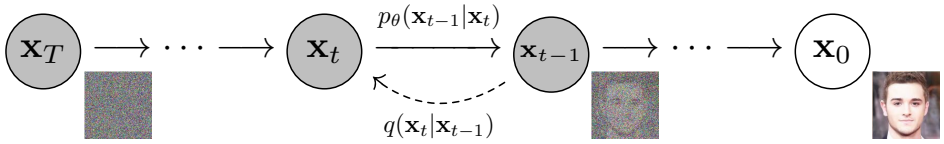

Figure 2: The directed graphical model for DDPM(Ho et al., 2020)

2.2 Learning foundation

2.2.1 Denoising diffusion probabilistic models (DDPM)

Denoising diffusion probabilistic models (DDPM) Ho et al. (2020); Nichol & Dhariwal (2021); Sohl-Dickstein et al. (2015) consist of two interconnected Markov chains: a forward diffusion process that gradually adds noise to the data, and a reverse process that removes noise to recover the data. The forward process transforms complex data distributions into a simpler prior, typically Gaussian noise, while the reverse process learns how to reconstruct the data from this noisy representation by modeling the reverse transitions. Data generation involves first sampling a random noise vector from the prior, and then applying the reverse chain, step-by-step, to iteratively refine the noise into meaningful data. The key challenge lies in training the reverse Markov chain so that it effectively mimics the true reversal of the forward process.

Mathematically, let the data be sampled from a distribution $x_0 \sim q(x_0)$. The forward Markov process produces a sequence of progressively noisier variables $x_1, x_2, ..., x_T$ through a transition kernel $q(x_t|x_{t-1})$. The joint distribution of these variables, conditioned on the original data x_0, can be expressed as:

$$q(x_1, ..., x_T|x_0) = \prod_{t=1}^{T} q(x_t|x_{t-1}). \tag{1}$$

Typically, the transition kernel is defined as a Gaussian distribution:

$$q(x_t|x_{t-1}) = \mathcal{N}(x_t; \sqrt{1-\beta_t}x_{t-1}, \beta_t\mathbf{I}), \tag{2}$$

where $\beta_t \in (0, 1)$ is a pre-determined noise schedule controlling the amount of noise added at each step.

In the reverse process, the goal is to recover the data by sampling from a reverse Markov chain. The chain starts with a noise sample $x_T \sim p(x_T) = \mathcal{N}(0, \mathbf{I})$ from a simple Gaussian prior, and transitions through a learnable kernel $p_\theta(x_{t-1}|x_t)$, parameterized by neural networks. This kernel takes the form:

$$p_\theta(x_{t-1}|x_t) = \mathcal{N}(x_{t-1}; \mu_\theta(x_t, t), \Sigma_\theta(x_t, t)), \tag{3}$$

where $\mu_\theta(x_t, t)$ and $\Sigma_\theta(x_t, t)$ represent the learned mean and variance, respectively. By iteratively applying this reverse kernel, we generate the data x_0 through a sequence of updates starting from the noise sample x_T and progressing through $x_{T-1}, x_{T-2}, \ldots, x_0$. Figure 2 illustrates the graphical model for DDPM.

This iterative sampling process captures the reverse dynamics of the original forward diffusion, gradually refining random noise into a meaningful data point, such as an image or text.

2.2.2 Denoising diffusion implicit models (DDIM)

This original DDPM formulation of the generation process in the form of a reverse Markov chain has more recently been complemented by a non-Markovian alternative denoted as denoising diffusion implicit models (DDIM), which offers a deterministic and more efficient generation process. In DDPM, the sampling process typically requires a large number of iterations to achieve satisfactory results. In contrast, the DDIM is designed to accelerate the sampling process by reducing the number of iterations needed. Here, a backward denoising step can be computed with

$$x_{t-1} = \frac{\sqrt{\bar{\alpha}_{t-1}}x_t - \sqrt{1-\bar{\alpha}_t}\epsilon_\theta(x_t, t)}{\sqrt{\bar{\alpha}_t}} + \sqrt{1-\bar{\alpha}_{t-1}}\epsilon_\theta(x_t, t). \tag{4}$$

One distinct advantage of this formulation of the denoising process is that it allows for accurate reconstruction of the original input video x_0 from the noise at time step T. This technique, called DDIM inversion, can be utilized for applications such as image and video editing.

2.2.3 Elucidated diffusion models (EDM)

EDM (Karras et al., 2022) introduce a unified and optimized framework for diffusion-based generative models by reinterpreting sampling and training processes. Unlike DDPMs, which rely on stochastic Markovian sampling, or DDIMs, which employ deterministic non-Markovian updates, EDMs aim to optimize both training and sampling efficiency by introducing tailored sampling schemes and reparameterization strategies. EDMs build upon the common framework of diffusion models by considering the data distribution $q(x_0)$ perturbed by Gaussian noise, leading to a sequence of noisy variables $\{x_t\}$ over time.

While DDPMs use a stochastic reverse process, EDMs leverage an ordinary differential equation (ODE) for deterministic sampling, as inspired by DDIMs. The probability flow ODE Song et al. (2020a) is expressed as:

$$\frac{dx}{dt} = -\sigma(t)\nabla_x \log p(x; \sigma(t)), \tag{5}$$

where $\sigma(t)$ is the noise schedule at time t. Unlike DDIMs, EDMs employ second-order solvers, such as Heun's method, to balance accuracy and computational efficiency.

To ensure stable training, EDMs redefine the loss function with noise-dependent preconditioning. The denoising target $D_\theta(x; \sigma)$ is expressed as:

$$D_\theta(x; \sigma) = c_{\text{skip}}(\sigma)x + c_{\text{out}}(\sigma)F_\theta(c_{\text{in}}(\sigma)x; c_{\text{noise}}(\sigma)), \tag{6}$$

where F_θ is a neural network, and c_{skip}, c_{out}, and c_{in} are scale-dependent coefficients. The overall training objective becomes:

$$\mathcal{L} = \mathbb{E}_{\sigma, x_0, \epsilon}\left[\lambda(\sigma)\|D_\theta(x + \sigma\epsilon; \sigma) - x_0\|^2\right], \tag{7}$$

where $\lambda(\sigma)$ is a weighting function that emphasizes intermediate noise levels during training.

Compared to DDPMs, EDMs achieve faster sampling by reducing the number of neural function evaluations through efficient solvers and noise schedules. Unlike DDIMs, which rely on deterministic updates, EDMs integrate adaptive techniques to minimize truncation errors further, further improving fidelity and flexibility. This unified and modular design allows EDMs to achieve better results while significantly reducing computational overhead(Karras et al., 2022).

2.2.4 Flow matching and rectified flow

Despite denoising diffusion being powerful for video generation tasks, another branch in the family of differential-equation-based generative models began to arise recently, namely the flow matching generative models(Lipman et al., 2023; Liu et al., 2022c; Tong et al., 2023). While diffusion models learn the score function of a specific SDE, flow matching aims to model the vector field implied by an arbitrary ODE directly. A neural network is used for approximating the vector field, and the ODE can also be numerically solved to obtain data samples. The design of such ODE and vector field often considers linearizing the sampling trajectory and minimizing the transport cost(Tong et al., 2023). As a result, flow matching models have simpler formulations and fewer constraints but better quality. VoiceBox(Le et al., 2023) shows the potential of flow matching in fitting large-scale speech data, and LinDiff(Liu et al., 2023b) shares a similar concept in the study of vocoders. More importantly, the rectified flow(Liu et al., 2022c) technique in flow matching models further straightens the ODE trajectory in a concise way. By training a flow matching model again but with its own generated samples, the sampling trajectory of rectified flow theoretically approaches a straightforward line, which improves the efficiency of sampling. *Rectified Flow*(Liu et al., 2022c; 2023d) is a generative model that efficiently transitions between two distributions π_0 and π_1 by solving ordinary differential equations (ODEs). Building on flow matching(Lipman et al., 2023) and stochastic interpolants(Albergo et al., 2023), Rectified Flow introduces a rectification mechanism to optimize the ODE path, improving the efficiency and stability of the sampling process. This approach establishes a strong theoretical baseline for diffusion acceleration and provides a unified perspective on generative models.

The core dynamics of Rectified Flow are governed by the following ODE:

$$\mathrm{d}Z_t = v(Z_t, t)\mathrm{d}t,$$

where Z_t represents the data point at time $t \in [0, 1]$, which evolves continuously along the flow. The vector field $v(Z_t, t)$ determines the direction and velocity of Z_t's movement. This vector field is parameterized using a neural network, which is optimized to align the trajectories with the target distributions. The term $\mathrm{d}t$ represents an infinitesimal time step, enabling a smooth transition between π_0 and π_1.

To learn the vector field v, Rectified Flow minimizes the following objective:

$$\min_v \int_0^1 \mathbb{E}\left[\|(X_1 - X_0) - v(X_t, t)\|^2\right] \mathrm{d}t,$$

where X_0 and X_1 are sampled from the initial distribution π_0 and target distribution π_1, respectively. The term $X_t = tX_1 + (1-t)X_0$ represents a linear interpolation between X_0 and X_1. The loss function measures the squared difference between the actual direction of interpolation $(X_1 - X_0)$ and the vector field $v(X_t, t)$. This ensures that v effectively captures the necessary dynamics to transition samples between the two distributions while preserving their structure.

A key theoretical advantage of Rectified Flow is that the ODE formulation guarantees that paths do not cross. The vector field $v(Z_t, t)$ ensures unique and deterministic trajectories for all starting points, avoiding ambiguities in sampling and maintaining stability during inference. With its focus on optimizing vector fields and straightening trajectories, Rectified Flow offers a powerful and efficient alternative to traditional diffusion models. By combining a strong theoretical foundation with practical efficiency, it sets a new benchmark for generative modeling tasks.

2.2.5 Learning from feedback and reward models

The integration of human feedback into video diffusion models has evolved significantly, beginning with foundational ideas in reinforcement learning and progressing to advanced mechanisms leveraging multimodal and AI-driven annotations. Early work C2M(Ardino et al., 2021) user interaction by selecting objects in the scene and specifying their final location through mouse clicks to generate video in complex scenes. InstructVideo (Yuan et al., 2023) further emphasized aligning video generation with human preferences by incorporating temporal coherence loss:

$$\mathcal{L}_{\text{coherence}} = \mathbb{E}\theta \left[\sum_{j=1}^{F-1} |(v_{j+1} - v_j) - (o_{j+1} - o_j)|_2^2 \right], \tag{8}$$

where v_j and o_j denote predicted and ground truth frames. This method enhanced temporal consistency but primarily focused on supervised fine-tuning with explicit human feedback signals. Subsequent research introduced more scalable methods for integrating feedback. (Furuta et al., 2024b) demonstrated the use of binary AI feedback from vision-language models (VLMs) to optimize dynamic object interactions in videos. Their unified reinforcement learning framework leveraged AI annotations to align outputs with human-like quality assessments, overcoming the limitations of manual data annotation. This concept was further extended in T2V-Turbo(Li et al., 2024d) and its subsequent version T2V-Turbo-V2(Li et al., 2024e), which significantly improved the quality and speed of text-to-video generation through the incorporation of AI feedback, enhancing dynamic object interaction.(Furuta et al., 2024a) In parallel, efforts to construct comprehensive preference datasets began to take shape. (Wu et al., 2024g) presented VIDEOPREFER, a large-scale dataset created using multimodal large language models (MLLMs) such as GPT-4 Vision. This dataset provided 135,000 preference annotations, allowing the training of VIDEORM, the first general-purpose reward model tailored for video preferences. VIDEORM incorporated temporal dynamics, significantly enhancing the alignment of video outputs with human expectations. (Furuta et al., 2024a) further proposed a robust framework for improving dynamic interactions in video generation, showcasing AI feedback as a critical factor for realistic object behavior in generated content. Other works, such as FreeScale(Qiu et al., 2024c)indirectly addressed alignment by improving high-resolution visual generation in video diffusion models. Their approach, while

not explicitly focused on feedback, laid the groundwork for integrating multi-scale visual consistency with human-preferred attributes in video content. Some advanced methods, like VINE(Lu et al., 2024b) also highlighted the robustness of feedback-aligned generative priors for specific tasks like watermarking and video editing. These innovations showed how feedback mechanisms could extend beyond video generation to broader applications, ensuring fidelity and alignment with user intent.

2.2.6 One-shot and few-shot learning

One-shot and few-shot fine-tuning techniques enable generative models to adapt to new tasks or domains with minimal training data. These approaches are particularly valuable in scenarios where acquiring large datasets is infeasible, yet high-quality outputs are required. By leveraging either a single example (one shot) or a small set of examples (few shots), these methods refine pretrained generative models to specialize in specific tasks while maintaining generalization capabilities.

One-shot learning refers to a model's ability to learn from just a single example. In generative modelling, this is particularly useful when only one instance of the target data is available. For example, Tune-A-Video (Wu et al., 2023b) demonstrates how a pre-trained text-to-image diffusion model can be fine-tuned on a single text-video pair, enabling it to generate new videos that maintain the temporal consistency of the original while adhering to text prompts. However, Tune-A-Video is based on the template video and edits it with different content prompts which will restrict the freedom of generative video.

Few-shot fine-tuning extends this capability by adapting models to new domains or tasks using a small number of training samples. Several techniques have emerged to enhance the generative capacity of models under few-shot scenarios. LAMP (Learn A Motion Pattern) (Wu et al., 2023c) proposes a motion learning model to capture the motion pattern from the training data and utilizes about 8$\tilde{1}$6 videos to tune the pretrained T2I model. However, it is constrained by their incomplete capture of image features. MAIM (Huang et al., 2025) addresses this by integrating image features via the CLIP encoder, enabling videos with intricate scenes and multiple objects.

2.2.7 Training-free methods

Training-free approaches enable direct video generation without additional training or fine-tuning, making them valuable for black-box scenarios.

Text2Video-Zero (Khachatryan et al., 2023) introduced cross-frame attention based on pretrained text-to-image diffusion model. FateZero (Qi et al., 2023) enhanced this through intermediate attention maps, and Free-Bloom (Huang et al., 2023a) combined GPT-3 with image diffusion models for improved semantic coherence. PEEKABOO (Jain et al., 2024b) enabled spatio-temporal control through masked diffusion using a latent diffusion model-based video generation model, while ControlVideo (Zhang et al., 2023e) extended ControlNet with an interleaved-frame smoother to generate consistent controllable and structurally smooth video. DreamVideo-2 (Wei et al., 2024b) proposed zero-shot subject-driven video customization with precise motion control, enabling subject-preserving and motion-specific video editing. Following this, VideoElevator (Zhang et al., 2024f) encapsulates T2V to enhance temporal consistency and harnesses T2I to provide more faithful details. Recent innovations include GPT4Motion (Lv et al., 2024)'s combination of GPT-4, Blender, and text-to-image diffusion models for physics-aware generation, AnyV2V (Ku et al., 2024)'s universal editing framework built on an image editing model combined with an existing image-to-video generation model to generate the edited video through temporal feature injection. Video Custom Diffusion (Magic-Me) (Ma et al., 2024e) built a training-free 3D Gaussian Noise Prior for video frame initialization, reconstructing inter-frame correlation to achieve identity-preserved generation.

2.2.8 Token learning

Token learning, such as Textual Inversion Gal et al. (2022), is another paradigm within generative modeling. Instead of fine-tuning the entire model, token learning focuses on training specific embeddings or tokens that represent new concepts or ideas. By using textual inversion, the model learns a new token that can be combined with existing tokens to guide generation without requiring large datasets or significant changes

to the model's architecture. However, optimizing the single token embedding vector has limited expressive capacity because of its limited optimized parameter size. In addition, using one word to describe concepts with rich visual features and details is very hard and insufficient. Animate-A-Story(He et al., 2023a) extended traditional textual inversion to timestep-variable textual inversion (TimeInv) and adapted it to video generation task to ensure flexible controls over structure and characters. DreamVideo(Wei et al., 2024c) further incorporated textual inversion to capture the fine appearance of the subject from provided images to generate videos with customized subjects.

2.3 Guidance

2.3.1 Classifier guidance

In generative modeling, diffusion models such as DDPM and DDIM can be guided using classifiers to improve the quality of conditional generation. This approach, called *classifier guidance* (Dhariwal & Nichol, 2021), integrates class information into the diffusion process by leveraging the gradients of a classifier trained on noisy data. The classifier's gradients help the model generate data conditioned on a given label, improving the overall sample quality for specific categories.

Mathematically, the classifier-guided diffusion process modifies the reverse noising process by incorporating the classifier's log-probability gradients. This guidance is applied at each timestep of the diffusion process, allowing the model to generate more accurate conditional samples.

The reverse noising process is represented as follows:

$$p_{\theta,\phi}(x_t|x_{t+1}, y) = Z \cdot p_\theta(x_t|x_{t+1}) \cdot p_\phi(y|x_t) \tag{9}$$

where p_θ is the reverse noising process from the original diffusion model, $p_\phi(y|x_t)$ is the classifier's conditional probability, and Z is a normalizing constant.

We now describe how this approach can be applied to both DDPM and DDIM frameworks. In particular, they(Dhariwal & Nichol, 2021) train a classifier $p_\phi(y|x_t, t)$ on noisy images x_t, and then use gradients $\nabla_{x_t} \log p_\phi(y|x_t, t)$ to guide the diffusion sampling process towards an arbitrary class label y.

Algorithm for classifier-guided DDPM sampling. In the DDPM framework, classifier guidance can be incorporated by modifying the reverse diffusion process. The update at each timestep involves sampling from a Gaussian distribution with a mean adjusted by the classifier gradients. Detailed workflow can be referred to Algorithm algorithm 1.

Algorithm 1 Classifier-guided DDPM sampling, given a diffusion model $(\mu_\theta(x_t), \Sigma_\theta(x_t))$, classifier $p_\phi(y|x_t)$, and gradient scale s.(Dhariwal & Nichol, 2021)

1: **Input:** class label y, gradient scale s
2: $x_T \leftarrow$ sample from $\mathcal{N}(0, I)$
3: **for** $t = T$ to 1 **do**
4: $\quad \mu, \Sigma \leftarrow \mu_\theta(x_t), \Sigma_\theta(x_t)$
5: $\quad x_{t-1} \leftarrow$ sample from $\mathcal{N}(\mu + s\Sigma\nabla_{x_t} \log p_\phi(y|x_t), \Sigma)$
6: **end for**
7: **return** x_0

Algorithm for classifier-guided DDIM sampling. For the DDIM framework, the deterministic nature of the sampling process requires a slightly different approach. The classifier gradient is used to modify the epsilon prediction, which guides the reverse sampling process in DDIM. Deatailed workflow can be referred to Algorithm algorithm 2.

In the DDIM case, it defines a new epsilon prediction $\hat{\epsilon}(x_t)$, which incorporates the classifier's guidance into the joint distribution of the diffusion model and the classifier:

$$\hat{\epsilon}(x_t) := \epsilon_\theta(x_t) - \sqrt{1 - \alpha_{\bar{t}}}\nabla_{x_t} \log p_\phi(y|x_t) \tag{10}$$

Algorithm 2 Classifier-guided DDIM sampling, given a diffusion model $\epsilon_\theta(x_t)$, classifier $p_\phi(y|x_t)$, and gradient scale s. (Dhariwal & Nichol, 2021)

1: **Input:** class label y, gradient scale s
2: $x_T \leftarrow$ sample from $\mathcal{N}(0, I)$
3: **for** $t = T$ to 1 **do**
4: $\quad \epsilon \leftarrow \epsilon_\theta(x_t) - \sqrt{1-\bar{\alpha_t}}\nabla_{x_t} \log p_\phi(y|x_t)$
5: $\quad x_{t-1} \leftarrow \frac{\sqrt{\bar{\alpha_{t-1}}}x_t - \sqrt{1-\bar{\alpha_t}}\epsilon}{\sqrt{\bar{\alpha_t}}} + \sqrt{1-\bar{\alpha_{t-1}}}\hat{\epsilon}$
6: **end for**
7: **return** x_0

This modified epsilon prediction is then used to guide the reverse sampling process, replacing the standard noise predictions from the original model.

The development of classifier guidance for diffusion models has sparked significant advances in video generation applications. (Shi et al., 2023a) explored compositionality in visual generation by using latent classifiers to guide diffusion models in semantic space, demonstrating effective control over multiple attributes and their relationships. (Chung et al., 2024) further reformulated classifier guidance to better respect manifold constraints crucial for temporal consistency in videos. (Lian et al., 2024) then incorporated large language models to generate dynamic scene layouts as intermediate representations, effectively guiding the diffusion process for coherent motion and interactions. These developments demonstrate the field's progression from basic guidance mechanisms to more sophisticated approaches specifically tailored for video generation challenges.

2.3.2 Classifier-free guidance

While classifier-based guidance successfully allows for the conditional generation of data by leveraging the gradients from a pre-trained classifier, it has several limitations. For instance, classifier guidance requires the maintenance of a separate classifier, and its performance is closely tied to the quality of this classifier. To address these concerns, *classifier-free guidance*(Ho & Salimans, 2022) offers an alternative that achieves similar results without the need for a dedicated classifier.

Classifier-free guidance modifies the model's predicted noise directly by using conditioning information, allowing for conditional generation without relying on external classifier gradients. This approach avoids the complexities of training and maintaining an additional classifier.

Rather than training a separate classifier model, they(Ho & Salimans, 2022) adopt an approach that jointly trains an unconditional denoising diffusion model, $p_\theta(x)$, and a conditional model, $p_\theta(x|y)$. Both models are parameterized through a shared score estimator: $\epsilon_\theta(x_t)$ for the unconditional case and $\epsilon_\theta(x_t, y)$ for the conditional case. They use a single neural network to parameterize both models and then perform sampling using a linear combination of conditional and unconditional scores, as shown in Equation 11.

$$\hat{\epsilon}_\theta(x_t, y) = (1 + w)\epsilon_\theta(x_t, y) - w\epsilon_\theta(x_t) \tag{11}$$

Here, w is a guidance scale that controls the strength of the conditional information. This formulation allows the model to perform conditional sampling without relying on classifier gradients.

Algorithm for Classifier-Free Guidance describes the sampling procedure for classifier-free guidance, which adjusts the score estimates directly within the diffusion model without requiring any classifier gradients. Algorithms algorithm 3 and algorithm 4 describe training and sampling with classifier-free guidance in detail.

This algorithm leverages the classifier-free guidance to adjust the sampling procedure by computing the guided score at each timestep. Instead of using gradients from a classifier, the model directly modifies its own score estimates to account for the conditional information.

Algorithm 3 Joint training a diffusion model with classifier-free guidance

Require: p_{uncond}: probability of unconditional training

repeat
  $(x, y) \sim p(x, y)$ ▷ Sample data with conditioning information from the dataset
  $y \leftarrow \emptyset$ with probability p_{uncond} ▷ Randomly discard conditioning to train unconditionally
  $\lambda \sim p(\lambda)$ ▷ Sample log SNR value
  $\epsilon \sim \mathcal{N}(0, I)$
  $x_\lambda = \alpha_\lambda x + \sigma_\lambda \epsilon$ ▷ Corrupt data to the sampled log SNR value
  Take gradient step on $\nabla_\theta \|\epsilon_\theta(x_\lambda, y) - \epsilon\|^2$ ▷ Optimize the denoising model
until converged

Algorithm 4 Conditional sampling with classifier-free guidance

Require: w: guidance strength
Require: c: conditioning information for conditional sampling
Require: $\lambda_1, \ldots, \lambda_T$: increasing log SNR sequence with $\lambda_1 = \lambda_{\min}, \lambda_T = \lambda_{\max}$

$x_0 \sim \mathcal{N}(0, I)$
for $t = 1, \ldots, T$ **do**
  $\tilde{\epsilon}_{t-1} \leftarrow (1 + w)\epsilon_\theta(x_{t-1}) - w\epsilon_\theta(x_{t-1})$ ▷ Form the classifier-free guided score at log SNR λ_{t-1}
  $x_t \leftarrow \frac{(x_{t-1} - \alpha_{\lambda_{t-1}} \tilde{\epsilon}_{t-1})}{\alpha_{\lambda_{t-1}}}$ ▷ Sampling step (could be replaced by another sampler, e.g., DDIM)
  $x_t \sim \mathcal{N}(\tilde{\mu}_{\lambda_{t-1}, \lambda_t}(x_{t-1}, x_t), \tilde{\sigma}^2_{\lambda_{t-1}, \lambda_t})$
end for
return x_T

2.4 Diffusion model frameworks

This section explores several key frameworks within diffusion models, highlighting their distinctive approaches and applications.

2.4.1 Pixel diffusion and latent diffusion

Remarkable progress has been made in developing large-scale pre-trained text-to-Video Diffusion Models (VDMs), including proprietary models (*e.g.*, Make-A-Video (Singer et al., 2023), Imagen Video (Ho et al., 2022c), Video LDM (Blattmann et al., 2023b), Gen-2 (Esser et al., 2023)) and open-sourced ones (*e.g.*, VideoCrafter (He et al., 2023b), ModelScopeT2V (Wang et al., 2023c). These VDMs can be categorized into two primary architectures: (1) Pixel-based VDMs and (2) Latent-based VDMs. The former directly operates on pixel values for denoising, as exemplified by Make-A-Video Singer et al. (2023), Imagen Video Ho et al. (2022c), and PYoCo Ge et al. (2023). The latter manipulates the compressed latent space within a variational autoencoder (VAE), as demonstrated by Video LDM Blattmann et al. (2023b) and MagicVideo Zhou et al. (2022). However, both of them have pros and cons. **Pixel-based VDMs** can generate motion accurately aligned with the textual prompt but typically demand expensive computational costs in terms of time and GPU memory, especially when generating high-resolution videos. **Latent-based VDMs** are more resource-efficient because they work in a reduced-dimension latent space. However, it is challenging for such a small latent space (*e.g.*, 8×5 for 64×40 videos) to cover rich yet necessary visual semantic details as described by the textual prompt. Thus, if the generated videos are often not well-aligned with the textual prompts or the generated videos are of relatively high resolution (*e.g.*, 256×160 videos), the latent model will focus more on spatial appearance but may also ignore the text-video alignment. Recently, Show-1(Zhang et al., 2023a) integrates the strengths of both pixel and latent VDMs, resulting in a novel video generation model that can produce high-resolution videos of precise text-video alignment at low computational cost (15G GPU memory during inference). LATTE Ma et al. (2024c) further proposes a novel latent diffusion transformer for video generation, which extracts spatio-temporal tokens from input videos and models video distribution in the latent space using Transformer blocks, achieving state-of-the-art performance across multiple video

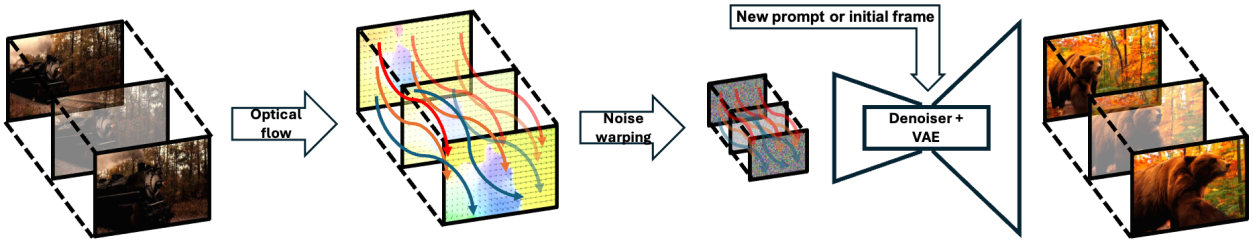

Figure 3: An example for optical flow usage in video scenario, Go-with-the-Flow (Burgert et al., 2025), a novel framework that predicts 3D scene dynamics across sequential frames, outperforming conventional single-frame approaches. By integrating multi-frame spatial-temporal relationships, it improves depth accuracy and visual fidelity in scene reconstruction.

generation datasets by exploring optimal design choices such as video clip patch embedding, model variants, timestep-class information injection, and temporal positional embedding.

2.4.2 Optical-flow-based diffusion models

Another distinct approach within diffusion models leverages optical flow to maintain temporal coherence between frames. Optical flow is a common approach to represent motion by estimating the displacement field between consecutive frames. Early approaches treated it as an optimization problem using handcrafted features to maximize visual similarity(Horn & Schunck, 1981; Black & Anandan, 1993; Bruhn et al., 2005; Sun et al., 2014). Incorporating deep learning-based methods revolutionized this field. FlowNet(Dosovitskiy et al., 2015) pioneered end-to-end optical flow estimation, demonstrating the potential of deep learning in this domain. Subsequent advancements on improved architectures and synthetic datasets further promoted the progress of optical flow estimation(Ilg et al., 2017; Ranjan & Black, 2017; Sun et al., 2018; 2021; Hui et al., 2018; 2020; Yang & Ramanan, 2019). RAFT(Teed & Deng, 2020) included iterative refinement with correlation volumes, significantly boosting performance, while FlowFormer(Huang et al., 2022b; Shi et al., 2023c) applied attention mechanisms within optical flow usage. VideoFlow(Shi et al., 2023b) extended optical flow to video generation scenarios and utilized temporal information across multiple frames, achieving high accuracy. (Hu et al., 2023)propose a Dynamic Multi-scale Voxel Flow Network (DMVFN) to explicitly model the complex motion cues of diverse scales between adjacent video frames by dynamic optical flow estimation to generate videos at lower computational costs. Also, Motion-I2V(Shi et al., 2024) further refined the motion modelling by a diffusion-based motion field predictor and motion-augmented temporal attention to generate more consistent videos even in the presence of large motion and viewpoint variation. By conditioning the optical flow between a previous and a subsequent frame, this framework achieves realistic motion continuity, which is critical for applications in video generation and motion synthesis. Additionally, recent advancements explore upgrading pretrained image diffusion models to video generation by temporally warping input noise. How I Warped Your Noise (Chang et al., 2024) proposed a novel noise representation called integral noise ($\int$*-noise*), preserving temporal correlations through an optical-flow-based noise warping algorithm. This foundational approach mitigated issues like high-frequency flickering and texture-sticking artifacts, laying the groundwork for temporally coherent video diffusion. Building upon this, Infinite-Resolution Integral Noise Warping (Deng et al., 2024b) method introduces a training-free approach where temporal correlations in noise are preserved by warping input noise using integral representations, enabling consistent frame generation while reducing computational overhead. These diffusion model frameworks demonstrate the versatility and adaptability of diffusion processes across different domains, from high-resolution static images to complex, temporally coherent videos. As shown in Figure 3, Go-with-the-Flow (Burgert et al., 2025) combined optical flow extraction from training videos with real-time noise warping and fine-tuning video diffusion models on paired warped noise and video data to enable robust and motion-controllable generation. Together, these methods demonstrate the progression from temporal correlation preservation to advanced motion control, showcasing the versatility and adaptability of diffusion models in video generation.

2.4.3 Noise scheduling

Diffusion models (Song et al., 2020b; Ho et al., 2020) perturb data with Gaussian noise through a diffusion process for training, and the reverse process is learned to transform the Gaussian distribution back to the data distribution. Perturbing data points with noise populates low data density regions to improve the accuracy of estimated scores, resulting in stable training and image sampling. The forward process is controlled by the handcrafted noise schedule. However, current noise scheduling strategies remain handcrafted for each dataset, such as VP (Ho et al., 2020), VE (Song et al., 2020b), Cosine (Nichol & Dhariwal, 2021) and EDM (Karras et al., 2022). These noise schedules perform well in low-resolution RGB spaces but yield poorer results in higher resolutions (Dhariwal & Nichol, 2021; Hoogeboom et al., 2023). Recent studies (Chen, 2023; Hoogeboom et al., 2023) propose carefully designed noise schedules that outperform VP, VE, and Cosine schedules in RGB space. Besides, (Guo et al., 2023a) analyzed the power spectrum, introduced a numerical quantification of noise levels, and proposed the weighted signal-to-noise ratio (WSNR) as a unified metric for noise levels in both RGB and latent spaces. WSNR-equivalent training noise schedules significantly enhance high-resolution model performance across both latent and RGB spaces.

2.4.4 Agent-based diffusion models

Agent-based approaches have revolutionized diffusion models for multimedia generation, where agents are implemented as specialized neural modules with distinct functionality and decision-making capabilities. DriveGAN (Kim et al., 2021) pioneered this direction by utilizing multi-agent frameworks for video generation through differentiable simulation. UniSim (Yang et al., 2024g) contributed by developing a neural closed-loop sensor simulator using coordinated agents for scene reconstruction and sensor data generation. MORA (Yuan et al., 2024c) established a comprehensive framework with five specialized agents for different generation stages, introducing self-modulated fine-tuning for dynamic agent contribution adjustment. VideoAgent (Soni et al., 2024b) advanced the framework by integrating multimodal LLM feedback and real-world execution for iterative refinement. AutoGen (Wu et al., 2024d) and MetaGPT (Hong et al., 2024a) extended these principles to broader generative tasks, implementing standardized communication protocols to enable scalable multi-agent collaboration. This progression shows how agent-based diffusion models have evolved from simple architectures to sophisticated multi-agent systems capable of handling complex generation tasks while maintaining consistency through structured collaboration and feedback mechanisms.

2.5 Architecture

As shown in Figure 4, most text-conditional visual generation models comprise three key modules: a variational autoencoder (VAE) compresses images and videos into a latent space. Second, a neural network—typically incorporating a U-Net or Transformer-based backbone—performs the denoising within this latent space. The denoising process can be enhanced using optical flow or human feedback to improve generation quality. A text encoder generates embeddings to guide the image or video generation process.

2.5.1 UNet

The UNet(Ronneberger et al., 2015) architecture has become foundational in designing denoising models for visual diffusion applications, originally developed for medical image segmentation and now adapted widely for generative tasks across images, video, and audio. In image generation tasks, a UNet typically encodes an input into progressively lower-resolution latent representations while increasing feature channels through a series of encoding layers. This encoded latent is then upsampled back to the original resolution by corresponding decoding layers.

In diffusion models, UNet can operate in either the pixel space or the latent space. For example, Latent Diffusion Models (LDMs) (Rombach et al., 2022) utilize UNet within a lower-dimensional latent space, which allows for more efficient, high-resolution generation. In pixel space, UNet implementations are used for direct denoising, maintaining the input's spatial resolution throughout the process.

Modern implementations of UNet in diffusion models build upon the original by replacing ResNet blocks with Vision Transformer (ViT) layers(Dosovitskiy et al., 2020). ResNet blocks apply 2D-Convolutions, focusing

Models	Backbone	VAE	Text Encoder	# Params	Training dataset and size	Resolution	Duration	# Frames	GPU size	GPU time
Academia open-source models										
VideoGPT(Yan et al., 2021)	-	VQVAE	-	-	UCF-101, BAIR	64×64	-	-	-	-
CogVideo(Hong et al., 2023a)	DiT	2D VAE	GPT-3	15.5B	WebVid-5.4M	480×480	-	-	$8 \times RTX6000$	-
CogVideoX(Yang et al., 2024j)	STDIT	3D VAE	-	2-5B	LAION-5B, COYO-700M	768×1360	10s	160	-	-
MagicVideo(Zhou et al., 2022)	3D UNet	VideoVAE	CLIP	-	WebVid-10M, HD-VG-130M	1024×1024	-	-	$1 \times$ A100	-
Make-A-Video(Singer et al., 2022)	UNet	2D VAE	CLIP	9.7B	WebVid-10M, HD-VG-100M	768×768	-	76	-	-
LVDM(Rakhimov et al., 2023)	3D UNet	3D VAE	CLIP	1.6B	UCF-101, TaiChi	128×128	-	1024	$8 \times V100s$	4.5 days
Video-LDM(Blattmann et al., 2023b)	3D UNet	-	-	-	WebVid-10M	512×1024	~ 4.7s	113	$2 \times$ A100s	-
Latent-shift(Sun et al., 2023c)	ViT	2D VAE	CLIP ViT-L	1.5B	WebVid-10M	256×256	2-8s	-	$1 \times$ A100	-
MagViT(Yu et al., 2023a)	UNet	2D VAE	-	464M	UCF-101	128×128	2-8s	16	$1 \times$ V100	-
MagViT-V2(Yu et al., 2024b)	-	3D VAE	MLM	307M	UCF-101	640×360	-	-	-	-
VideoFusion(Zhou et al., 2023)	UNet	-	CLIP	2B	UCF101, Taichi-HD, SkyTimelapse	128×128	-	16	-	-
VideoComposer(Jiang et al., 2023a)	3D UNet	-	CLIP	-	WebVid-10M	256×256	-	16	-	-
InstructVideo(Yuan et al., 2023)	UNet	-	CLIP	-	WebVid-10M	-	-	-	$4 \times$ A100s	-
ModelScope(Wang et al., 2023c)	3D UNet	VQGAN	T5	$\sim$1.7B	WebVid	256×256	-	-	A100	-
HiGen(Qing et al., 2024)	3D UNet	-	CLIP	-	WebVid-10M	448×256	-	32	$8 \times$ A100s	-
Dysen-VDM(Zhao et al., 2023a)	3D UNet	2D VAE	CLIP	-	UCF-101, MSRVTT	256×256	2s	16	$16 \times$ A100s	-
VideoGen(Chen & Sun, 2023)	UNet	-	CLIP	-	WebVid-10M	256×256	-	16	$64 \times$ A100s	-
Animate-A-Story(He et al., 2023a)	3D UNet	-	CLIP	-	WebVid-10M	256×256	-	16	-	-
AnimateDiff(Guo et al., 2023c)	UNet	2D VAE	-	-	Web Vid	1024×576	-	-	-, -	
AnimateDiff-V2	UNet	-	CLIP	-	-	1024×1024	-	-	-, -	
SimDA(Xing et al., 2024b)	UNet	-	T5-XXL	1.1B	WebVid-10M	256×256	-	-	$1 \times$ A100	-
AnimateLCM(Wang et al., 2024a)	-	-	CLIP	-	UCF-101	512×512	2s	16	$1 \times$ A100	-
Snap Video(Menapace et al., 2024)	DiT	3D VAE	T5-XXL	3.90B	UCF-101, MSRVTT	288×512	-	16	A100	-
VideoDirGPT(Lin et al., 2024a)	UNet	2D VAE	CLIP	-	UCF-101, MSR-VTT	-	-	-	$16 \times A6000$	
SiT(Ma et al., 2024a)	DiT	2D VAE	CLIP ViT-L	675M	LAION-5B	512×512	-	-	-	-
Open-Sora(Zheng et al., 2024c)	STDiT	3D VAE	T5-XXL	1.1B	WebVid-10M, Panda-70M HD-VG-130M, MiraData Vript, Inter4K	1280×720	2-16s	16	$8 \times$ H100s	3.5k hrs
Open-Sora-Plan(Lab & etc., 2024)	DiT	WF-VAE	mT5-XXL	-	Panda-70M	256×256	-	25-49	$8 \times NPUs$	-
I4VGEN(Guo et al., 2024a)	UNet	2D VAE	CLIP	-	-	512×512	2-8s	16	$1 \times V100$	-
Zeroscope-v2	-	-	-	$\sim$1.7B	-	1024×576	3-12s	-	-	-
CausVid(Yin et al., 2024)	DiT	-	-	-	-	640×352	10s	128	$64 \times$ H100s	2 days
RepVideo(Si et al., 2025)	-	-	-	-	-	-	-	-	$32 \times$ H100s	-
Industry commercial models										
GEN-1	-	-	-	-	-	1280×720	$\sim$8s	-	-	-
GEN-2	-	-	-	-	-	2048×1080	$\sim 4s$	-	-	-
GEN-3 Alpha	-	-	-	-	-	4096×2160	Variable	-	-	-
Imagen video(Ho et al., 2022a)	UNet	-	T5-XXL	16.2B	-	Up to 1280×768	Up to 5.3s	-	-	-
W.A.L.T(Gupta et al., 2023)	DiT	-	T5-XXL	3.00B	UCF-101, MSRVTT	512×896	2-5s	-	$8\times$ A6000s	-
Phenaki(Villegas et al., 2022)	C-ViViT	2D VAE	T5-XXL	0.8B		64×64	-	11-15	-	-
MiracleVision	-	-	-	-		1920×1080	60s	1,440	-	-
Lavie(Wang et al., 2023g)	UNet	2D VAE	CLIP	$\sim$ 3B	Vimeo25M	1280×2048	$\sim$ 10-20s	16-61	-	-
Seine(Chen et al., 2024d)	UNet	VQGAN	CLIP	-	WebVid-10M	320×512	-	16	-	-
VLogger(Zhuang et al., 2024)	UNet	VQVAE	CLIP	1.3B	WebVid-10M	320×512	$\sim$ 2-3s	16	-	-
Optis(Chen et al., 2024d)	-	-	CLIP	1.3B	WebVid-10M	320×512	5min	320	A100	-
Vchitect-2.0	-	-	-	$\sim$ 2B	-	720×480	$\sim$ 10-20s	-	$8 \times$ A100s	-
Pika	-	-	-	-	-	1920×1080	3-7s	-	-	-
MovieGen	DiT	TAE	MetaCLIP+UL2+ByT5	30B	-	1920×1080	16s	-	6,144 H100s	1000k hrs
Show-1	UNet	-	T5-XXL	-	WebVid-10M	576×320	-	-	$48 \times$ A100s	-
Kling	DiT	3D VAE	-	-	-	1920×1080	up to 3min	-	-	
Wanx 2.1	DiT	-	-	-	-	1920×1080	-	-	-	-
Nova Real	-	-	-	-	-	1280×720	$\sim$ 6s	-	-	-
Veo-1	-	-	-	-	-	1920×1080	$\sim$ 1min	-	-	-
Veo-2	-	-	-	-	-	4096×2160	$\sim$ 2min	-	-	-
LumaAI Dream Machine	-	-	-	-	-	1360×752	$\sim$ 5s	-	-	-
LumaAI Ray 2	-	-	-	-	-	1280×720	$\sim$ 5-9s	-	-	-
VideoPoet	-	-	T5 XL	1.1 B	270M videos	896×512 8 fps	-	-	-	-
Lumiere	UNet	-	T5 XL	-	30M videos	- 16 fps	5s	-	-	-
Hailuo AI	-	-	-	-	-	1280×720	3- 5s	-	-	-
Mira	-	-	-	-	MiraData	-	10s-2min	-	-	-
VideoCrafter1(Chen et al., 2023a)	U-ViT	Video VAE	CLIP	-	Laion-coco-600M, Webvid-10M	1024×576	-	-	-	-
VideoCrafter2(Chen et al., 2024a)	U-ViT	Video VAE	-	-	WebVid-10M	512×320	-	-	-	
Vidu	-	-	-	-	-	1920×1080	4-8s	-	-	-
EasyAnimate(Xu et al., 2024c)	DiT	3D VAE	T5-XXL	-	-	1024×576	-	up to 144	-	-
Mochi 1(Team, 2024a)	DiT	3D VAE	T5-XXL	$\sim$10B	-	1280×720	$\sim 5.4s$	-	$4 \times$ H100s	-
Jimeng(Lin et al., 2024b)	-	-	-	-	-	-	5s	-	-	-
Allegro	-	-	-	-	-	1280×720	-	-	-	-
LTX-Video(HaCohen et al., 2024)	DiT	Video-VAE	T5-XXL	-	-	768×512	5s	121	$1 \times$ H100	-
STIV(Lin et al., 2024b)	DiT	-	-	8.7B	-	512×512	-	-	-	-
Sora	DiT	3D VAE	Multiple LLMs	$\sim$30B	-	1920×1080	5-20s	-	-	-
HunyuanVideo(Kong et al., 2025)	DiT	3D VAE	MLLM	$\sim$13B	-	1280×720	$\sim$5s	-	-	-
Step-Video-T2V(Ma et al., 2025)	DiT	Video VAE	CLIP, Step-LLM	$\sim$30B	-	768×768	-	204	H100	-
SkyReels-V1(SkyReels-AI, 2025)	DiT	3D VAE	MLLM	-	-	544×960	-	97	-	-
Magic-1-For-1(Yi et al., 2025)	DiT	Video VAE	CLIP, LLM	-	-	-	-	-	-	-

Table 1: Comparison of modules and parameters in different diffusion generative models and their industry applications. New models can be found in video generation arena leaderboard and vbench leaderboard. (TAE refers to temporal autoencoder, and MLLM refers to multimodal large language model). Papers about related component and dataset: VideoVAE(Zhou et al., 2022), mT5-XXL(Xue, 2020), WebVid(Bain et al., 2021), UCF-101(Soomro et al., 2012), MSR-VTT(Xu et al., 2016), MiraData(Ju et al., 2024), Laion-coco 600M(LAION, 2023) Taichi-HD(Siarohin et al., 2019), SkyTimelapse(Xiong et al., 2018), Panda-70M(Chen et al., 2024c), FaceForensics(Rössler et al., 2018), Inter4K(Stergiou & Poppe, 2023), Vimeo25M(Huang et al., 2023b), MiraData(Zhao et al., 2023d), Vript(Yang et al., 2024a)

.

on extracting spatial features, while the ViT blocks introduce spatial self-attention and cross-attention mechanisms. This configuration allows the model to condition generation based on text prompts or specific time steps. Matching resolution layers in the encoder and decoder are connected by residual connections, ensuring efficient information flow.

UNet has been further adapted to handle temporal information for video-based diffusion tasks. Extensions like AnimateDiff incorporate temporal attention layers within the UNet to capture dependencies across

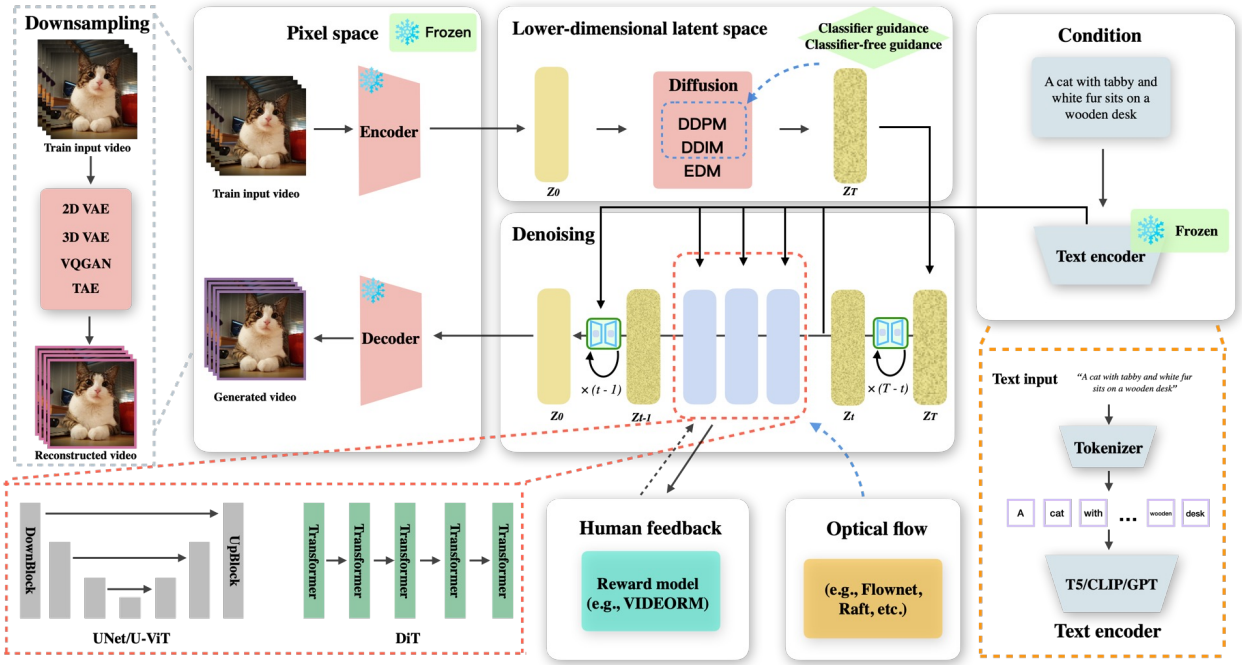

Figure 4: A pipeline for diffusion-based visual content generation leverages a pre-trained variational autoencoder (VAE), such as 2D VAE, 3D VAE, VQGAN, or TAE, to encode input images or videos into a lower-dimensional latent representation. Within this latent space, diffusion models (e.g., DDPM, DDIM, EDM) iteratively introduce noise and employ neural architectures, such as U-Net or Transformer-based models, to learn a denoising process that reconstructs high-fidelity outputs. User-provided textual prompts undergo refinement through large language models (e.g., T5, CLIP, GPT) before being mapped into an embedding space via a trained text encoder. This embedding space serves as a conditioning mechanism, guiding the diffusion process to ensure semantic coherence with the input prompt. Furthermore, the framework integrates optical flow estimation methods (e.g., FlowNet, Raft) to enhance motion consistency in generated video sequences and incorporates human feedback mechanisms (e.g., VIDEORM) to iteratively improve generation quality.

frames. (An et al., 2023) keep using 2D UNet and enable motion learning by shifting the feature channels along the temporal dimension. Other modifications include transitioning from classic 2D-UNet to spatial-temporal factorized 3D UNet architecture. VDM (Ho et al., 2022c) propose a spatial-temporal factorized 3D UNet by adding temporal blocks for video generation, as a natural extension of the standard image diffusion model. Similarly, (Ho et al., 2022a) builds on the similar video U-Net architecture to the cascaded image diffusion model Imagen Saharia et al. (2022), while (He et al., 2022), MagicVideo(Zhou et al., 2022), and ModelScope(Wang et al., 2023c)apply it to the latent space (Rombach et al., 2022), as shown in Table 1. MoVideo(Liang et al., 2025) further generates the depth and optical flow of the whole video by utilizing a 3D UNet architecture by adding extra-temporal modules, including temporal convolution and temporal attention layers after spatial convolution and spacial attention layers, improving frame consistency and visual quality for video generation.

2.5.2 Diffusion transformers

The Diffusion Transformer (DiT) replaces UNet's traditional convolutional design with a Vision Transformer (ViT) framework, offering improved spatial attention capabilities suited for generative tasks across images and videos(Peebles & Xie, 2023). DiT achieves this through a 2D patchification process, where individual image frames are divided into patches that are then treated as tokens, allowing the model to capture

detailed spatial dependencies within each frame. GenTrone(Chen et al., 2024b) adapted DiT from class to text conditioning and scaled GenTrone from approximately 900M to over 3B parameters demonstrating Transformer-based diffusion models can be used in the visual generative domain. From Table 1, models including CausVid(Yin et al., 2024), SiT(Ma et al., 2024a), and Sora also use DiT in video generation settings. However, for video generation, 2D tokenization alone is insufficient to capture the sequential dependencies critical for temporal coherence across frames. Approaches such as ViViT(Arnab et al., 2021) and STDiT(Zheng et al., 2024c) address this limitation by extending DiT's patchification from 2D to 3D, introducing a 3D tokenization approach that simultaneously captures both spatial and temporal relationships. One representative work is CogVideoX (Hong et al., 2023a), which uses STDiT to model spatial-temporal evolution in video generation, capturing long-range dependencies for improved motion consistency and semantic fidelity. In this structure, consecutive frames are processed as spatiotemporal patches, enabling the model to understand dynamic changes across frames. Building on these approaches, frameworks like VDT(Lu et al., 2024a) incorporate both causal attention, which restricts attention to previous frames, and sparse causal attention, which further limits the focus to a subset of recent frames. VersVideo(Xiang et al., 2023) incorporated multi-excitation paths for spatial-temporal convolutions with dimension pooling across different axes and multi-expert spatial-temporal attention blocks to further boost the model's spatial-temporal performance instead of simply extending 2D operations with temporal operations to significantly escalate training and inference costs.Text2Performer(Jiang et al., 2023b)proposes ae continuous VQ-diffuser to directly output the continuous pose embeddings for better motion modeling. These mechanisms enhance model's effectiveness for video-based diffusion tasks.

2.5.3 VAE for latent space compression

Diffusion and denoising in RGB pixel space, as demonstrated in (Ho et al., 2020; Dhariwal & Nichol, 2021; Saharia et al., 2022; Ramesh et al., 2022; Ho et al., 2022b), require high computational resources, significantly increasing both training cost and inference latency. To mitigate its resource consumption, Latent Diffusion Models (LDM)(Rombach et al., 2022) leverage variational autoencoders (VAEs) to compress images from pixel space into a more compact latent space enabling the diffusion process to occur in this optimized space. This approach enhances both training and inference efficiency by reducing the complexity of the data representation.

Classical VAEs for image and video compression include standard VAEs(Kingma, 2013), quantized versions like VQVAE(Esser et al., 2021), VQGAN(Van Den Oord et al., 2017), and their GAN-enhanced variants, which improve reconstruction quality for higher compression. For example, VideoGPT(Yan et al., 2021) use a 3D-VQVAE in the latent space for video generation. Seine(Chen et al., 2024d) and MAGVIT(Yu et al., 2023a) integrate 3D-VQGAN with discriminators for latent space encoding to achieve better visual quality. The VAE framework not only compresses effectively but also enable the training of multiple generative tasks across downstream tasks.

By integrating VAE in model building, some image generation models(Ho et al., 2022a; Li et al., 2024b; Podell et al., 2023; Bao et al., 2023b; Peebles & Xie, 2023; Lu et al., 2024c; Ma et al., 2024a; Chen et al., 2023c; Li et al., 2024j; Team, 2024b; Esser et al., 2024) also leverage latent space encoding/decoding, freezing VAE parameters during diffusion training and inference. Some diffusion models, including Make-A-Video(Singer et al., 2022), Imagen(Ho et al., 2022a), Show-1(Zhang et al., 2023a), directly learn pixel distributions generating videos, as shown in Table 1. However, video generation involves both spatial and temporal complexity, leading to higher computational costs. Besides, some representative diffusion video generation models, including Sora(Liu et al., 2024e), Phenaki(Villegas et al., 2022), VideoCrafter(Chen et al., 2023a), AnimateDiff(Guo et al., 2023c), and VideoPoet(Kondratyuk et al., 2023), start using VAE compression in video settings before training and inference in latent space. Many video generation models, including Latte(Ma et al., 2024c), Lavie(Huang et al., 2023b), MagicVideo(Zhou et al., 2022), Align-your-latent(Blattmann et al., 2023b), and AnimateDiff(Guo et al., 2023c), are devrived from Stable Diffusion's image 2D VAEs, as training a full 3D latent space from scratch is challenging. However, temporal compression in 2D VAE-based video models relies on uniform frame sampling, which ignores motion information, leading to low FPS and less smooth video generation.

Some approaches also start to utilize hybrid 2D-3D or fully 3D VAEs. For example, MagViT(Yu et al., 2023a), EasyAnimate(Xu et al., 2024c), Open-Sora(Zheng et al., 2024c; Lab & etc., 2024), and CogVideo-X(Yang et al., 2024j) employ hybrid 2D-3D VAEs, leveraging volumetric encoding for video generation. MAGViT(Yu et al., 2023a) adopting 3D VQGAN structures integrating both 3D and 2D downsampling, and MAGViT-V2(Yu et al., 2024b) utilizing a fully 3D VAE with 3D convolutional encoder and overlapping downsampling for enhanced spatial-temporal fidelity. HunyuanVideo(Kong et al., 2025), Kling, Mochi 1 (Team, 2024a), and SkyReels-V1(SkyReels-AI, 2025) continue leveraging 3D VAEs for compressed training in latent space in industry scenarios. Step-Video-T2V(Ma et al., 2025) and Magic-1-For-1(Yi et al., 2025) introduce novel Video VAE structures for efficient generation. However, training a video VAE independently without ensuring compatibility often leads to a latent space gap, preventing accurate projection into pixel space (Zhao et al., 2024b). CV-VAE (Zhao et al., 2024b) introduces a novel approach using latent space regularization to train a video VAE that extracts continuous latent for generative video models while maintaining compatibility with existing pretrained image and video models. Also, to trade off lower memory and computational cost with slightly lower reconstruction quality, the latest video generation model, Moive Gen(teamMeta, 2024) further uses interleaved 2D-1D convolutional encoders in its VAE. This approach balances efficiency and quality by reducing the redundancy of temporal information while maintaining spatial coherence.

2.5.4 Text encoder

In text-conditional visual generation models, the text encoder plays a crucial role in capturing semantic information from input text prompts, directly affecting the generated content. Early text-to-image models used text encoders trained on paired text-image datasets, either trained from scratch(Nichol et al., 2021; Ramesh et al., 2021) or fine-tuned from pre-trained models such as CLIP(Radford et al., 2021). CLIP, which employs contrastive learning to align text and image embedding spaces, enables the text encoder to effectively represent both visual and linguistic semantics after being trained on large-scale multimodal datasets. Once an input text prompt is tokenized and embedded, it serves as a conditioning mechanism for the diffusion model's generative backbone. CLIP-based text encoders are widely used in text-to-image diffusion models, as shown in Table 1, including DALLE-2(Ramesh et al., 2022), Stable Diffusion(Rombach et al., 2022), DiT(Bao et al., 2023a; Peebles & Xie, 2023), Fit(Lu et al., 2024c), SiT(Ma et al., 2024a), HunyuanDiT(Li et al., 2024j), and Scaling Diffusion (Esser et al., 2024; Labs, 2024). In these models, the text encoder's parameters are often frozen to reduce computational and memory overhead during training, ensuring that most training resources are allocated to the diffusion process itself.

However, CLIP often struggle with understanding detailed text descriptions. To address this, large language models (LLMs) trained on extensive text corpora provide stronger text comprehension and generation capabilities. Imagen(Ho et al., 2022a) compared CLIP with pre-trained LLMs such as BERT(Devlin et al., 2019) and T5(Raffel et al., 2020) as text encoders. Their findings showed that scaling the size of the text encoder improves the quality of text-to-image generation. Notably, (Ho et al., 2022a) found that the T5-XXL encoder significantly enhances image-text fidelity, leading to its adoption in several models such as Latte(Ma et al., 2024c), Open-Sora(Zheng et al., 2024c), and SimDA(Xing et al., 2024b). Some approaches further combine CLIP and T5 to enhance text comprehension. Step-Video-T2V(Ma et al., 2025) integrates CLIP, Step-LLM, and Video-VAE to refine alignment between textual descriptions and generated video content. To improve text encoding, ByT5(Xue et al., 2022b) introduced a byte-level tokenization-free approach, effectively handling diverse text inputs. This has been leveraged in Movie-Gen, where ByT5 combined with MetaCLIP and UL2 jointly enhances text understanding for improved video generation. Multilingual contexts also benefit from LLM-based encoders. Open-Sora-Plan (Lab & etc., 2024) incorporates multilingual T5 (mT5-XXL) alongside WF-VAE, optimizing text representations for video synthesis across diverse linguistic structures. Recent image(Tan et al., 2024c; Team, 2024b) and video(Yang et al., 2024j; Yi et al., 2025), generation models employ large language models such as Baichuan(Yang et al., 2023a), Llama(Touvron et al., 2023a;b), and ChatGLM(Du et al., 2021) to enhance the semantic understanding of complex text. SkyReels-V1(SkyReels-AI, 2025) and HUnyuanVideo(Kong et al., 2025) further integrate pre-trained Multimodal Large Language Model (MLLM) as their text encoders to enhance visual-text alignment and improve instruction adherence in diffusion models.

3 Implementation

In this part, we present a detailed analysis of the datasets, training engineering techniques, and evaluations of video generation.

3.1 Datasets

In this part, we review the most popular datasets used for video generation, as summarized in table 2. Specifically, we split the datasets into academic and commercial datasets.

Academic benchmark datasets. As a long-standing problem, there exist numerous traditional text-to-video benchmark datasets, such as MSR-VTT (Xu et al., 2016), DiDeMo (Hendricks et al., 2017), LSMDC (Rohrbach et al., 2015), and VATEX (Wang et al., 2019), which consist of videos and corresponding captions collected from the real world or annotators. However, those datasets are always small, low quality, and cover only a small number of different areas, such as sports, cooking, and movies.

Building upon those traditional benchmark datasets, researchers have recently introduced datasets (Sanabria et al., 2018; Zellers et al., 2021; Lee et al., 2021; Chen et al., 2024c; Ju et al., 2024) with a large number of videos. For example, YT-Temporal-180M (Zellers et al., 2021) contains 180M videos collected from YouTube. InternVid (Wang et al., 2023h) takes over 7 million videos lasting nearly 760K hours, yielding 234M video clips accompanied by detailed descriptions of a total of 4.1B words. Also, researchers noticed that video quality, such as resolution, is also important. Inter4k-1k (Stergiou & Poppe, 2023), as a pioneer, introduces 1k videos with a resolution of 4k, enabling the understanding and generation of high-resolution videos.

On the other side, as manually collecting datasets is time-consuming and expensive, researchers started to generate datasets using off-the-shelf models. VidProM (Wang & Yang, 2024) contains 1.67 million unique text-to-video prompts generated by Pika, VideoCraft2 (Chen et al., 2024a), and Text2Video-Zero (Khachatryan et al., 2023).

On the other side, other researchers focus on providing comprehensive video generation benchmark datasets (Huang et al., 2024a; Wang & Yang, 2024) from different perspectives, *e.g.*, temporal consistency, style consistency, semantic consistency, and video quality. VBench takes 100 prompts to evaluate video generation models from different perspectives. FETV (Liu et al., 2023e) reuses the texts from the MSR-VTT test set and WebVid for open-domain text-video pairs, guaranteeing the diversity of prompts. It also contains manually written prompts describing scenarios that are unusual in the real world, and cannot be found in existing text-video datasets.

Except for the benchmark dataset for video generation, there are also some datasets targeting face video generation, video inpainting, and video restoration. For example, VFHQ (Xie et al., 2022) is proposed for the face super-resolution, which contains over 16, 000 high-fidelity clips of diverse interview scenarios.

Commercial benchmark datasets. There are also some companies providing high-quality image/video-text paired data such as Pond5, Adobe Stock, Shutterstock, Getty, Coverr, Videvo, Depositphotos, Storyblocks, Dissolve, Freepik, Vimeo, and Envato, which are widely used in training video generation methods (Zheng et al., 2024c).

3.2 Training engineering

A comprehensive pipeline for data curation, preprocessing, and training is needed to train a large foundation model for video generation. In this part, we present an overview of data preprocessing, training techniques, and acceleration methods.

Data preprocessing. Instead of directly using the original data from the dataset, more and more methods (Zheng et al., 2024c; Li et al., 2024j; Yang et al., 2024j; Blattmann et al., 2023a) have started to select, filter, and enhance video-text paired data before training the model as shown in fig. 5. OpenSora (Zheng et al., 2024c), as a representative open-sourced method, first splits videos into shorter clips using scene detection (Ravi et al., 2025). Later, clips are evaluated using the aesthetic and optical flow scores, and the clips with low scores are removed from training. After that, the qualified clips are captioned using machine

Datasets	Modalities	Vision	Text	Duration	Resolution	Domains	# of samples	Sources	License
Academia datasets									
UCF-101 (Soomro et al., 2012)	V, A	Real	-	AVG. 7 s	320x240	-	V (13,320)	YouTube	CC-BY
Kinetics-400 (Carreira & Zisserman, 2017)	V, A	Real	-	AVG. 10 s	-	-	V (306,245)	YouTube	-
BSCV (Liu et al., 2023c)	V	Real	-	-	480P	-	V (28 k)	-	-
VFHQ (Xie et al., 2022)	V	Real	-	-	700x700	-	V (16,827)	FFHQ, VoxCeleb1	-
DMLab-40k (Yan et al., 2023b)	V	Synthetic	-	-	-	3D Rendered	V (40 k)	-	-
Habitat (Yan et al., 2023b)	V	Synthetic	-	-	-	3D Rendered	V (200 k)	-	-
Minecraft (Yan et al., 2023b)	V	Synthetic	-	-	-	3D Rendered	V (200 k)	-	-
DEVIL (Szeto & Corso, 2022)	V	Real	-	-	-	Camera Infos	V (1,250)	Flickr	MIT
Inter4K-1k (Stergiou & Poppe, 2023)	V	Real	-	AVG. 5 s	4K	-	V (1 k)	-	-
MSR-VTT (Xu et al., 2016)	V, T, A	Real	Real	AVG. 15 s	320x240	-	T/V (10 k)	Youtube	-
DiDeMo (Hendricks et al., 2017)	V, T, A	Real	Real	AVG. 7 s	-	-	T/V (27 k)	Flickr	BSD 2-Clause
LSMDC (Rohrbach et al., 2015)	V, T, A	Real	Real	AVG. 5 s	1080p	-	T/V (118 k)	-	-
VATEX (Wang et al., 2019)	V, T, A	Real	Real	AVG. 10 s	-	-	T/V (41 k)	Youtube	CC-BY-4.0
YouCook2 (Zhou et al., 2018a)	V, T, A	Real	Real	AVG. 5 mins	-	-	T/V (14 k)	Youtube	-
How2 (Sanabria et al., 2018)	V, T, A	Real	Real	AVG. 90 s	-	-	T/V (79 k)	Youtube	Creative Commons BY-SA 4.0
ActivityNet Caption (Heilbron et al., 2015)	V, T, A	Real	Real	AVG. 120 s	-	-	T/V (100 k)	Youtube	-
VideoCC3M (Nagrani et al., 2022)	V, T, A	Real	Real	AVG. 10 s	-	-	T/V (10.3 M)	-	-
WebVid10M (Bain et al., 2021)	V, T	Real	Real	AVG. 18 s	360p	-	T/V (10.7 M)	-	AGPL-3.0
WTS70M (Stroud et al., 2021)	V, T	Real	Real	AVG. 10 s	-	-	T/V (70 M)	-	-
HowTo100M (Miech et al., 2019)	V, T, A	Real	Auto Captioning	AVG. 4 s	240p	-	T/V (136 M)	Youtube	Apache License 2.0
HD-VILA-100M (Xue et al., 2022a)	V, T	Real	Auto Captioning	AVG. 13 s	720p	-	T/V (100 M)	-	See license
YT-Temporal-180M (Zellers et al., 2021)	V, T, A	Real	Real	-	-	-	T/V (180 M)	Youtube	-
ACAV100M (Lee et al., 2021)	V, T, A	Real	Real	AVG. 10 s	-	-	T/V (100 M)	-	MIT License
Vript-400k (Yang et al., 2024a)	V, T, A	Real	Real	AVG. 11 s	720p	-	T/V (420 k)	-	-
VidProdM (Wang & Yang, 2024)	V, T	Synthetic	Real	AVG. 2 s	-	-	T (1.67 M), V (6.69 M)	-	CC-BY-NC 4.0
FETV (Liu et al., 2023e)	V, T	Real	Real	-	-	-	T (619), V (541)	MSR-VTT and WebVid	CC-BY-NC 4.0
InternVid (Wang et al., 2023h)	V, T	Real + Synthetic	Auto Captioning	AVG. 12 s	720p	-	T/V (234 M)	-	CC BY-NC-SA 4.0
AIGCBench (Fan et al., 2024)	I, V, T	Real	Real	-	-	-	T/I (2,928), T/V (1,000)	-	Apache License 2.0
AVE (Argaw et al., 2022)	V, T	Real	Real	AVG. 4 s	-	-	V (196k)	-	-
Panda-70M (Chen et al., 2024c)	V, T	Real	Auto Captioning	AVG. 9 s	720p	-	T/V (70 M)	-	See license
HD-VG-130M (Wang et al., 2024f)	V, T	Real	Auto Captioning	-	720p	-	T/V (130 M)	-	See license
MiraData-77k (Ju et al., 2024)	V, T	Real	Auto Captioning	AVG. 72 s	720p	Camera Infos	V (330 k)	-	GPL-v3
LAION-AESTHETICS 6.5+	I, T	Synthetic	Real	-	-	-	T/I (625 k)	-	-
Animate bench	I, T	Synthetic	Real	-	-	-	T/I (105)	-	Apache License 2.0
DrawBench (Saharia et al., 2022)	I, T	Real	Real	-	-	-	I/T (200)	-	-
PartiPrompts (Yu et al., 2022b)	I, T	Real	Real	-	-	-	T (1.6 k)	-	Apache License 2.0
Commercial datasets									
Midjourney-v5-1.7M	I, T	Synthetic	Real	-	-	-	T/I (1.7 M)	-	Apache License 2.0
Midjourney-Kaggle-Clean	I, T	Synthetic	Real	-	-	-	T/I (250 k)	-	ce0-1.0
Unsplash-lite	I, T	Synthetic	Real	-	-	-	T/I (250 k)	-	See license
Mixkit	V, T	Real	Real	AVG. 18 s	720p	-	T/V (1,234)	-	Commercial and non-commercial
Pixabay	I, V, T	Real	Real	AVG. 25 s	720p	-	T/V (31,616)	-	Commercial and non-commercial
Pexels-400k	V, T	Real	Real	-	720p	-	T/V (400,476)	-	MIT

Table 2: The overview of most popular datasets used in training video generation models. We also include image datasets as they are usually used in training. "I", "V", "T", and "A" represent image, video, text, and audio. Other commercial datasets include those released by Pond5, Adobe Stock, Shutterstock, Getty, Coverr, Videvo, Depositphotos, Storyblocks, Dissolve, Freepik, Vimeo, and Envato.

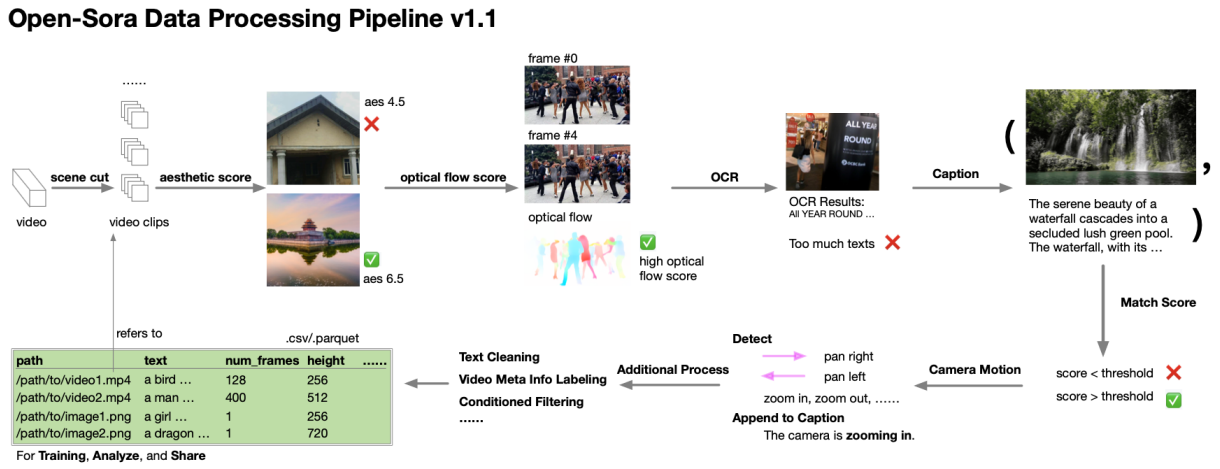

Figure 5: The data preprocessing pipeline of Open-Sora Zheng et al. (2024c).

captioners (Hong et al., 2024b; Li et al., 2025; Xu et al., 2024d) and a matching score will be employed to evaluate the alignment between clips and their captions. Finally, samples with adequate scores (high aesthetic quality, large video motion, and strong semantic consistency) are used for training the model. The overall pipeline is presented in fig. 5. Similarly, SVD (Blattmann et al., 2023a) filters out samples with low text-video alignment evaluated by CoCa (Yu et al., 2022a), static videos (evaluated by optical flow), and high text overlays.

Training techniques. Video generation models (Blattmann et al., 2023a; Zheng et al., 2024c) are usually initialized with image models and pretrained with image data. Then, the models are pretrained with video data for learning efficient video representations. After that, models are trained using high-quality data to form the final video generation models. However, due to the difficulty of the video generation problem, different training techniques (Blattmann et al., 2023a; Xing et al., 2023; Hong et al., 2023a; Yang et al., 2024j) are proposed. For example, CogVideoX (Yang et al., 2024j) employs a multi-resolution frame pack strategy to enable the generation of videos with varied lengths. And a progressive training strategy is employed to generate videos of different resolutions. On the other side, to scale up the training of video generation models, multi-node parallelization and VRAM-efficient scheduling are utilized Yang et al. (2024j); Zheng et al. (2024c).

Video generation acceleration techniques. Due to the high computational requirements of training and inferencing video generation methods, researchers have developed several acceleration techniques. For example, Open-Sora (Zheng et al., 2024c) employs flash attention (Dao et al., 2022), ZeRO (Rajbhandari et al., 2020), and gradient checkpoint for kernel optimization, hybrid parallelism, and larger batch size training. Moreover, Open-Sora employs efficient STDiT as the vision encoder while preprocessing text and video data for acceleration. On the other side, parameter-efficient fine-tuning (PEFT) (Geng et al., 2024a; Jia et al., 2022), which is widely applied in training large foundation (language and vision-language) models (Li et al., 2025; Touvron et al., 2023a;b), could be used in video generation for training acceleration (Xing et al., 2024b; Pan et al., 2022). We also include a detailed discussion on long video generation acceleration techniques in section 4.5.

3.3 Evaluation metrics and benchmarking findings

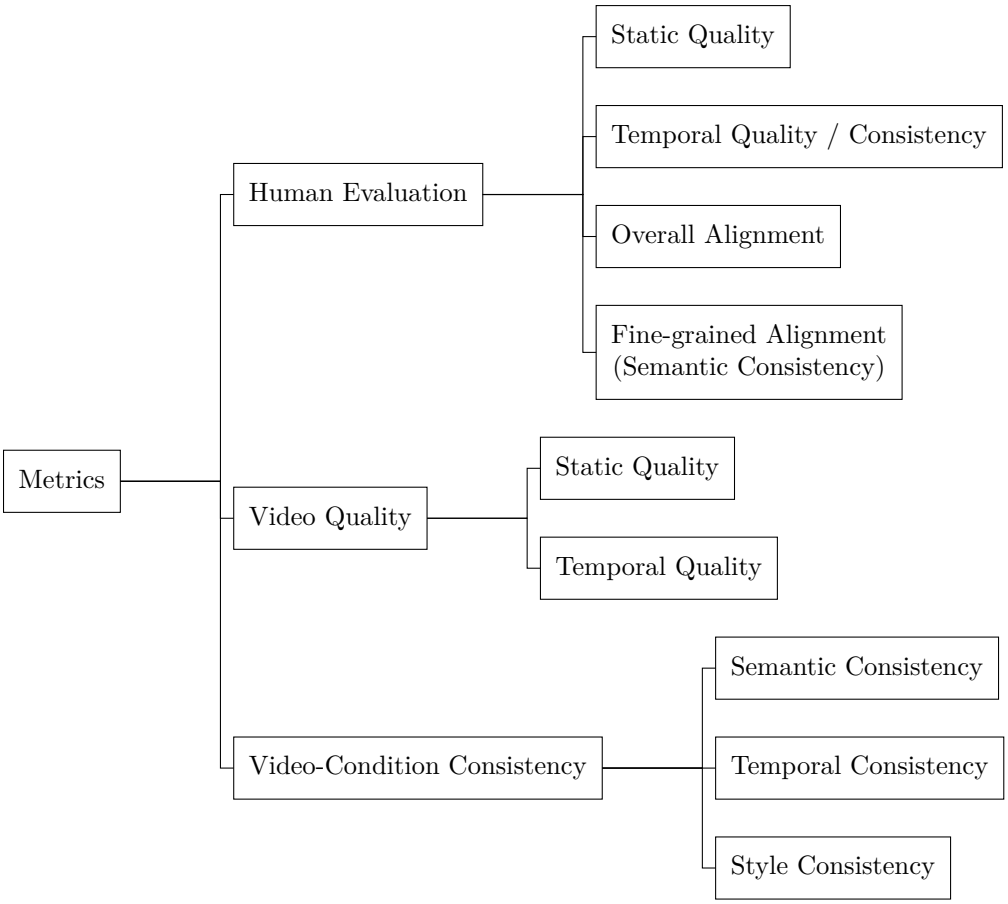

Existing evaluation metrics include human evaluation and auto evaluation. Human evaluation (Liu et al., 2023e; Huang et al., 2024a) always includes several aspects such as static quality, temporal quality (consis-

tency), overall alignment, and fine-grained alignment (semantic consistency). And human evaluation is always employed to test the alignment between auto-evaluation and human evaluators, such as VBench (Huang et al., 2024a), which uses 16 human evaluations on 16 different dimensions mainly focusing on temporal and semantic consistency. A human-verified metric is STREAM (Kim et al., 2023b), testified under the same dimensions using auto-evaluation and human evaluation.

On the other side, as auto-evaluation (Huang et al., 2024a;b; Fan et al., 2024) is cheaper and faster, it is widely applied to evaluate video quality and conditioned quality (semantic consistency and temporal consistency). Video quality usually only contains video as the input of metrics while conditioned quality also uses other modal inputs such as image, text, or audio to evaluate the generated video.

Video quality consists of static quality and temporal quality. 1) For static quality, AIGCBench (Fan et al., 2024) employs a pre-trained optical flow estimation model, *i.e.*, RAFT (Teed & Deng, 2020), and calculates the mean square of the average flow score between adjacent frames from the generated video for estimating the motion effects as Flow-Square-Mean. Dover (Wu et al., 2023a) is also employed for evaluating the static quality from aesthetic and technical perspectives. Moreover, the **number of video frames** is used for accessing the quality. On the other side, FETV (Liu et al., 2023e) employs FID (Heusel et al., 2017) and FVD (Unterthiner et al., 2019) metrics. 2) For temporal quality, AIGCBench assesses it by calculating the average similarity between adjacent frames using CLIP (Radford et al., 2021) noted as GenVideo Clip (Adjacent frames). VBench (Huang et al., 2024a) evaluates it by subject, background, temporal flickering, motion, dynamic degree, aesthetic quality, and imaging quality using multiple pre-trained models including DINO, CLIP, Amt, RAFT, and LAION. Bonneel et al. (2015) proposes a warping error for improving the consistency between frames. Except for those methods, STREAM (Kim et al., 2023b) is proposed to avoid the problem of FVD, which has a stronger emphasis on the spatial aspect than the temporal naturalness of video and demonstrates considerable instability and diverges from human evaluations. It evaluates temporal and semantic quality at the same time.

The metrics for evaluating conditioned quality can be categorized into semantic consistency, temporal consistency, and style consistency. 1) In semantic consistency, for image/video-video metrics, AIGCBench (Fan et al., 2024) employs Mean Squared Error (MSE First) and Structural Similarity Index Measure (SSIM First) for evaluating the first generated frames. To further understand how the semantics are preserved across frames, AIGCBench calculates the cosine similarity between the input image and each frame of generated video using CLIP (Image-GenVideo CLIP). Moreover, GenVideo-RefVideo SSIM is also employed to measure the spatial structural similarity of the generated videos to the reference videos by calculating the SSIM (Structural Similarity Index Measure) between the corresponding frames of the generated and reference videos as the referenced video is at hand. For Text-to-Video metrics, AIGCBench employs GenVideo-Text Clip and GenVideo-RefVideo CLIP (Keyframes), calculating the similarity between the input text / referenced video and keyframes from generated videos using CLIP. Similar to AIGCBench, FETV (Liu et al., 2023e) propose to use stronger models, such as CLIP finetuned on MSR-VTT, BLIP, and UMP, and VQA models for evaluating the semantic consistency. Moreover, FETV also introduces a novel QA-based metric (Otter-VQA). This metric generates yes-no questions on key elements from the text prompt via the Vicuna model and calculates the average number of questions that receive a positive answer by feeding the generated (or ground-truth) videos and questions into the Video LLM as the score. VBench (Huang et al., 2024a) evaluates the semantic consistency by objects, humans, color, relationships, scene, appearance, and temporal style using ViCLIP, CLIP, Tag2Text, UMT, and GRiT. 2) For temporal consistency, researchers usually directly employ the temporal quality metrics. Recently, TC-bench Feng et al. (2024c) proposed to focus on the transition of objects, relations, and background for better temporal consistency. 3) For style consistency, VBench employs CLIP and ViCLIP to assess the similarity between generated videos and the style description.

Except for those metrics, VBench (fig. 6) and Video Generation Arena also set up online evaluation platform, providing an accessible leaderboard for researchers.

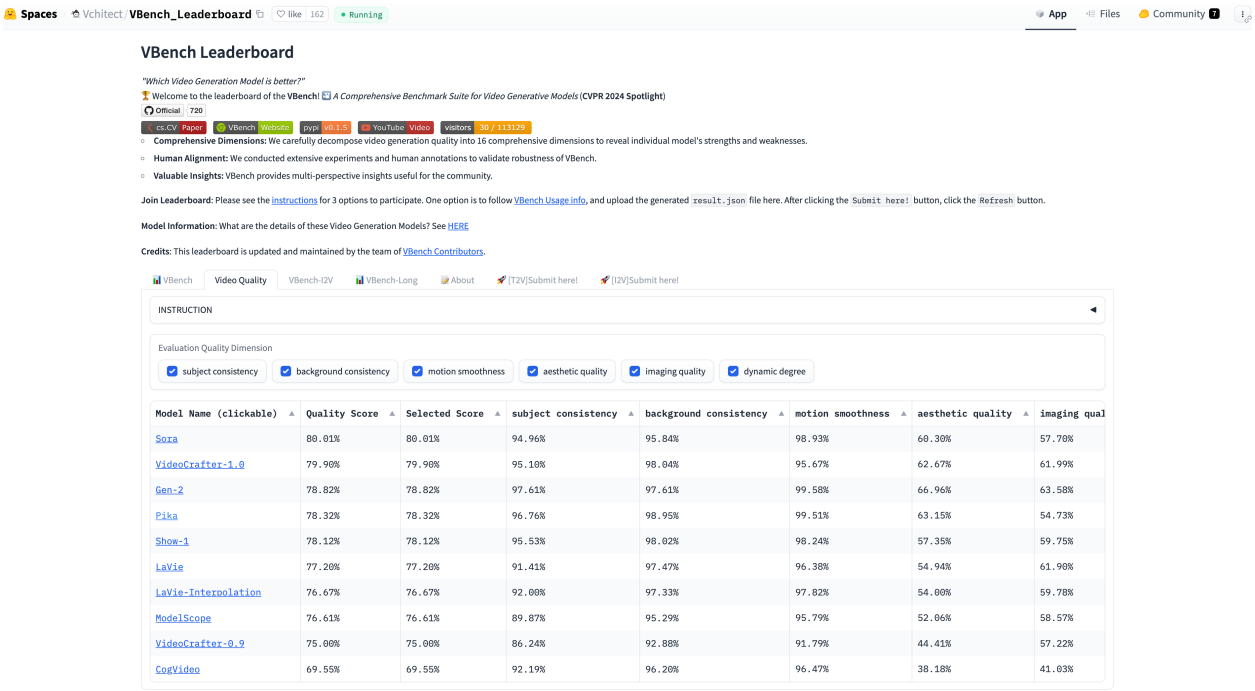

Spaces Vchitect / VBench_Leaderboard like 162 Running App Files Community 7

VBench Leaderboard

"Which Video Generation Model is better?"

Welcome to the leaderboard of the **VBench**! *A Comprehensive Benchmark Suite for Video Generative Models* (**CVPR 2024 Spotlight**)

Official 720

cs.CV Paper VBench Website pypi v0.1.5 YouTube Video visitors 30 / 113129

- **Comprehensive Dimensions:** We carefully decompose video generation quality into 16 comprehensive dimensions to reveal individual model's strengths and weaknesses.
- **Human Alignment:** We conducted extensive experiments and human annotations to validate robustness of VBench.
- **Valuable Insights:** VBench provides multi-perspective insights useful for the community.

Join Leaderboard: Please see the instructions for 3 options to participate. One option is to follow VBench Usage info, and upload the generated `result.json` file here. After clicking the `Submit here!` button, click the `Refresh` button.

Model Information: What are the details of these Video Generation Models? See HERE

Credits: This leaderboard is updated and maintained by the team of VBench Contributors.

VBench | Video Quality | VBench-I2V | VBench-Long | About | [T2V]Submit here! | [I2V]Submit here!

INSTRUCTION

Evaluation Quality Dimension

subject consistency | background consistency | motion smoothness | aesthetic quality | imaging quality | dynamic degree

Model Name (clickable)	Quality Score	Selected Score	subject consistency	background consistency	motion smoothness	aesthetic quality	imaging qual
Sora	80.01%	80.01%	94.96%	95.84%	98.93%	60.30%	57.70%
VideoCrafter-1.0	79.90%	79.90%	95.10%	98.04%	95.67%	62.67%	61.99%
Gen-2	78.82%	78.82%	97.61%	97.61%	99.58%	66.96%	63.58%
Pika	78.32%	78.32%	96.76%	98.95%	99.51%	63.15%	54.73%
Show-1	78.12%	78.12%	95.53%	98.02%	98.24%	57.35%	59.75%
LaVie	77.20%	77.20%	91.41%	97.47%	96.38%	54.94%	61.90%
LaVie-Interpolation	76.67%	76.67%	92.00%	97.33%	97.82%	54.00%	59.78%
ModelScope	76.61%	76.61%	89.87%	95.29%	95.79%	52.06%	58.57%
VideoCrafter-0.9	75.00%	75.00%	86.24%	92.88%	91.79%	44.41%	57.22%
CogVideo	69.55%	69.55%	92.19%	96.20%	96.47%	38.18%	41.03%

Figure 6: The VBench leader board at Feb. 3rd, 2025. SORA still scores the highest on some of the metrics, *e.g.*, quality score and selected score.

3.4 Industry solutions

As shown Backbone column in Table 1, video generation industry has evolved significantly with the adoption of diffusion models that leverage advanced architectures like DiT, UNet, and U-ViT. DiT (Diffusion Transformer) is widely used in models like W.A.L.T(Gupta et al., 2023), MovieGen, Kling, and Mochi 1(Team, 2024a), excelling in capturing long-range dependencies for sharp, coherent visuals in video generation tasks. UNet, utilized in models like Imagen video, Lavie(Wang et al., 2023g), Seine(Chen et al., 2024d), and VLogger(Zhuang et al., 2024), is known for its ability to handle both local and global features, making it ideal for high-resolution video generation. U-ViT (U-Transformer for video) is another backbone seen in models like VideoCrafter1(Chen et al., 2023a) and VideoCrafter2(Chen et al., 2024a), effective at processing both spatial and temporal dependencies for more accurate video generation. These architectures continue to shape the industry's approach to advanced video generation.

Variational Autoencoders (VAE) are widely used in industry to learn latent video representations. As shown VAE column in Table 1, models such as HunyuanVideo(Kong et al., 2025), Mochi 1(Team, 2024a), and Kling utilize 3D VAE for temporal consistency. On the other hand, models like Lavie(Wang et al., 2023g) and Phenaki(Villegas et al., 2022) utilize 2D VAEs, which offer greater computational efficiency but are less effective at capturing the temporal dynamics of video content. Meanwhile, VQ-VAE, used in models like VLogger(Zhuang et al., 2024) and Vchitect-2.0, introduces vector quantization to improve efficiency by discretizing the latent space. Additionally, Video VAE architectures, such as in VideoCrafter(Chen et al., 2023a) and LTX-Video(HaCohen et al., 2024), are specifically designed for video generation, optimizing the ability to handle both spatial and temporal complexities. The choice of VAE architecture thus directly influences the quality, efficiency, and temporal coherence of video generation.

Text encoders, such as T5-XXL, are essential for aligning video with textual descriptions. Based on the column text encoder in the Table 1, models like Imagen video, W.A.L.T.(Gupta et al., 2023), and MovieGen use T5-XXL for precise video-text alignment, enhancing generative capabilities. Meanwhile, models like Lavie(Wang et al., 2023g) and Seine(Chen et al., 2024d) leverage CLIP-based encoders, which offer flexibility

for generating both short clips and full-length videos. T5-XXL excels in large-scale generation, while CLIP provides versatility for diverse visual styles and content.

The scale of models varies, as shown in the parameter column of Table 1, with larger models like Sora (with $\sim 30B$ parameters) and MovieGen (with $\sim 30B$ parameters) offering scalability for large-scale production. Smaller models including Vchitect-2.0 and VideoPoet maintain strong performance while using fewer parameters (1B–2B) to balance performance and computational cost.

Training datasets such as WebVid-10M(Bain et al., 2021) and Vimeo25M(Huang et al., 2023b) are commonly used for large-scale models like Seine(Chen et al., 2024d), Lavie(Wang et al., 2023g) and Show-1 from Table 1, ensuring diverse outputs. Models including Lumiereand VideoPoet choose to gather video and image data directly from public websites, rather than relying on pre-existing datasets.

Resolution plays a key role in video output quality. As shown in the resolution coulmn in the Table 1, GEN-3 Alpha and Sora support high resolutions like 4090×2160 and 1920×1080, ideal for cinematic production. In contrast, models like Seine(Chen et al., 2024d) and Phenaki(Villegas et al., 2022) offer lower resolutions like 320×512 or 64×64, balancing quality and computational efficiency.

Video duration is also a key consideration. Based on the duration column in the Table 1, W.A.L.T(Gupta et al., 2023) and VLogger(Zhuang et al., 2024) excel in generating short-duration videos for platforms such as social media, while models such as Kling and Mira are capable of creating longer videos, suited for film production or extended content.

GPU requirements for training and inference vary. As shown in the GPU size and GPU hours column in the Table 1, Large models such as Show-1 and MovieGen need substantial GPU resources, with Show-1 requiring around 48 A100 GPUs. Smaller models like LTX-Video(HaCohen et al., 2024) can achieve faster processing, offering practical real-time video generation for commercial use.

The video generation industry continues to grow with models such as MovieGen and Sora catering to high-end production, while consumer-focused models like VLogger(Zhuang et al., 2024) and EasyAnimate (Xu et al., 2024c) offer fast solutions for short-form video content. The challenge remains to optimize video quality while managing computational resources for broader accessibility.

4 Applications

4.1 Conditions

In this section, we examine a variety of "conditions" that researchers use to guide the video generation process. Unlike purely unconditional or text-based generation, which can lack specific control or produce unsatisfactory temporal consistency, leveraging additional forms of conditioning provides more precise and robust ways to steer the synthesis. These conditions can stem from many sources—images, spatial constraints, camera parameters, audio signals, high-level editing instructions, or even physical simulations—and can serve different roles, from specifying global traits like style and identity to prescribing detailed frame-by-frame motion.

We organize these conditions into subtopics based on the type of guidance they offer. First, we discuss image-based methods (Image condition 4.1.1), where a single reference image or a sequence of images conveys both coarse semantic cues and fine-grained details for video generation. We then explore spatial conditions (Spatial condition 4.1.2), such as trajectories, bounding boxes, or scene layouts, which grant users exact control over object movement and scene composition. Next, we address camera parameter inputs (Camera parameter condition 4.1.3) for 3D-consistent view synthesis and cinematic manipulation. We also cover audio-based approaches (Audio condition 4.1.4) for synchronizing speech, music, or other sound cues with visual content. Finally, we examine methods that focus on high-level editing (High-level video condition 4.1.5) and specialized application constraints (Other conditions 4.1.6), including incorporating physics-based realism, working with physiological signals, and utilizing timestamp information as conditions. Through these diverse forms of conditioning, researchers aim to create video generation systems that balance creative freedom with strong user control, opening the door to a wide range of potential applications.

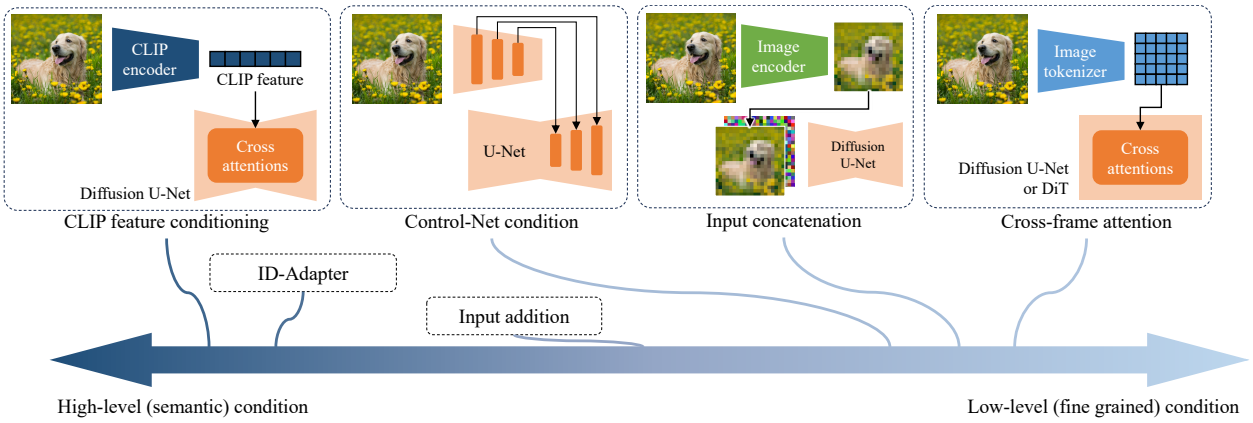

Figure 7: Methods for controlling video generation using image-based conditions. We categorize these methods along a spectrum ranging from high-level semantic conditions to low-level conditions. Additionally, we illustrate four classic approaches commonly used to condition input images.

4.1.1 Image condition

Controlling video generation with images is a crucial capability, as images offer visually intuitive and fine-grained control over content that text alone cannot achieve. This functionality serves as a foundational building block for various video applications, such as identity-preserving video generation and image animation.

Depending on how the conditioning image is integrated into the diffusion model, the methods can be broadly categorized into two types: semantic-level image conditioning and fine-grained image conditioning.

Semantic-level conditioning. Similar to text-conditioned video diffusion, semantic-level image conditioning provides high-level coarse guidance for video generation. This is typically achieved by encoding the input image into a low-dimensional feature that retains rich semantic information, such as identity. These features are then fed into the video model through cross-attention layers in a manner similar to how text embeddings are incorporated into the network. For instance, DreamVideo (Wei et al., 2024c) employs an identity adapter to encode the identity of the conditioning image, while ID-Animator (He et al., 2024d) uses a face adapter to capture the facial identity of a human face. Additionally, CLIP features are commonly utilized to extract global information from the image, which is then used to condition video generation (Zhang et al., 2023d; Xing et al., 2023; Wang et al., 2023e; Xu et al., 2024b; Jiang et al., 2024b; Zhao et al., 2024a).

Fine-grained-level conditioning. High-level control is not always desirable. In some cases, we aim to fully control every detail of the generated video. At the extreme, fine-grained conditioning means the conditioning image directly corresponds to one of the frames in the generated video. This is achieved by exposing the network to the fine-grained features of the conditioning image.

The most straightforward approach is to concatenate the image (or its latent representation) with the noise input. This concatenation typically occurs along the channel axis, with the conditioning image often serving as the first frame of the training video. This approach is widely adopted in many video generation models, including SVD (Blattmann et al., 2023a), VDT (Lu et al., 2024a), Motion I2V (Shi et al., 2024), AtomoVideo (Gong et al., 2024), and CogVideoX (Yang et al., 2024j). Since the model predicts multiple frames simultaneously and the conditioning image is usually a single frame, the image can either be repeated across all frames or temporally padded with black pixels, accompanied by an additional mask channel to indicate the validity of the condition for each frame. Notably, this concatenation-based approach is also widely used in image generation Brooks et al. (2023); Ke et al. (2024); Zeng et al. (2024c); He et al. (2024c).

Concatenation can also be done along the temporal axis (Shi et al., 2024; Ma et al., 2024b; Zhang et al., 2024i; Gu et al., 2024a; Dai et al., 2023), where the conditioning image is explicitly set as the first frame of the predictions. This method avoids the need for modifications to the model architecture.

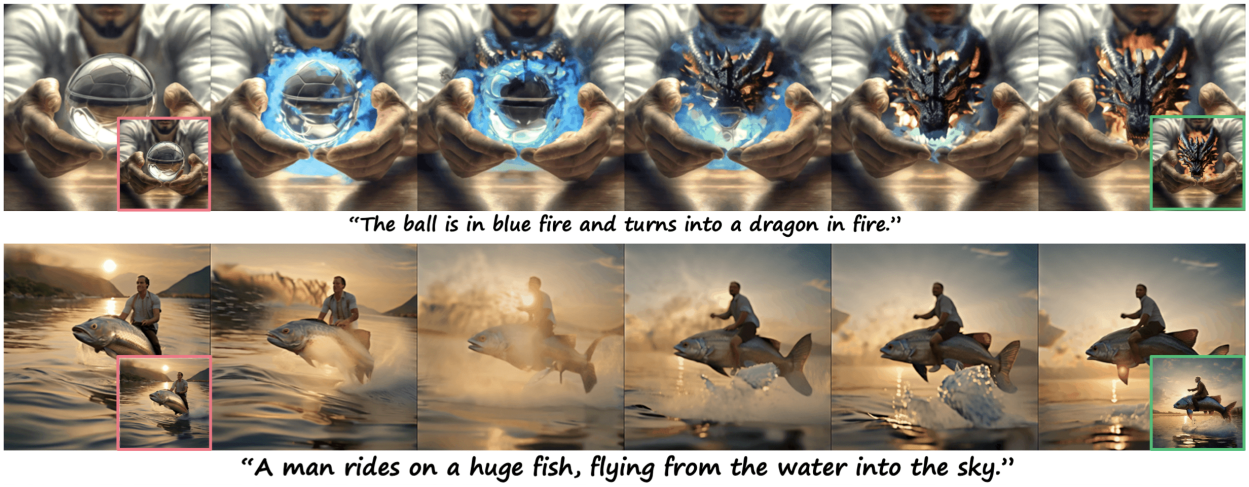

Figure 8: Make Pixel Dance Zeng et al. (2024a) shows that by conditioning both on the first and last frame, the model implicitly learns to generate large-scale motion.

While concatenation is often used for conditioning on the first frame, Make Pixel Dance (Zeng et al., 2024a) demonstrates that conditioning on both the first and last frames enables the model to implicitly learn large-scale motion generation, as shown in Fig. 8

MagDiff (Zhao et al., 2024a) designs a pyramid structure to encode conditioning images, effectively capturing contextual information at multiple scales and enhancing the robustness of the input.

PIA (Zhang et al., 2023f) introduces a plug-and-play image conditioning approach that enables seamless conditioning across various personalized text-to-image models without the need for fine-tuning. This is achieved by non-invasively injecting conditioning features into the first convolutional layer of the U-Net.

Image conditioning can also be implemented using a ControlNet-like approach (Zhang et al., 2023b). For instance, DreamVideo (Wang et al., 2023a) incorporates image conditioning by forwarding the conditioning image through the downsampling blocks of the diffusion U-Net and injecting the resulting intermediate feature maps into the video model. Similarly, SparseCtrl (Guo et al., 2024b) employs a ControlNet-like structure but extends it to support temporally sparse conditions, enabling the use of one or more frames as conditioning inputs.

I2V-Adapter (Guo et al., 2023b) highlights a potential challenge of concatenating: when fine-tuning a video model initialized from a text-to-video model, directly concatenating the input image can disrupt the fundamental weights. To address this, they propose cross-frame attention mechanisms to enhance the image condition. Specifically, additional cross-frame attention layers are introduced after each self-attention layer, where keys and values are derived from the first frame, and learned queries target each output frame. This architecture is later adopted in EMO (Tian et al., 2024). VideoCrafter (Chen et al., 2023a) also use cross attentions for image conditioning, but uses an additional projection network to align the image embeddings with text embeddings.

Moreover, with the incorporation of optical flow, image conditions can be utilized more explicitly. By warping the image features using optical flow and decoding the warped image, the generated frames effectively "copy" information from specific locations in the conditioning image. This approach is employed in several flow-based video generation methods (Ni et al., 2023; Li et al., 2024i).

Multi-level condition. Semantic-level and fine-grained conditions are often combined to achieve more robust and precise control. For instance, both concatenation and CLIP feature cross attention can be integrated into the U-Net together to improve conditioning consistency (Xu et al., 2024b; Xing et al., 2023;

Zhang et al., 2023d), VideoBooth (Jiang et al., 2024b) combines CLIP feature cross-attention with image latent cross-frame attention to provide a balance of coarse guidance and fine detail control.

VideoComposer (Wang et al., 2023e) controls the details of generated videos by employing a Spatio-Temporal Condition Encoder, which encodes various modalities, such as images, sketches, depth maps, and edge maps. Simultaneously, it leverages the CLIP embedding of an image to control the style of the generated video.

ConsistI2V (Ren et al., 2024) enhances image conditioning by integrating multiple branches that support both coarse and fine control. These include noise concatenation, image cross-attention, and temporal attention. Additionally, it introduces layout control by using the low-frequency components of the input image as noise initialization for the video generation process.

4.1.2 Spatial condition

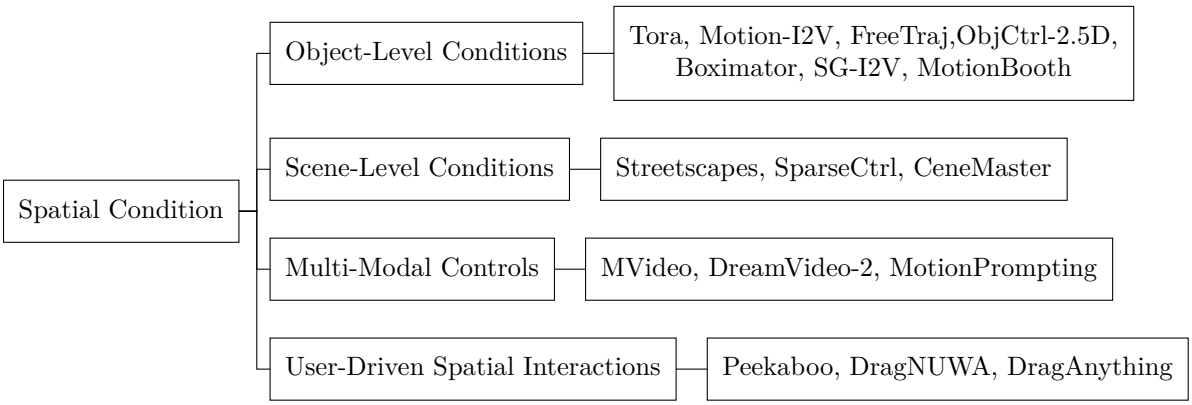

Spatial-conditioned video generation leverages explicit spatial information and constraints to guide the synthesis process, granting users greater control over the layout, movement, and dynamics of video elements. These spatial conditions may appear at multiple levels of granularity—from direct object trajectories and manipulations to structural guidance via depth maps or scene layouts—and can be combined with other modalities to ensure coherence and consistency. Ultimately, spatial conditions form the backbone for controlling motion, be it object-level movement or global camera transitions, resulting in videos that more faithfully align with user intent.

Object-level conditions. This category emphasizes controlling the motion and placement of individual objects, often through explicit trajectory specification. Such approaches give users fine-grained command over how objects appear and move throughout the generated scene.

Early examples include Tora (Zhang et al., 2024g), which enables users to input detailed trajectories for multiple objects, resulting in high-fidelity, multi-object videos that precisely follow the prescribed paths. Similarly, Motion-I2V (Shi et al., 2024) accepts sparse trajectory annotations and motion brushes directly on a reference image, ensuring temporal consistency and accurate object-level motion control.

Building upon these ideas, FreeTraj (Qiu et al., 2024a) supports free-form, user-defined trajectories to guide object motion, allowing flexible and intuitive spatial control. By integrating trajectory information into latent space features and employing temporal consistency modules, FreeTraj ensures seamless motion across frames while maintaining coherent scene appearances. Taking this concept further, ObjCtrl-2.5D (Wang et al., 2024i) introduces object-centric trajectory control in a 2.5D latent space. Users can define paths—including rotations, translations, and interactions—across multiple objects. With techniques like keyframe-based interpolation and motion-aware attention, ObjCtrl-2.5D guarantees spatial fidelity and smooth transitions.

Beyond trajectory drawing, object localization methods also facilitate spatial conditioning. Boximator (Wang et al., 2024d) allows users to control object positions through bounding boxes, incorporating a self-tracking mechanism to maintain motion coherence without retraining. Similarly, SG-I2V (Namekata et al., 2024) introduces a training-free approach that leverages bounding boxes and user-defined trajectories in an image-to-video diffusion pipeline. By aligning self-attention feature maps across frames and applying frequency-

based post-processing, SG-I2V enforces temporal consistency, preserves high-frequency details, and enables precise zero-shot motion control without additional fine-tuning. Such bounding-box-based approaches complement trajectory-driven methods, offering additional avenues for achieving granular and visually consistent object movements. Additionally, MotionBooth (Wu et al., 2024c) fine-tunes text-to-video (T2V) models for subject-level control, introducing tailored losses (e.g., subject region and subject token cross-attention losses) that preserve object identity while enabling flexible subject movement. Its training-free "motion injection" allows users to define unique object trajectories on the fly with minimal overhead, maintaining fidelity to the customized subject's appearance even under significant motion changes.

Scene-level conditions. While object-level conditions dictate the movement of individual elements, scene-level constraints shape the overall layout, geometry, and camera perspective. Methods like Streetscapes (Deng et al., 2024a) rely on street maps, height maps, and camera trajectories to ensure spatial coherence and temporal stability in city-scale videos. SparseCtrl (Guo et al., 2024b) uses sparse sketches or depth maps at keyframes to propagate structural guidance through the sequence, reducing the need for dense inputs while maintaining spatial fidelity. CineMaster (Wang et al., 2025) further emphasizes 3D-aware scene manipulation by integrating precise 3D bounding box placement, flexible object and camera motion, and interactive layout control into a two-stage workflow.

Multi-modal controls. A natural extension of spatial conditioning involves integrating other modalities, such as text, images, or optical flow, to provide more holistic guidance. MVideo (Zhou et al., 2024a) fuses semantic (textual) and spatial (image and trajectory) inputs, employing motion-aware attention mechanisms to ensure that these heterogeneous signals inform both appearance and temporal dynamics, thus allowing for richer and more contextually grounded video generation.

By combining spatial and trajectory conditions, methods can align object movements and appearances across time. DreamVideo-2 (Wei et al., 2024c) exemplifies this synergy by using a dual-stream diffusion architecture. Its Appearance Stream preserves spatial features while a Motion Stream enforces trajectory-based temporal dynamics. Optical flow maps and frame-wise image conditioning further ensure spatial consistency. Similarly, MotionPrompting (Geng et al., 2024b) maps explicit motion prompts—representing object or camera trajectories—into latent space and refines them through a two-stage generation process, achieving both stable global motion patterns and precise spatial fidelity.

User-driven spatial interactions. Beyond automated integration of spatial cues, several works empower users to interactively manipulate scene content. Peekaboo (Wu et al., 2020) enables direct control over object placement and movement via spatial and temporal masks, offering flexible adjustments without retraining the model. DragNUWA (Yin et al., 2023a) allows users to guide arbitrary object movements and camera shifts by combining trajectories with textual and image inputs, unlocking complex video editing through multi-modal manipulation. Extending this idea further, DragAnything (Wu et al., 2024f) leverages draggable points on objects so users can intuitively reposition and pose them across frames, enhancing interactivity and customization within video diffusion frameworks.

In essence, spatial conditions and motion controls are tightly interconnected. Specifying spatial guidance through trajectories, bounding boxes, scene layouts, or depth maps sets the stage for orchestrating how objects and viewpoints evolve over time. By blending object-level trajectories, scene-scale structures, and interactive user cues, these methods collectively push toward more controllable and user-aligned video generation.

4.1.3 Camera parameter condition

Camera parameter conditioning, which precisely manipulates camera poses and trajectories, is crucial for achieving realistic 3D consistency in video generation. Equally important is local object motion control—defining how specific entities move within the scene—so that the overall dynamic is both coherent and visually compelling. Recent works interweave these two aspects, providing new ways to blend cinematographic flexibility with targeted motion editing.

Methods like CameraCtrl (He et al., 2024a) rely on camera pose and trajectory inputs to guide video generation with geometric representations and temporal attention, allowing creators to simulate dynamic

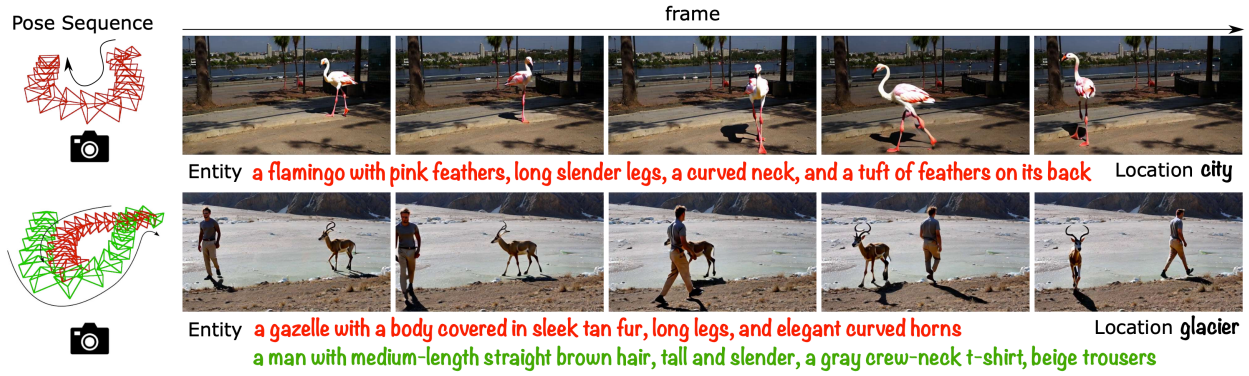

Figure 9: An example of integrating camera poses and object motion control for video generation (Fu et al., 2024).

viewpoints for virtual reality and film production. Extending these ideas, CVD (Kuang et al., 2024) enforces epipolar constraints to maintain geometric and motion consistency across multiple perspectives. Further exploring 3D constraints, CamCo (Xu et al., 2024b) adopts Plücker coordinates to ensure coherent epipolar geometry, while Cavia (Xu et al., 2024a) employs cross-view and cross-frame attention layers to align spatial and temporal cues in multi-view videos. VD3D (Bahmani et al., 2024d) uses scene representations like depth maps or NeRF, merging appearance and geometry streams for more realistic 3D effects, and AC3D (Bahmani et al., 2024b) integrates Plücker coordinates with hierarchical training and cross-frame attention to manage complex motions across multiple viewpoints. Augmenting these efforts, MotionBooth (Wu et al., 2024c) introduces a lightweight latent shift module for training-free camera motion control, synchronizing smooth camera movements with subject fidelity via concise loss functions and attention alignment. For more in-depth discussion on camera conditioning, please refer to Sec. 4.6.3.

On the object motion side, various approaches link bounding-box–level or trajectory-based editing to camera control for deeper storytelling. Direct-A-Video (Yang et al., 2024i) allows users to specify camera movements such as panning or zooming alongside simple bounding-box manipulation for objects, removing the need for explicit motion annotations. MotionCtrl (Wang et al., 2024j) goes further by letting users provide detailed trajectory paths for both objects and the camera, integrating these into a diffusion-based model to achieve precise movements and strong frame-to-frame consistency. Likewise, 3DTrajMaster (Fu et al., 2024) incorporates 6DoF pose sequences for multi-entity 3D motion control, using a 3D-motion–grounded injector architecture that fuses text and pose embeddings and a gated attention mechanism within a diffusion pipeline. CineMaster (Wang et al., 2025) further couples bounding-box–based object manipulation with camera parameter specification in a two-stage pipeline. A Blender-based interface collects 3D bounding boxes and camera trajectories, which are automatically interpolated before guiding a specialized diffusion model that disentangles camera from object motion for enhanced 3D alignment. By merging camera parameters with object trajectories, these methods deliver more comprehensive control over how scenes unfold, enabling cohesive, lifelike video generation.

4.1.4 Audio condition

Audio conditions enable synchronization between sound and visuals, crucial for applications like talking head generation and co-speech gesture animation. By leveraging audio inputs, models generate videos that reflect the nuances of speech, emotion, and rhythm inherent in the audio signal.

Several works have focused on generating expressive talking head videos synchronized with speech. EMO (Tian et al., 2024) conditions video generation on audio input and a single reference image, using facial bounding box masks and head movement speed as weak conditions. By integrating audio features

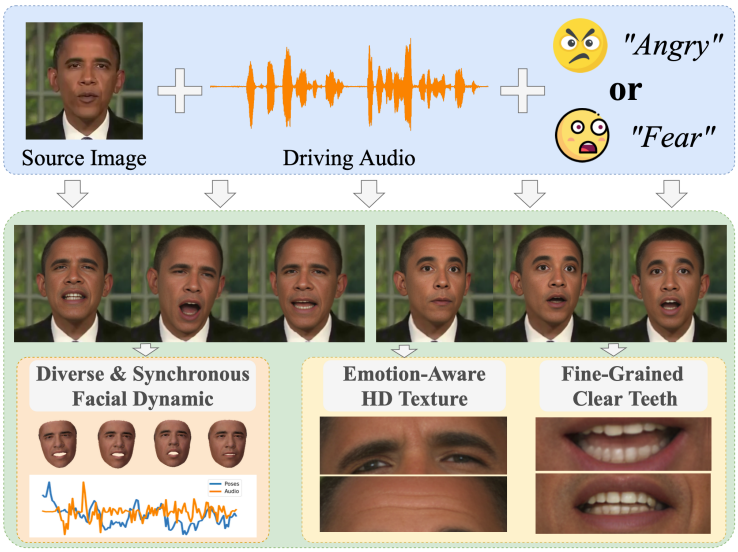

Figure 10: In audio-conditioned video generation, in conjunction with traditional conditions (e.g., image, text), audio information is usually adopted to augment synchronization with talking motion (facial expressions, head movements, lip and teeth dynamics) to create a more realistic and emotionally expressive animation (Tan et al., 2024a).

from pretrained models like wav2vec into a diffusion-based framework, EMO synchronizes facial expressions and lip movements with the input audio, capturing emotional tones.

Similarly, VASA-1 (Xu et al., 2024e) and DreamTalk (Ma et al., 2023) utilize audio features extracted with wav2vec models to generate talking face videos. VASA-1 incorporates audio features from previous frames to maintain temporal consistency, employing classifier-free guidance for motion generation. DreamTalk uses a transformer-based audio encoder to process audio windows, producing synchronized lip movements and expressions with the help of a lip synchronization expert and a style predictor. Speech2Lip (Wu et al., 2023e) builds on these ideas by adopting a decomposition-synthesis-composition strategy, where a speech-driven implicit model focuses on lip movement in a canonical space while a geometry-aware mapping (GAMEM) handles pose variability for speech-insensitive elements like head movements. A contrastive sync loss further boosts synchronization quality, even with limited training data, yielding sharper visuals and more accurate lip alignment than previous methods. Expanding beyond facial animations, ANGIE (Liu et al., 2022b) addresses co-speech gesture generation by learning motion representations through unsupervised learning. It constructs codebooks of reusable gesture patterns and predicts future motions based on quantized motion codes and audio inputs, resulting in natural gesture animations synchronized with speech. Similarly, OmniHuman (Lin et al., 2025) extends audio-driven generation for more comprehensive human animation tasks such as full-body movements and human-object interactions, leveraging a multi-condition training strategy (text, audio, and pose) in a progressive manner, and delivers realistic motion synthesis and robust lip-sync accuracy.

For emotional expressiveness, EMOPortraits (Drobyshev et al., 2024) integrates a speech-driven mode into one-shot head avatar synthesis, using a multi-view dataset of extreme facial expressions (FEED) to generate highly expressive facial animations driven by audio inputs. FlowVQTalker (Tan et al., 2024a) combines normalizing flow and vector quantization to model and generate emotional talking face videos, predicting facial dynamics using audio inputs, a source image, and an emotion label.

To capture subtle expressions and head movements, AniTalker (Liu et al., 2024d) and AniPortrait (Wei et al., 2024a) utilize motion representations learned through self-supervised learning. AniTalker introduces a variance adapter to synthesize speech with controlled attributes, serving as input to a diffusion-based motion generator. AniPortrait employs a two-stage method, obtaining 3D representations from audio inputs and converting them into high-quality portrait animations using a diffusion model.

Additionally, CCVS (Le Moing et al., 2021) (Context-aware Controllable Video Synthesis) incorporates audio tracks as ancillary information to influence the video's rhythm and mood, maintaining temporal coherence by utilizing context frames and object trajectories.

4.1.5 High-level video condition

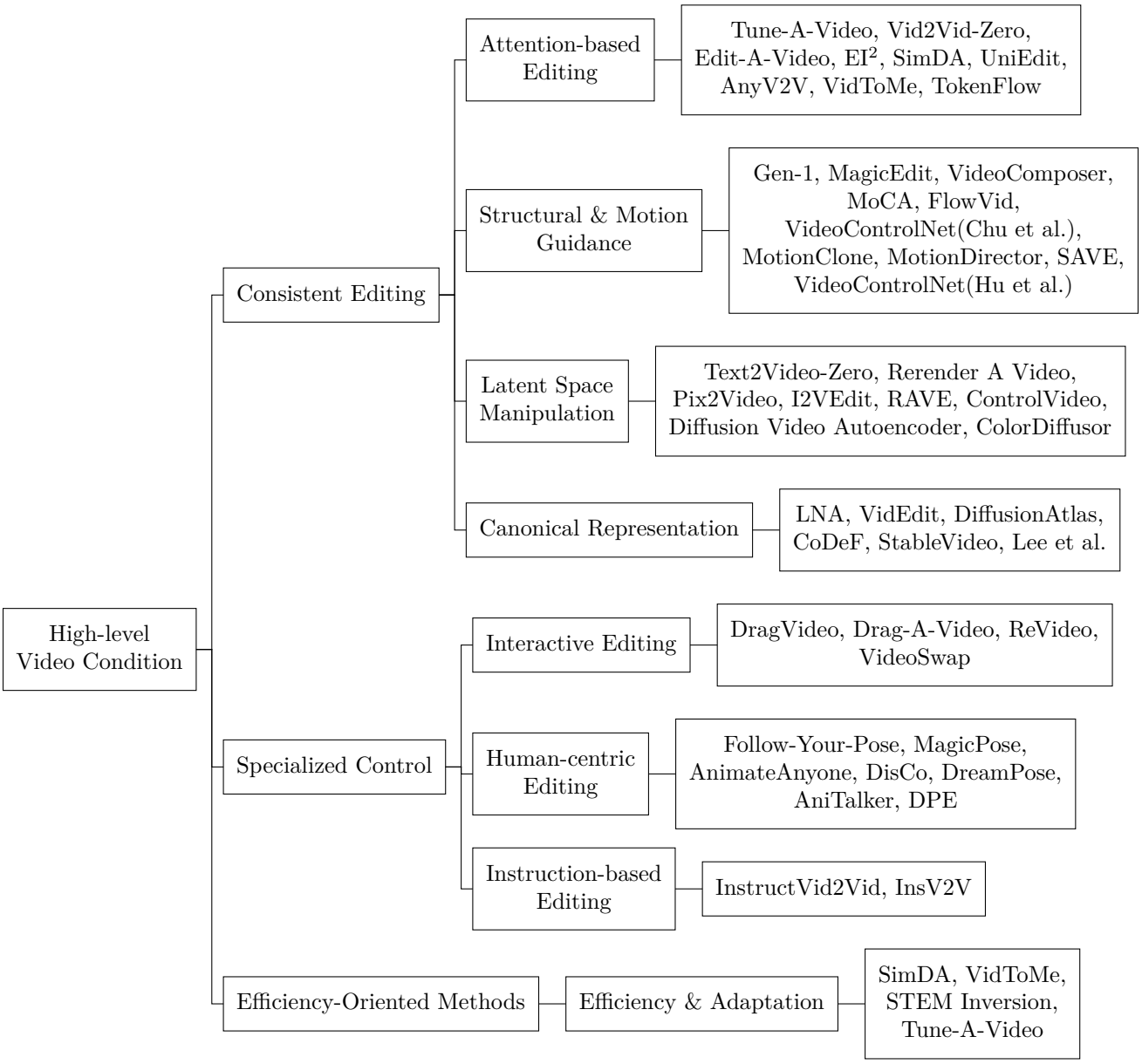

In recent years, diffusion-based video editing has become a powerful paradigm for synthesizing and manipulating videos while maintaining consistency in appearance, motion, and structure. Research in this domain has flourished across different dimensions, including strategies for preserving spatio-temporal coherence, specialized user controls, and approaches that boost efficiency. Below, we group these methods under three broad categories and detail the core ideas within each.

Consistent editing. A large body of work addresses how to preserve uniformity across frames, focusing on refined attention mechanisms, structural and motion guidance, latent space manipulation, and canonical representations. In terms of *attention-based approaches*, some of the earliest breakthroughs emerged when text-to-image diffusion models were extended to video. Tune-A-Video(Wu et al., 2023b) introduced

sparse-causal spatio-temporal attention to adapt Stable Diffusion for one-shot video editing, while Vid2Vid-Zero(Wang et al., 2023d) developed a dense spatial-temporal attention module and cross-frame attention to capture longer-range temporal dependencies. Edit-A-Video(Shin et al., 2024) likewise addressed temporal flicker by injecting attention maps from previous frames and applying a novel temporal-consistent blending method. Further enhancements came from methods like EI^2(Zhang et al., 2024j) and SimDA(Xing et al., 2024b), which minimized feature shifts via Shift-restricted Temporal Attention Modules, instance centering, spectral normalization, and Latent-Shift Attention to achieve smoother updates with fewer parameters. Some techniques also explicitly combine spatial and temporal features: UniEdit(Bai et al., 2024) and AnyV2V(Ku et al., 2024) fuse self-attention features across frames or integrate DDIM inversions to preserve both content and motion. Token-level operations further enhance frame alignment, with VidToMe(Li et al., 2024g) merging redundant tokens locally and globally, and TokenFlow(Geyer et al., 2023) identifying nearest-neighbor tokens to propagate consistent structure.

Beyond direct attention, some methods leverage explicit structural or motion signals to guide the diffusion process. Gen-1(Esser et al., 2023) demonstrated that providing depth maps alongside noisy latents ensures coherent scene geometry, while MagicEdit(Liew et al., 2023) and VideoComposer(Jiang et al., 2023a) used ControlNet or spatio-temporal encoders for depth, pose, or sketch guidance. Optical flow is also popular for ensuring consistent movement: MoCA(Yan et al., 2023a) projects edits from the initial frame onto subsequent frames through flow warping, FlowVid(Liang et al., 2024a) conditions the diffusion on flow-aligned features, and VideoControlNet(Chu et al., 2023) uses similar flow-based constraints to reduce flicker. Motion-Clone(Ling et al., 2024c) instead relies on internal temporal attention signals to extract dominant motion cues, making it training-free. Splitting appearance and motion into separate pathways further enhances flexibility, as in MotionDirector(Zhao et al., 2023c) (with dual-path LoRA) and SAVE(Song et al., 2023) (with a motion word and motion-aware cross-attention loss). A specialized example is VideoControlNet (Hu et al.)(Hu & Xu, 2023), which segments the video into I-, P-, and B-frames for independent generation, motion-guided updates, and interpolation, respectively.

Latent space manipulation is another powerful direction for preserving consistency. Text2Video-Zero(Khachatryan et al., 2023) and Rerender A Video(Yang et al., 2023b) warp the latent codes of initial or subsequent frames to guide motion while keeping appearance stable. Pix2Video(Ceylan et al., 2023) and I2VEdit(Ouyang et al., 2024b) inject self-attention features from prior frames to ensure visual continuity. Other methods, such as RAVE(Kara et al., 2024) (noise shuffling and the grid trick) or ControlVideo(Zhang et al., 2023e) (an interleaved-frame smoothing pipeline), unify frame latents during denoising. Diffusion Video Autoencoder(Kim et al., 2023a) explicitly disentangles identity, motion, and background within latent representations to simplify partial edits, and ColorDiffusor(Liu et al., 2023a) addresses color drift with dedicated Color Propagation Attention and an Alternated Sampling Strategy.

Finally, canonical representations use a consistent 2D atlas or parameterization to propagate edits across frames. Methods like Layered Neural Atlases(Kasten et al., 2021), VidEdit(Couairon et al., 2023), and DiffusionAtlas(Chang et al., 2023b) map videos into an atlas space, apply edits there, and then map them back to the original frames. CoDeF(Ouyang et al., 2024a) extends this concept using a hash-based design for canonical and deformation fields, while StableVideo(Chai et al., 2023) and Lee et al.(Lee et al., 2023) propagate keyframe edits via atlas-based correspondences, with the latter estimating dense semantic links to handle shape changes.

Specialized control. Several methods emphasize more direct or domain-specific control, whether through user interaction, human-centric capabilities, or language-based instructions. Interactive editing systems like DragVideo(Deng et al., 2023) and Drag-A-Video(Teng et al., 2023) adapt point-based image manipulation to the video domain by tracking user-selected points across time and optimizing latent codes for smooth motion. ReVideo(Mou et al., 2024) lets users edit the first frame and then specify new motion trajectories, supported by a three-stage training strategy that decouples content and motion. VideoSwap(Gu et al., 2024b) targets subject swapping via semantic point correspondences and layered atlases, maintaining consistent appearances in dynamic scenes.

Human-centric editing often centers on preserving identity, pose, and expressions across multiple frames. Approaches like Follow-Your-Pose(Ma et al., 2024d) and MagicPose(Chang et al., 2023a) typically train for

appearance control first and then refine temporal or pose-specific features using modules like ControlNet. Specialized appearance encoders, as in AnimateAnyone(Hu, 2024) or MotionEditor(Tu et al., 2024), capture high-fidelity details that are integrated into the denoising process for better motion generation. Broader subject or background manipulations appear in DisCo(Wang et al., 2024e), DreamPose(Karras et al., 2023), and AniTalker(Liu et al., 2024d), leveraging ControlNet-based architectures to separate or recombine different video elements. DPE(Pang et al., 2023) focuses specifically on decoupling pose and expression through a bidirectional cyclic training scheme, skipping 3D Morphable Models for simpler pipelines.

Instruction-based editing harnesses natural language to guide transformations in video, making them accessible to non-experts. InstructVid2Vid(Qin et al., 2024) and InsV2V(Cheng et al., 2023) adapt Prompt-to-Prompt editing for multi-frame scenarios by generating training data from captioning systems. They preserve coherence via specialized objectives like an Inter-Frames Consistency Loss and strategies such as Long Video Sampling Correction.

Efficiency-oriented methods. Since diffusion-based pipelines can be computationally intensive, numerous works focus on streamlining editing without degrading consistency. SimDA(Xing et al., 2024b) employs Latent-Shift Attention and lightweight adapters, while VidToMe(Li et al., 2024g) uses Token Merging (ToMe) to compress attention tokens both locally and globally, saving compute cycles across frames. STEM Inversion(Li et al., 2024f) applies an EM algorithm to find compact bases for each frame, reducing the dimensionality of video representations and speeding up inference. On a similar note, Tune-A-Video(Wu et al., 2023b) demonstrates that carefully designed sparse spatio-temporal attention modules can maintain temporal stability while significantly cutting resource usage.

4.1.6 Other conditions

Recent advancements in video generation have incorporated various special conditions to enhance control, realism, and applicability. These conditions include audio inputs, physical simulations, trajectories, scene layouts, and physiological signals. Below, we survey these developments, categorizing the works based on the special conditions they employ.

Physics-based video generation. Incorporating physics-based conditions ensures that generated motions adhere to real-world dynamics. PhysGen (Liu et al., 2024c) conditions video generation on external forces and physical parameters like gravity and friction to simulate realistic object motion. Starting from a single image, it extracts physical properties, simulates dynamics using a physics engine, and renders the motion using diffusion models, allowing for physically grounded and controllable video sequences.

Similarly, MotionCraft (Aira et al., 2024) uses physics-based optical flow derived from simulations to guide video generation. By warping the latent space of a pretrained diffusion model according to the optical flow, it animates the starting frame with the desired motion, enabling the synthesis of complex movements without retraining the model.

Extending physics-based conditioning to interactive scenarios, VideoAgent (Soni et al., 2024a) introduces multi-agent interactions guided by instructional text prompts and environmental contexts. By simulating agent behaviors that adhere to physical laws, it generates purposeful videos involving multiple interacting agents.

Physiological signal conditioning. Incorporating physiological signals opens avenues for health-related applications Synthetic Generation of Face Videos with Plethysmograph Physiology (Wang et al., 2022c) uses a given PPG signal to guide video generation, reflecting physiological signals like heart rate. Starting from a single image, it introduces variations to enhance the training of remote photoplethysmography models.

Timestamp conditioning. Timestamp conditions pinpoint precisely *when* events occur, ensuring proper sequencing and duration. MinT (Wu et al., 2024h) exemplifies this by binding each event to a designated time range, using Rescaled Rotary Positional Encoding for coherence, and leveraging scene cut conditioning for seamless transitions. With an LLM-based prompt enhancer to expand event captions, MinT maintains smooth multi-event progression, improves text alignment, and preserves subject integrity, highlighting the importance of time-based control for narrative-rich video generation.

4.2 Enhancement

The enhancement of image and video qualities has been a long-lasting and well-studied topic in computer vision. Early literature focused on low-level (i.e., pixel-level) video enhancement, where we process videos based on low-level photometric or geometric features to resolve specific issues such as video noise, motion blur, *etc.* However, in recent years, the success of generative models including GANs and diffusion models has offered new options to tackle these traditional low-level tasks. In this chapter, we review and discuss the potential of these new generative models on traditional video enhancement tasks including video denoising, video inpainting, video super-resolution, video interpolation and prediction.

4.2.1 Video denoising and deblurring

Video denoising aims to enhance video quality by reducing noise and restoring degradation issues like out-of-focus blur, motion blur, and compression artifacts such as moiré patterns (Rota et al., 2023). The noise or degradation defined in these tasks is low-level meaning that it generally does not require much high-level (semantic/object-level) understanding of the video.

Interestingly, the latest diffusion models are inspired and structured with a denoising framework, so they seem to be a direct fit for video denoising. However, they have completely different focuses. The latest diffusion models are mostly designed for highly creative generation tasks, where we use the model to generate from an image of complete noise. The whole process is more about "imagining" what might be hidden beneath the noise, rather than simply "removing" the noise. With large datasets, diffusion models learn the overall distribution of images rather than focusing on refining individual local patches based on appearance. In contrast, video denoising assumes that the input videos, although noisy, should start with enough quality, where at least the main content should be be recognizable. The goal is to reduce noise while keeping the main content unchanged in the video, leaving little room for creativity compared to generative diffusion models.

More broadly, there have been few successful generative models, not just diffusion models, specifically developed for video denoising tasks. The reasons are three-fold.

- **Different focus**: Video denoising requires the model to strictly maintain the original content of the video and avoid introducing extra new information. The task itself limits creativity, so generative modesls generally do not fit very well in this area.
- **Existence of good traditional methods**. Since the task primarily only involves minor local refinement, video denoising is generally not a very challenging task. Also, due to its long history in research, many effective traditional methods already exist and can address the problem reliably. Using generative models for this relatively simple task may seem overkilling.
- **Efficiency**. Compared to traditional methods, generative models are much more complex, making them harder to train and less efficient in practical applications.

4.2.2 Video inpainting

Video inpainting is a process used to fill in the missing or corrupted parts of a video Quan et al. (2024). A masked area is usually specified as a part of the input, and the task is aimed at filling in that area using spatial and temporal cues to make the video appear seamless and coherent. Note that the masked area can be specified in various ways depending on the application scenario. Here are some examples.

- In applications where the goal is to restore a corrupted area in the video, the masked area is defined as the region of corruption, and the task mainly focuses on filling in the area based on the local continuity of the frame.
- In applications where the goal is to remove unwanted objects, the mask area is defined as the object masks, and the task focuses more on finding temporal correspondences to fill in the background behind the object.

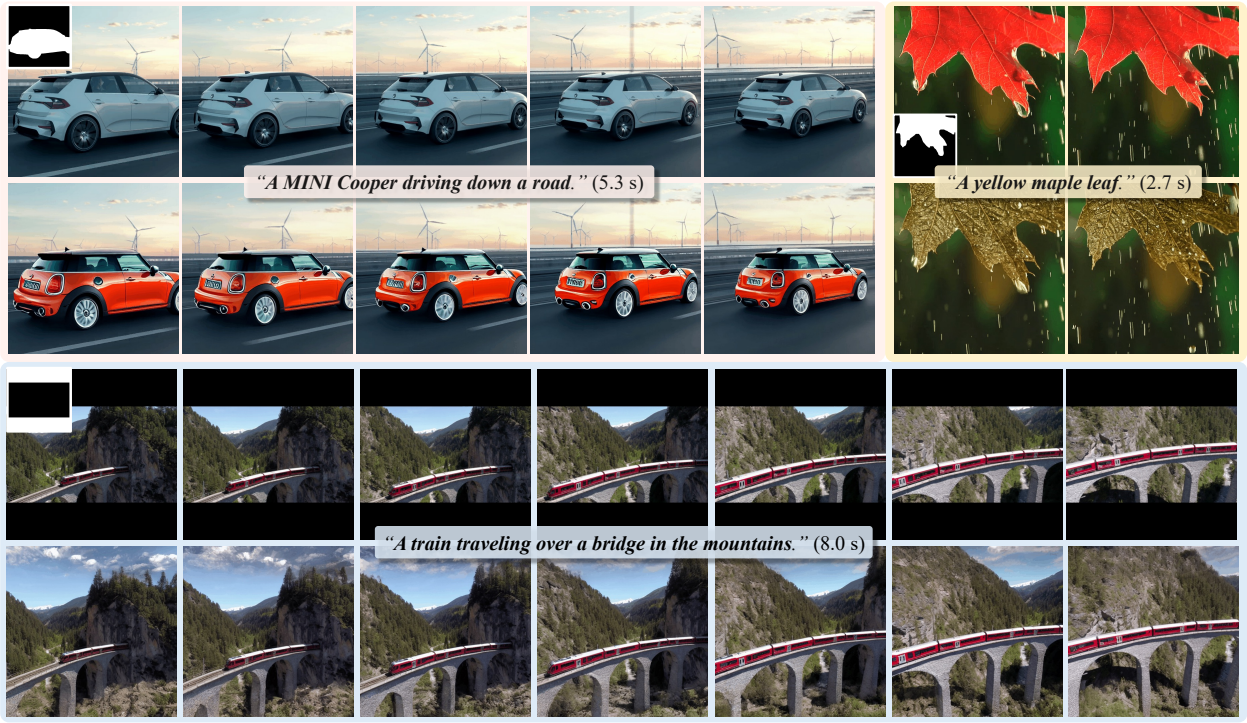

Figure 11: Example of video inpainting with text instructions for video generation. The contents in the masked regions are inpainted under text instrubtions. Original figure from AVID (Zhang et al., 2024h)

While traditional methods typically adhere to a predefined problem setting with a specified masked area, recent diffusion methods aim to be more creative by incorporating language instructions and addressing more challenging cases through complex generation. One such example is shown in Figure 11, where masks and instructions are provided to enable video editing applications as a video inpainting task (Zhang et al., 2024h).

GAN (Generative Adversarial Network) models were first adopted to solve the inpainting problem from a generative perspective. Starting from image inpainting, Pathak et al. (2016) uses inpainting as a self-supervised task to learn video representations, where an adversarial loss is introduced to produce sharper results. Yu et al. (2018) also introduced local and global WGANs for enhanced results. Recently, Chang et al. (2019) extended this idea to free-form video inpainting, where the masks can have arbitrary shapes such as text captions, and proposed a temporal PatchGAN loss to enhance temporal consistency.

Diffusion moodels have also been explored for inpainting tasks, and such explorations mainly start from image inpainting. RePaint (Lugmayr et al., 2022) applied a pretrained unconditional DDPM and modified the standard denoising strategy by sampling the masked regions from the diffusion model and sampling the unmasked areas from the given image. SmartBrush (Xie et al., 2023) explored image inpaiting with both text and shape guidance with precision control. They try to generate a new object to be filled in the shape specified by the masks. To preserve the background and improve consistency, they add an extra mask prediction module in the diffusion process, which is used to guide the sampling process in the inference stage. For video inpainting, Green et al. (2024) reframe the task as a conditional generative modeling problem tackled with conditional video diffusion models. They use sampling schemes specific to inpainting problems to capture long-range dependencies and show that their model can inpaint diverse novel objects that are semantically consistent with the context.

To better utilize the multi-modal capability of diffusion models, some research work has focused on adding inputs of other modalities, such as text instructions, into video inpainting, paving the way for real applications

like text-guided video editing. AVID (Zhang et al., 2024h) builds on existing text-guided image-inpainting models and improves temporal consistency by integrating motion modules. They also proposed a structure guidance module tailored for different types of masks, and a middle-frame attention guidance method for longer videos. Subsequently, CoCoCo (Zi et al., 2024) proposes a more efficient motion capture module and an instance-aware region selection method for better "consistency, controllability, and compatibility" (and hence the name "CoCoCo").

Furthermore, UniPaint (Wan et al., 2024) presents an interesting argument that video inpainting and interpolation can be unified and mutually enhanced as both tasks involve filling missing information in the spatial and temproal domains, respectively, for which they propose a spatial-temporal masking strategy during training. Wu et al. (2024b) introduces a pure language-driven video inpainting task, where the specified inpainting masks are no longer needed. Instead, they use natural language instructions, such as instructions to remove objects, to guide and condition the inpainting process.

4.2.3 Video interpolation and extrapolation/prediction

Video interpolation aims to generate intermediate frames between two consecutive frames to increase the video's frame rate. In contrast, video extrapolation or prediction focuses on forecasting the next frame following the input frames. Both tasks involve generating new frames along the temporal dimension and thus depend heavily on understanding the motion between frames.

Traditionally, video interpolation and extrapolation/prediction are distinct tasks approached with different methodologies. Video interpolation focuses on finding or synthesizing intermediate frames to reflect the motion between existing frames, while video extrapolation requires more creativity and may rely on external domain knowledge or common sense to help predict future frames. Moreover, video interpolation has clear and direct real-life applications and generally produces more reliable results because it uses temporal cues from both preceding and succeeding frames. As a result, video interpolation has traditionally been of greater interest compared to video extrapolation/prediction.

However, from the perspective of diffusion models, video interpolation and extrapolation can be tackled in a more unified framework. One example is illustrated in Figure 12. Therefore, we discuss both tasks together in this chapter.

With the rise of large pretrained diffusion models, video interpolation and extrapolation are increasingly viewed as conditional generation tasks, rather than relying heavily on motion analysis and image warping. In both cases, generative methods follow the same approach—generating new frames based on the surrounding context frames. This allows a unified diffusion model to be trained to handle both interpolation and extrapolation.

One early example is MCVD (Masked Conditional Video Diffusion) (Voleti et al., 2022), where a diffusion model is trained to generate current frames conditioned on past and future frames. By randomly masking these frames, the model adapts to different tasks. If both past and future frames are masked, the model performs unconditional video frame generation. If only either past or future frames are masked, it handles past frame or future frame prediction, respectively. When neither are masked, the model performs video interpolation. This random masking enables MCVD to learn video interpolation, prediction, and generation in a unified framework. Similar ideas also appeared in RaMViD (Random-Mask Video Diffusion) (Höppe et al., 2022), but instead of masking in the temporal dimension, RaMViD apply masks in the spatial domain and use a unified framework to tackle video interpolation, infilling, and upsampling.

Moreover, some later methods also specifically explored the power of diffusion models on video interpolation. VIDIM uses cascaded diffusion models, where low-resolution target frames are first generated before generating high-resolution versions conditioned on these generated low-resolution frames(Jain et al., 2024a). LDMVFI explored latent diffusion models to achieve better perceptual generation quality for video interpolation (Danier et al., 2024).

Some other recent work has also adapted video interpolation/extrapolation to specific application scenarios. Fu et al. (2023) proposes MMVG (Multi-modal Masked Video Generation) to tackle a new adapted task called text-guided video completion (TVC) motivated by the uncertainty of frame prediction. Specifically, a

Figure 12: Examples of video extrapolation/prediction (Row 1&2) and interpolation (Row 3). For diffusion models, it is possible to add text instructions for a better control. Original figure from Fu et al. (2023)

video can have multiple potential future outcomes, so it is better to add text guidance to describe a specific future that we want to generate. Apart from that, some work explored interpolation for specific styles such as cartoon (Xing et al., 2024a).

Overall, we have seen great differences between traditional and generative methods.

- **Creativity**: Traditional methods adhere to the original content, motion, and physics in the video, while generative methods can generate in a more creative way.

- **Dependence on motion**: Traditional methods mostly rely on strong motion assumptions such as motion smoothness and linearity, so they may fail if the underlying motion is complex, nonlinear, or ambiguous (Jain et al., 2024a). Also, these smooth motion assumptions often result in overly smoothed predictions by traditional methods. However, diffusion models are less vulnerable to these problems due to their low dependence on motion understanding.

- **Difficulty**: Traditional methods are typically designed for simple settings, where only one intermediate or future frame is predicted from context frames, with short time intervals between them to maintain smooth motion assumptions. In contrast, generative methods can handle more complex tasks, such as interpolating or predicting 5-10 frames at a time, and the context frames can be far apart in time. An extreme example would be having only the first and last frames of a 5-second video. In this case, generative models are well-suited to generate the entire video since most of the information is completely made up. Traditional methods, however, would struggle to handle this scenario due to lack of context. We will discuss more about long video generation in Section 4.5.

4.2.4 Video super-resolution

Video super-resolution is another well-established task in video restoration, focusing on enhancing low-resolution videos by upsampling the video frames to produce clearer and sharper high-resolution outputs. Early research focused more on image super-resolution algorithms, followed by video super-resolution meth-

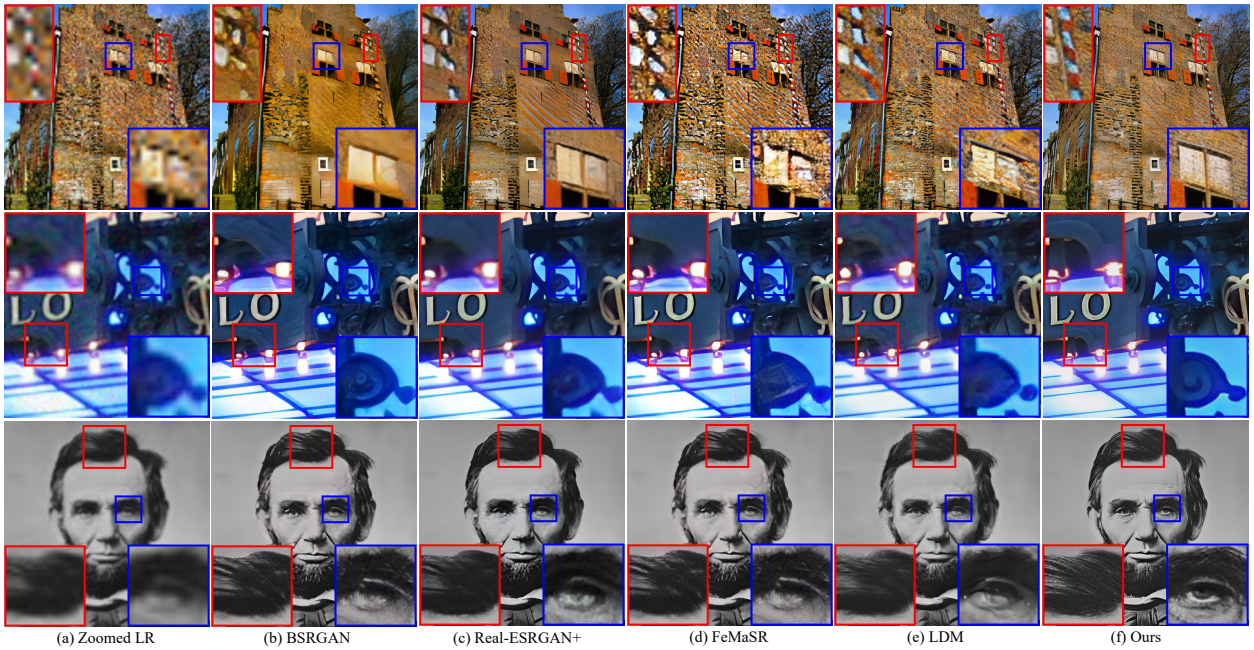

Figure 13: Video super-resolution examples of latest methods. Original figure from StableSR (Wang et al., 2024c)

ods, which introduced temporal consistency as an additional optimization objective. Some visual examples are shown in Figure 13.

In recent years, diffusion models have also been applied to super-resolution tasks. StableSR (Wang et al., 2024c) explored leveraging the prior knowledge from pre-trained diffusion models to improve super-resolution quality. They employed a frozen Stable Diffusion model to generate high-resolution images conditioned on the low-resolution features computed from a pretrained super-resolution model. A trainable time-aware encoder module was added to combine the super-resolution features with the diffusion features. Similarly, Yuan et al. (2024b) proposed to utilize a frozen pre-trained text-to-image diffusion model as the base to accomplish text-to-video super-resolution. They first use the image diffusion model to generate high-resolution images one-by-one and then refine the results through a temporal adapter.

Some latest methods have also investigated different ways to combine super-resolution networks (mostaly a VAE) and diffusion networks (U-Net). SATeCo (Chen et al., 2024e) combined the super-resolution (VAE) and diffusion model (U-Net) by inserting the U-Net structure in between the VAE encoder and decoder, together with some adapation or alignment modules. The latest VEnhancer (He et al., 2024b) also shares a similar structure with additional space-time data augmentation and video-aware conditioning, which are trained to enhance AI-generated video on both space and time resolutions. In comparison, Upscale-A-Video (Zhou et al., 2024b) is more designed for long videos. They first utilize the U-Net to generate each video segment given optical flow inputs and perform a global recurrent latent propagation to ensure consistency across a longer time range. The VAE decoder is then applied to decode high-resolution images. Both structures have shown pros and cons on flexibility, fidelity and quality.

In addition to using diffusion models to enhance video resolutions, some research work has also studies how to enhance/adapt low-resolution image/video generation models so that it can also work well on high-resolution tasks. Guo et al. (2025) propose a tuning-free method through a pivot replacement strategy that leverages reliable semantic guidance from the low-resolution model, as well as a tuning method that integrate learnable multi-scale upsampler modules to learn structural details at the new higher resolution.

To follow up, FreeScale (Qiu et al., 2024c) introduces a tuning-free inference paradigm that fuses features from different perceptive scales and extracts the desired frequency for each part of the frame.

4.2.5 Combining multiple video enhancement tasks

As we have discussed in the previous chapters, many diffusion methods have unified and tackled multiple enhancement tasks at the same time. To recall a few, UniPaint Wan et al. (2024) combines video inpainting and video interpolation, and MCVD (Voleti et al., 2022) unifies video interpolation and video prediction. Notably, VEnhancer (He et al., 2024b) is a plug-and-play method used to enhance a low-quality video generated by other generation models by removing artifacts and increasing both of its spatial and temporal resolutions.

This trend mainly stems from the flexibility of diffusion models which can be trained to generate outputs in a task-agnostic manner. As a result, the differences among enhancement models are more based on different training data and strategy instead of model structures.

4.2.6 Summary

In summary, recent diffusion-based methods have significantly advanced traditional video enhancement techniques, improving tasks such as video denoising, inpainting, interpolation, extrapolation/prediction, and super-resolution. From this review, we can see a clear trend as follows.

- Diffusion-based methods introduce greater creativity into traditional low-level video enhancement tasks. Leveraging the strength of pretrained diffusion models, these approaches can tackle more complex and challenging scenarios where traditional methods often fall short.
- Diffusion models have also enabled the use of multi-modal inputs, allowing enhancement tasks to be performed with additional inputs like text instructions. This advancement is revolutionary, as text-based input provides an effective means of making the enhancement process more controllable and customizable, opening new possibilities for video editing.
- From the perspective of diffusion models, the distinction between image and video is becoming less significant. Traditional methods often develop image and video enhancement algorithms separately, as video enhancement requires careful attention to temporal correspondences and alignment (the "physics" of motion). In contrast, diffusion models, which are less dependent on explicit motion understanding, allow for a more seamless and scalable adaptation between image and video models.
- Nevertheless, diffusion models can introduce more fidelity issues due to the inherent randomness of the diffusion process. In video enhancement, the output is expected to preserve the original content or subject matter, but diffusion models may introduce new elements that were not originally present. Finding ways to balance fidelity and quality can be an interesting topic for future research.

4.3 Personalization

Personalization in video generation is essential for creating content that accurately represents specific subjects, capturing their unique identities, expressions, and motions. Two primary approaches enable this personalization: subject-specific fine-tuning and subject-specific-driven inference. While fine-tuning approaches carefully adapt model parameters to a particular subject, inference-based methods rely on minimal references—often a single image—to guide identity preservation and motion synthesis without retraining.

Subject-specific fine-tuning. Subject-specific fine-tuning involves adapting a pre-trained model to a particular subject by retraining or modifying its parameters using data specific to that subject. This approach allows the model to embed detailed subject characteristics directly into its learned representation.

DreamVideo (Wei et al., 2024c) fine-tunes an identity adapter on a few static images of the subject, capturing subject-specific identity traits, while separately training a motion adapter on target motion patterns. This decoupling allows the system to integrate both identity and motion seamlessly into the final output.

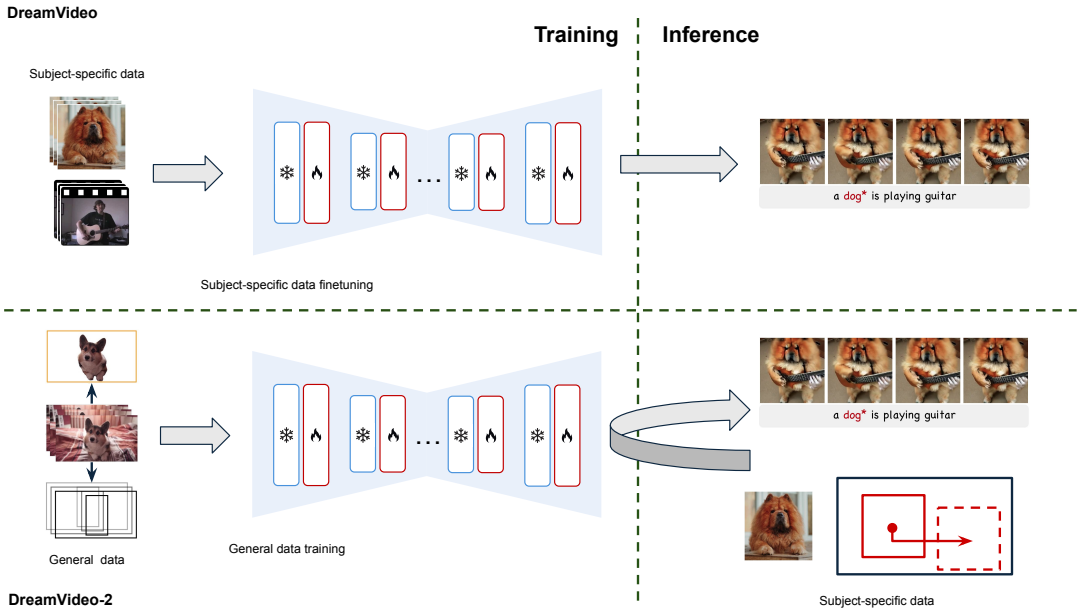

Figure 14: A high-level comparison of two personalization paradigms—subject-specific finetuning and subject-specific-driven inference—illustrated by DreamVideo (Wei et al., 2024c) and DreamVideo-2 (Wei et al., 2024b). In DreamVideo, each new subject (its images and desired motion) is used to finetune the model. In contrast, DreamVideo-2 leverages a pretrained diffusion model trained on general videos (decomposed into subjects and bounding boxes); it then generates videos for a new subject based on a single image and bounding boxes—without requiring additional finetuning.

Similarly, PersonalVideo (Li et al., 2024c) adopts a fine-tuning strategy to preserve high identity fidelity without degrading the model's motion and semantic capacities. By integrating an isolated identity adapter into the spatial self-attention layers of a pre-trained text-to-video diffusion model, PersonalVideo fine-tunes identity features without disrupting motion dynamics. This method enhances robustness through simulated prompt augmentation, ensuring that even with limited reference images, the model achieves reliable identity preservation alongside customizable style and motion.

By extending these techniques to scenarios without specialized video data, Still-Moving (Chefer et al., 2024) leverages text-to-image (T2I) customization and introduces lightweight spatial and temporal adapters for text-to-video pipelines. By training on duplicated still images (or "frozen videos"), it retains motion priors while aligning T2I and T2V features, enabling diverse personalization with only a handful of static images. In parallel, Dynamic Concepts (Abdal et al., 2025) addresses more inherently dynamic concepts—subjects whose characteristic motion is as integral to their identity as appearance—by fine-tuning a Diffusion Transformer in two stages. First, it learns an appearance "basis" from an unordered set of frames, and then refines temporal dynamics by freezing the learned parameters and focusing on motion consistency. Finally, Video Alchemist (Chen et al., 2025) expands personalization to multi-subject, open-set scenarios by fine-tuning a Diffusion Transformer, and personalizes both foreground objects and backgrounds while mitigating overfitting through targeted data augmentation.

Subject-specific-driven inference. Subject-specific-driven inference personalizes video outputs at runtime without retraining the model for each new subject. These methods typically rely on a single reference image (and sometimes auxiliary inputs like audio or text prompts) to guide identity preservation and expression synthesis.

Many audio-driven talking head frameworks fall into this category. EMO (Tian et al., 2024), VASA-1 (Xu et al., 2024e), AniTalker (Liu et al., 2024d), and AniPortrait (Wei et al., 2024a) generate expressive talking head videos from a single reference image and an audio input. They rely on diffusion-based models and

carefully designed motion encoding strategies to preserve subject identity while animating expressions and head movements. Approaches like DreamTalk (Ma et al., 2023), EMOPortraits (Drobyshev et al., 2024), and FlowVQTalker (Tan et al., 2024a) extend this concept by incorporating emotional expressiveness, predicting personalized emotion intensity from audio without additional style references, and ensuring identity consistency even under intense expressive variations. Beyond facial animation, ANGIE (Liu et al., 2022b) expands this paradigm to co-speech gesture generation, personalizing gesture patterns from minimal inputs while retaining the speaker's characteristic style.

Recent works further refine and expand subject-specific-driven inference into broader video customization scenarios. For instance, DreamVideo-2 (Wei et al., 2024b) introduces zero-shot subject-driven video generation with precise motion control. Using only a single reference image and bounding box sequences to define the subject's trajectory, it employs reference attention mechanisms and mask-guided motion modules to integrate subject appearance with flexible, fine-grained motion paths—achieving personalization without additional fine-tuning steps.

Building on this idea of inference-time personalization, IPT2V (Yuan et al., 2024a) demonstrates how decomposing identity features into low-frequency (global facial contours) and high-frequency (fine details) components can ensure identity preservation in text-driven synthesis. By integrating these components into a pre-trained Diffusion Transformer, IPT2V consistently captures the subject's essential features across varying poses and expressions, all without retraining for each subject. In a similar vein, ConsisID (Yuan et al., 2024a) also leverages frequency decomposition to reinforce identity consistency, but it further employs coarse-to-fine training strategies and dynamic mask losses to stabilize both facial outlines and subtle textures. This tuning-free workflow allows ConsisID to generate text-aligned videos that faithfully reproduce the subject's identity.

Lastly, MCNet (Hong & Xu, 2023) addresses motion transfer scenarios, animating a still image to follow the dynamics of a driving video while preserving identity through an implicit identity representation conditioned memory module. By extracting and reusing structural and appearance details from a single reference image, MCNet maintains subject fidelity throughout complex motions—again, without retraining on the target subject. Together, these approaches illustrate the growing versatility of inference-based frameworks that balance flexible control, identity preservation, and visual fidelity without the burden of subject-specific fine-tuning.

4.4 Consistency

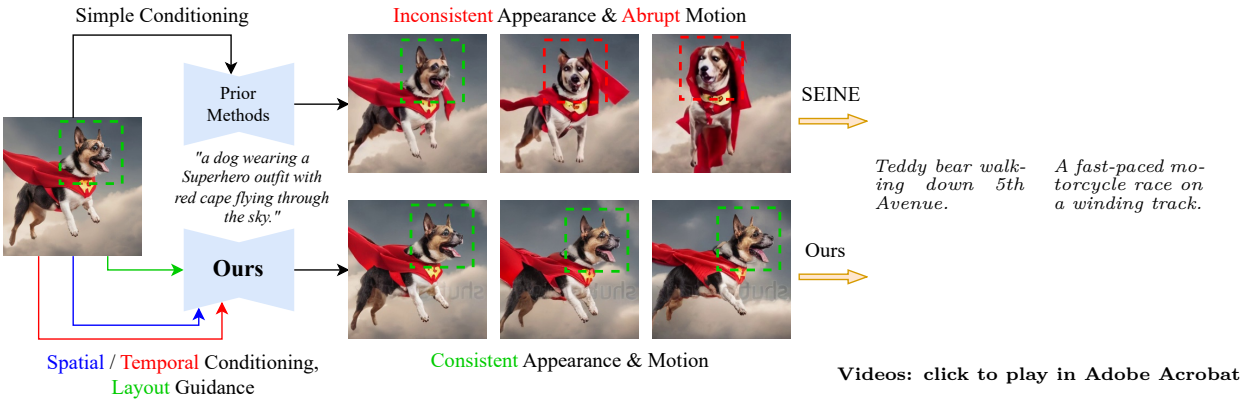

Figure 15: Comparison of image-to-video generation results obtained from SEINE and ConsistI2V. SEINE shows degenerated appearance and motion as the video progresses, while ConsistI2V maintains visual consistency utilizing spatial and temporal conditions.

Improving the consistency of generated videos has been a hot topic recently. Researchers have been working on improving consistency in two different perspectives, *i.e.*, semantic consistency, and motion consistency.

Early attempts (Yu et al., 2021; Skorokhodov et al., 2022; Shen et al., 2023; Zhang et al., 2023c) for GAN-based video generation methods mainly add additional discriminators or learned representations for controlling consistency. For example, DI-GAN (Yu et al., 2021) introduces an implicit neural representations-based video generator that improves motion dynamics by manipulating space and time coordinates along with a motion discriminator for temporal consistency. StyleGAN-V (Skorokhodov et al., 2022) employs continuous motion representations as positional embeddings.

Diffusion models. Semantic consistency (Ren et al., 2024; Zhang et al., 2024i; Jiang et al., 2024b; Li et al., 2024g; Zhou et al., 2024d; Sun et al., 2023b) ensures the semantic meaning including objects and relationships between objects are smooth between different frames. The biggest problem is semantic drifting, which refers to the gradual shift or change in the meaning or context of visual content as a video progresses. StableVideo (Chai et al., 2023), as a pioneer work, proposes to propagate the representation to the next frame to ensure consistency. Similarly, TokenFlow (Geyer et al., 2023) preserves consistency by explicitly propagating diffusion features based on inter-frame correspondences using sampled tokens for video editing. GLOBER (Sun et al., 2023a) employs a novel adversarial loss along with conditioning the generation on the global features extracted by a video encoder for global consistency. Specifically, for face video generation, EMO (Tian et al., 2024) preserves visual/identity consistency by encoding a reference image/video/audio and cross-attention for video generation.

Motion consistency consists of multiple aspects, such as video smoothness, reasonable object motion, and stable camera movement, while two different frameworks, including residual-based framework (Deng et al., 2024a; Zhou et al., 2024d) and optical flow-based framework, are proposed to ensure the motion consistency of generated videos. For the residual-based methods, they usually add additional motion representation extracted from previous frames or text prompts. As a representative work, Cinemo (Ma et al., 2024b) learns to generate residual images between a previous frame and a later frame for motion control. Moreover, it also incorporates a new noise refinement with discrete cosine transformation for controlling the input noise. VideoComposer (Wang et al., 2023f) uses motion vectors, depth sequences, mask sequences, and sketch sequences to assist in the generation of video frames. On the other side, in addition to the image-based residual, StoryDiffusion (Zhou et al., 2024d) proposes to split the long text prompts into multiple short text prompts to improve consistency.

For the optical flow-based models, they usually learn to generate optical flow between a previous frame and a later frame to maintain consistency. LFDM (Ni et al., 2023) introduces a flow predictor during training and injects flows into the denoising procedure for motion consistency. Similarly, Motion-I2V (Shi et al., 2024) consists of two stages. It first generates optical flows based on the input image and then videos are generated conditioned on the concatenation of these optical flows. For video editing, CAMEL (Zhang et al., 2024b) improves consistency through a frequency-based perspective, where the video is decomposed using low- and high-pass filters. Moreover, it learns additional motion prompts for further stabilize the video.

Apart from these methods, another popular paradigm for consistency is controlling the noise used in diffusion models. PYoCo (Ge et al., 2023) is first proposed to employ a novel correlated noise model, which consists of a noise shared among all frames and an individual noise conditioned on the previous frames. Following this, a $\int$-noise (Chang et al., 2024) is proposed to warp noise following the flow and preserve the spatial Gaussian property, which is able to preserve the motion and semantic consistency at the same time.

One application of consistency is long video generation, which poses high requirements for motion and semantic consistency. long video generation (Ouyang et al., 2024c) is always achieved by ensuring a smooth transition and semantic consistency among different frames. StoryDiffusion (Zhou et al., 2024d) proposes to use a novel consistent self-attention and a semantic space temporal prediction for object consistency. Similarly, StreamingT2V (Henschel et al., 2024) employs a long-term memory block, a short-term memory block, and also a new blending approach for infinitely long video generation. The short-term block focuses on consistency between adjacent frames, while the long-term block forces the model to depend on the first several frames to avoid forgetting. Later, SEINE (Chen et al., 2024d) proposes to employ a random-mask model for generating transitions based on textual descriptions. Multiple randomly masked images can be seen as images from different scenes and they can provide an overall comprehensive angle to consistency and long video generation. On the other side, 3D scene mesh (Fridman et al., 2023) is also used for generating

videos, which can be seen as another application of consistency. Specifically, the video frames and meshes are updated through several pre-trained models and the consistency between different frames is preserved through the iterated refinement of the mesh.

4.5 Long video

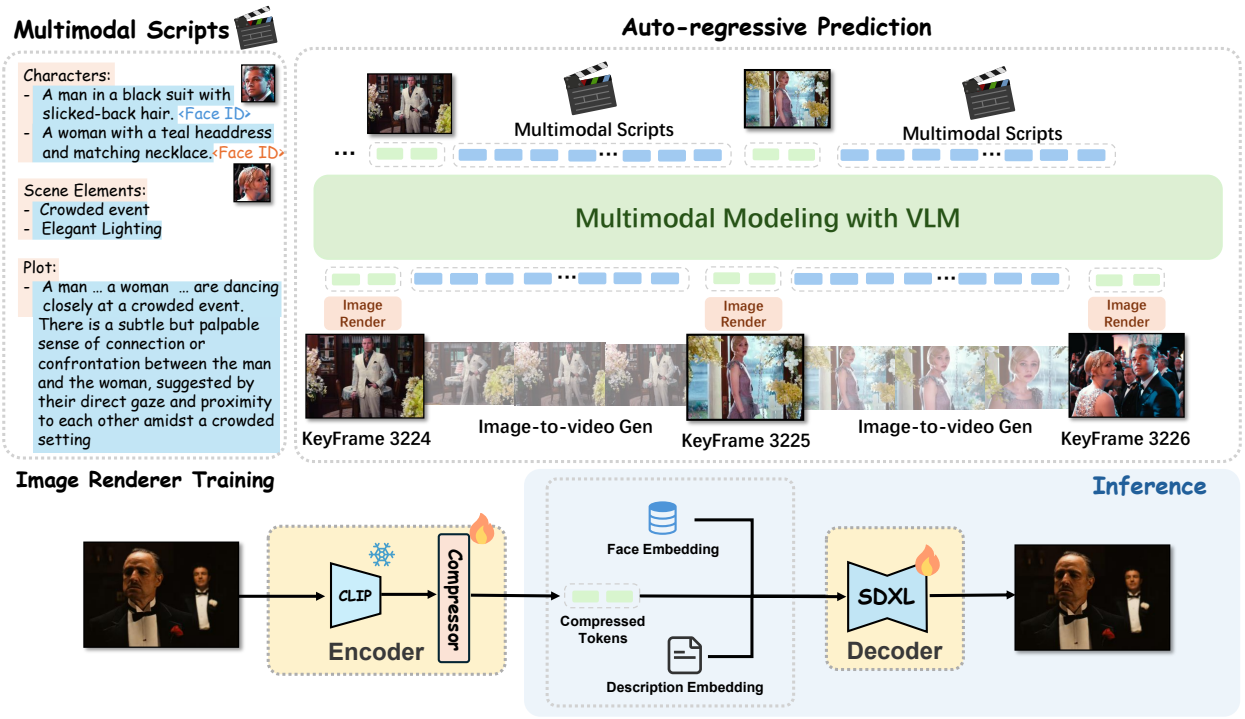

Figure 16: The framework of MovieDreamer. The autoregressive model takes multimodal scripts as input and predicts the tokens for keyframes. These tokens are then rendered into images, forming anchor frames for extended video generation. MovieDreamer ensures long-term coherence and short term fidelity in visual storytelling with the character's identity well preserved.

Long video understanding, including retrieval, classification, and generation, has been a challenging problem for a long time. Videos are always of different lengths and might be infinitely long, such that models find it hard to keep content consistent among different frames. In this part, we will introduce representative methods in long video generation.

Almost all the **traditional long video generation methods** are divide-and-conquer-based methods. They usually first generate keyframes and then generate other frames conditioned on these generated keyframes. TATS (Ge et al., 2022) uses multiple models (interpolation and autoregressive transformers) to ensure the transition between frames is consistent. Later, to further improve the flexibility of long video generation, Brooks et al. (2022) generates low-resolution sequences, which are then enhanced to high resolution. Besides, CogVideo (Hong et al., 2023a) further interpolates non-key frames with the help of keyframes and text conditions with a two-stage-based framework. Another work by Zhang et al. (2023c) is built upon StyleGAN-v (Skorokhodov et al., 2022), which suffers from undesired content jittering for long video generation. They further proposed a novel B-Spline-based motion representation to ensure temporal smoothness.

Diffusion models. Different from traditional models, the solutions in diffusion models are more diverse and can be split into two main categories, *i.e.*, divide and conquer (sliding windows and keyframes), autoregressive models (including sliding windows), and consistency. For **divide-and-conquer**-based methods (EMO), the generation of long videos is split into several stages and for each stage, the video is generated based on the

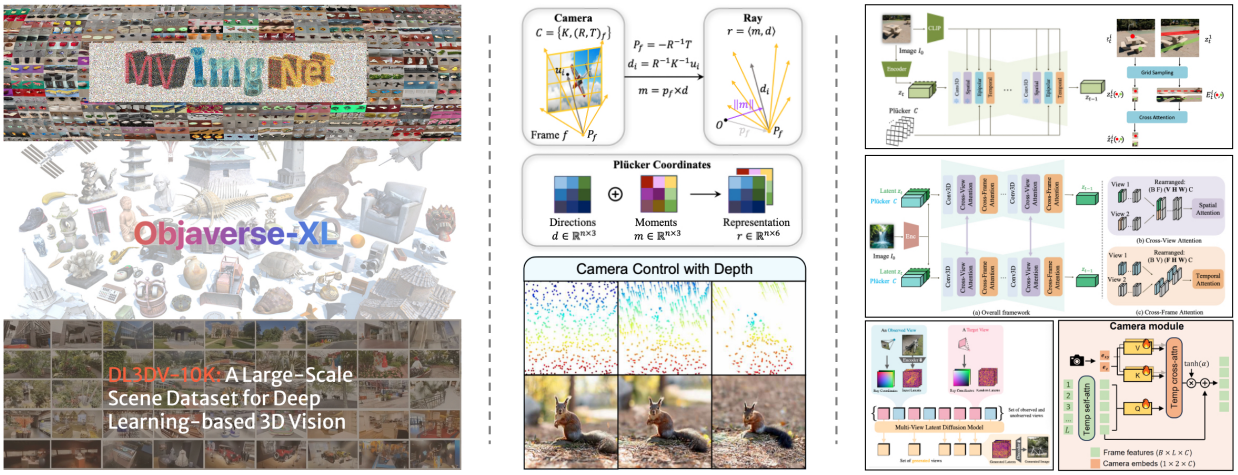

Training on 3D dataset | Camera conditioning | 3D-aware architecture

Figure 17: For a video diffusion model to be 3D aware, the general paradigm includes training on 3D dataset, adding camera control to the model, and introducing 3D-aware model architectures.

previous one or the input condition for refinement. NUWA-XL (Yin et al., 2023b) employs a hierarchical method for generating long videos. Specifically, a global diffusion model is first applied to generate the keyframes across the entire time range, and then local diffusion models recursively fill in the content between nearby frames. An earlier work (Harvey et al., 2022) proposes a RAG-style generation pipeline for generating adapted long video frames continued on any other videos along with a novel generation scheme (attention map) for not forgetting the early frames. Gen-L-Video (Wang et al., 2023b) also employs a hierarchical strategy to construct long videos through a set of short videos. FreeNoise (Qiu et al., 2024b), as an example, employs a sequence of noises for long-range correlation and performs temporal attention over them by sliding windows. Moreover, it also uses a motion injection method to condition the generation of long videos on multiple text prompts. Besides, instead of considering directly generating long videos, MAVIN (Zhang et al., 2024a) chooses to first generate several small clips and then generate the transition between them to maintain consistency with a boundary frame guidance module and a noise sampling strategy.

On the other side, autoregressive methods are drawing more and more research attention. For example, a sliding window, which can be seen as an application of autoregressive methods, is used to enable a short-video generator to generate long videos while the hidden representation of the video is interpolated when conditioning on different prompts. Moreover, many methods (Gao et al., 2024; Zhao et al., 2025; Xie et al., 2024a) are proposed with multimodal autoregressive models. MovieDreamer uses a multimodal autoregressive model with diffusion models to generate long videos conditioned on multimodal scripts. The multi-modal autoregressive model is designed to capture the key semantics in the multimodal conditions. (Xie et al., 2024a) further shows that existing models can be easily extended to autoregressive video diffusion models by varying the noise level instead of using a stable noise level.

Apart from these methods, more models are proposed to address the high computational requirements and the efficiency using diverse strategies and solutions (Diffusion Forcing). Specifically, to speed up the generation procedure, Video-Infinity (Tan et al., 2024b) is proposed to distribute the generation for one long video to multiple GPUs with the proposed clip parallelism and dual-scope attention modules. It is able to generate videos up to 2,300 frames in approximately 5 minutes with 8 × Nvidia 6000 Ada GPUs (48G), which is 100 times faster than the current methods.

4.6 3D-aware video diffusion

The world exists in three spatial dimensions plus time, while a video represents a 2D projection of this 3D world. Consequently, video diffusion models should adhere to certain 3D constraints. These models gener-

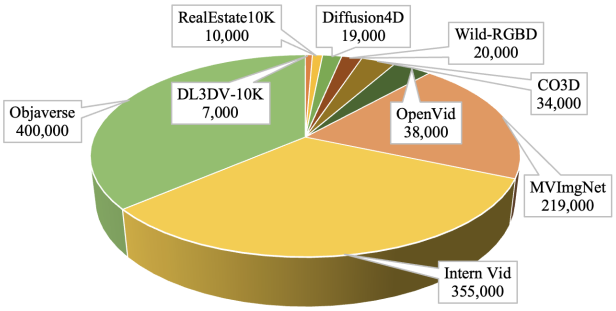

Figure 18: A visualization of the 3D datasets used by Cavia (Xu et al., 2024a).

ate multiple frames simultaneously and capture inter-frame relationships through attention layers spanning different frames. Existing research, such as SORA (Li et al., 2024h), demonstrates that by training on large-scale datasets, networks can implicitly learn 3D priors embedded within the data.

While this approach highlights a promising direction for learning 3D priors, there remains significant value in explicitly incorporating 3D awareness into video diffusion models. Doing so could improve 3D controllability and facilitate easier and more effective learning for the model.

4.6.1 Training on 3D dataset

Video diffusion models are typically trained on in-the-wild videos that feature arbitrary camera motions and dynamic scenes, making it challenging for these models to learn robust 3D priors. To enhance a model's ability for 3D generalization and multi-view consistency, one straightforward approach is to fine-tune the video diffusion model using datasets that explicitly capture 3D characteristics.

SV3D (Blattmann et al., 2023a) fine-tunes a pre-trained stable video diffusion model on orbiting videos of 3D synthetic objects from the GSO (Downs et al., 2022) and OmniObject3D (Wu et al., 2023d) datasets. These orbiting videos include both static orbits, where the camera circles an object at regularly spaced azimuths with a fixed elevation, and dynamic orbits, where the camera trajectory is irregular. Similarly, V3D (Chen et al., 2024f) fine-tunes on the Objaverse dataset, leveraging 360-degree orbiting videos, along with proprietary datasets featuring similar setups (Junlin Han, 2024; Melas-Kyriazi et al., 2024).

Generative Camera Dolly (Van Hoorick et al., 2024) introduces two synthetic datasets, Kubric-4D and ParallelDomain-4D, which provide multi-view videos of dynamic scenes. By fine-tuning a Stable Video Diffusion (SVD) model solely on these synthetic datasets, they achieve zero-shot generalization to real-world novel view synthesis tasks.

CamCo (Xu et al., 2024b) fine-tunes a video diffusion model on real-world camera fly-through data from the WebVid10M dataset (Bain et al., 2021), using estimated camera poses. This enables the model to generate scene-level videos with precise camera controls. Similarly, CVD (Kuang et al., 2024) combines RealEstate10K (Zhou et al., 2018b) and WebVid10M (Bain et al., 2021) to train a camera-controllable video diffusion model.

Diffusion4D (LIANG et al., 2024) extends video diffusion into the realm of 4D generation by fine-tuning on orbiting videos where both the camera and object are in motion, enabling models to capture spatiotemporal dynamics more effectively.

Cavia (Xu et al., 2024a) focuses on camera-conditioned image-to-multi-view-video generation. They train their model on a large-scale dataset of approximately 0.4 million videos annotated with camera poses. These videos are sourced from a diverse collection of datasets, including Wild-RGBD (Xia et al., 2024), MVImgNet (Yu et al., 2023c), RealEstate10K (Zhou et al., 2018b), CO3D (Reizenstein et al., 2021), DL3DV-10K (Ling et al., 2024b), Objaverse (Deitke et al., 2022; 2023), Diffusion4D (LIANG et al., 2024), OpenVid (Nan et al., 2024), and InternVid (Chen et al., 2023b). A visualization of the dataset collections used in Cavia can be seen in Fig. 18.

HumanVid (Wang et al., 2024h) introduces a human-centric dataset enriched with camera annotations, enabling precise modeling of human-centric video generation.

KFC-W (Chou et al., 2024) introduces an auxiliary task of multi-view inpainting for training video models. This approach enables the model to learn 3D priors from large-scale, unposed internet photos.

CineMaster (Wang et al., 2025) proposes a customized data labeling pipeline that leverages existing depth prediction (Yang et al., 2024e;f), instance segmentation (Ravi et al., 2024) and scene reconstruction (Zhang et al., 2024d) models to generate labeled data. This enables a 3D-aware model to train on large-scale, in-the-wild video data.

4.6.2 Architecture for 3D diffusion models

In addition to data-driven approaches for learning 3D priors, another promising strategy involves designing 3D-specific model architectures that incorporate inductive biases for generating view consistent images. Traditional U-Net based video diffusion models typically capture inter-frame relationships using temporal attention layers, which are implemented through per-pixel attention along the temporal dimension. While this enables information flow between frames at the same spatial positions, it is suboptimal for achieving 3D awareness.

Recently, multi-view diffusion models (Shi et al., 2023d; Tang et al., 2023; Yang et al., 2024b; Liu et al., 2024b;f; Hu et al., 2024; Kant et al., 2024; Yang et al., 2024d; Oh et al., 2023; Tang et al., 2024) have gained significant attention for static 3D scene generation. By employing cross-frame attention, these models effectively enhance the spatial relationships necessary for 3D consistency. For static 3D scene generation, epipolar-constrained attention (Xu et al., 2024b; Huang et al., 2023c; Zheng et al., 2024a) further enforces strict adherence to 3D constraints, ensuring greater structural accuracy.

This concept has also been extended to multi-view video diffusion models (Li et al., 2024a; Xie et al., 2024b; Xu et al., 2024a). By integrating both cross-frame and cross-view attention mechanisms, video models are fine-tuned to support 4D generation, enabling them to produce spatiotemporally consistent videos that adhere to 3D principles.

In DiT-like structures (Gao∗et al., 2024; Chou et al., 2024; Liang et al., 2024b; Gu et al., 2025; Wang et al., 2025), cross-frame attention is inherently achieved as tokens for different temporal and spatial locations are jointly mixed through transformer, allowing the model to learn 3D priors directly from data.

4.6.3 Camera conditioning

Cameras serve as a bridge between the 3D world and 2D images. Given a 3D scene, intrinsic and extrinsic camera parameters determine how the 3D scene is projected into a 2D image. Adapting a video diffusion model to be 3D-aware involves conditioning the model with camera parameters, allowing users to control the generated views. Typically, fine-tuning is required after introducing this additional conditioning, as discussed in Sec. 4.6.1.

Several commonly used approaches exist for conditioning video diffusion models with camera parameters:

- **MLP-based embedding**. A straightforward method is to use a fully connected multi-layer perceptron (MLP) to embed camera parameters. These parameters are often represented as elevation and azimuth angles, as in SV3D (Voleti et al., 2024; Yang et al., 2024c), panning and zooming movement (Yang et al., 2024h), or as a relative camera extrinsic matrix (Van Hoorick et al., 2024; Wang et al., 2024k; 2025). This embedding serves as a global condition, typically introduced into the diffusion model via cross-attention layers.

- **Ray map**. A camera defines a mapping from each pixel location in image space to a ray in 3D space. This mapping can be represented as a "ray map," which stores the ray origin and direction for each pixel location instead of RGB color. The ray map forms a spatially aligned representation with six channels, matching the resolution of an image. This method is particularly suited for scene-level

video diffusion models requiring pixel-aligned conditioning (Gao∗et al., 2024; Watson et al., 2024; Wu et al., 2024e).

- **Plücker coordinates**. Plücker coordinates are an alternative to a ray map, parameterizing a ray as $(\mathbf{o} \times \mathbf{d}, \mathbf{o})$, where $\mathbf{o}$ is the ray origin, $\mathbf{d}$ is the normalized ray direction, and $\times$ denotes the cross product. This representation provides a uniform way to encode rays, making it a suitable positional embedding for video diffusion models (Xu et al., 2024b;a; Bahmani et al., 2024d;b; He et al., 2024a; Kuang et al., 2024; Yao et al., 2024; Wang et al., 2024h; Zheng et al., 2024a; Liang et al., 2024b).

- **Point-based**. Camera conditioning can also be achieved implicitly by motions of 2D or 3D points. For instance, I2VControl-Camera (Feng et al., 2024b) employs point trajectories in the camera coordinate system as control signals, enabling precise control over the generated views. Similarly, Motion Prompting (Geng et al., 2024a) converts camera poses into image-space point trajectories. This is achieved by projecting a 3D point cloud, estimated using a monocular depth estimator, onto 2D points in image space. Diffusion as Shader (Gu et al., 2025) leverages a tracking video of dense 3D points as control signals to train a video DiT model, enabling detailed control over both camera and motion controls.

4.6.4 Inference-time tricks

Interestingly, there are a few efforts being made to explore whether it is possible to directly use a pre-trained video diffusion model for 3D-aware video generation without any fine-tuning. ViVid-1-to-3 (Kwak et al., 2024) combines a video diffusion model with Zero-1-to-3 XL to jointly denoise multi-view videos, effectively leveraging the 3D priors from Zero-1-to-3 XL alongside the temporal consistency inherent in video diffusion models. NVS-Solver (You et al., 2024) guides the sampling process of a pre-trained Stable Video Diffusion (SVD) model by iteratively modulating the score function with the given scene priors represented derived from warped input views, effectively achieving novel view synthesis from sparse input views. CamTrol (Hou et al., 2024) directs video generation by employing DDIM inversion noise derived from point cloud renderings, enabling 3D-aware video synthesis without the need for model fine-tuning.

5 Benefits to other domains

5.1 Video representation learning

Video representation learning (Ravanbakhsh et al., 2024), as a foundational task in video understanding, it provides downstream tasks with powerful backbones and useful representations. Early methods (Seo et al., 2020; Wu et al., 2022a) primarily relied on 2D Convolutional Neural Networks (CNNs) (He et al., 2016; Krizhevsky et al., 2012) to extract spatial features from individual frames. These methods treated video data as sequences of static images, which limited their ability to capture temporal dynamics. To address this, researchers began incorporating Recurrent Neural Networks (RNNs) (Hopfield, 1982) and Long Short-Term Memory (LSTM) (Hochreiter & Schmidhuber, 1997) networks to model temporal dependencies across frames. However, these approaches (Liu et al., 2016; 2018) often struggled with capturing complex, long-range temporal relationships and integrating spatial-temporal information efficiently.

The development of 3D CNNs marked a significant advancement, enabling simultaneous modeling of spatial and temporal features by applying convolutions across both space and time dimensions. This shift allowed for more holistic video representation (Tran et al., 2015), leading to better performance in tasks such as action recognition (Yang et al., 2019; Kong et al., 2017) and video captioning (Yan et al., 2022). More recently, attention mechanisms and Transformers (Vaswani et al., 2017) have been introduced to further enhance video representation learning (Zhao et al., 2022; Gabeur et al., 2020; Cao et al., 2022; Botach et al., 2022; Wu et al., 2022b). These models, especially those utilizing self-attention, can capture long-range dependencies and complex interactions between frames, leading to more robust and generalizable video representations. The evolution of video representation learning has been characterized by a gradual shift from static image processing to dynamic, sequence-based modeling, reflecting the unique challenges of video data.

On the other side, video-language learning (Radford et al., 2021; Li et al., 2022) has been boosted by the integration of advanced models (Vaswani et al., 2017; He et al., 2016) and the increasing complexity of tasks that involve understanding both visual and textual information. Early attempts at video representation learning (Lei et al., 2021) relied heavily on separate processing of video and language inputs, where modality-dependent models were used to extract features from video frames and textual data independently. However, this approach often fails to capture the intricate relationships between the two modalities. The introduction of Transformer-based models (Ye et al., 2023) marked a significant advancement, enabling more effective modeling of cross-modal interactions through self-attention mechanisms. These models can jointly process video and language inputs (Zhao et al., 2023b), leading to improved performance on tasks, *e.g.*, video captioning (Li et al., 2023), video retrieval (Wang et al., 2024b), and video question answering (Pan et al., 2023).

As shown by previous works in image generation (Chi et al., 2024), a pretrained video generative model might be able to serve as prior, loss, or regularize in learning video representations. Recently, a pioneer work (Yeh et al., 2024) employs image and video generative models for hateful visual content recognition. It queries well-trained SOTA image and video generative models to automatically scale up training data pairs for hateful visual content recognition, achieving superior performance.

5.2 Video retrieval

Video retrieval, mainly video-text retrieval (VTR), which involves cross-modal alignment and abstract understanding of temporal images (videos), has been a popular and fundamental task of language-grounding problems (Wang et al., 2020a;b; 2021; Yu et al., 2023b). Most existing conventional video-text retrieval frameworks (Yu et al., 2017; Dong et al., 2019; Zhu & Yang, 2020; Miech et al., 2020; Gabeur et al., 2020; Dzabraev et al., 2021; Croitoru et al., 2021) focus on learning powerful representations for video and text and extracting modality-dependent representations with modality-dependent encoders. Inspired by the success of self-supervised pretraining methods (Devlin et al., 2019; Radford et al., 2019; Brown et al., 2020) and vision-language pretraining (Li et al., 2020; Gan et al., 2020; Singh et al., 2022) on large-scale unlabeled cross-modal data, recent works (Lei et al., 2021; Cheng et al., 2021; Gao et al., 2021; Ma et al., 2022; Park et al., 2022; Wang et al., 2022a;b; Zhao et al., 2022; Gorti et al., 2022; Luo et al., 2022; Liu et al., 2022d;a; Cao et al., 2022) have attempted to pretrain or fine-tune video-text retrieval models (Gorti et al., 2022; Lei et al., 2021).

With the rapid progress in video generation, leveraging the advancement in video generation (Chen et al., 2024b; Muaz et al., 2023) to advance video retrieval by reranking (Zhou et al., 2024e; Dutta et al., 2021) or other methods becomes more and more promising. On the other side, retrieval augmented generation could also help faithful video generation (Arefeen et al., 2024; Rosa, 2024; Tevissen et al., 2024; He et al., 2023a).

5.3 Video QA and captioning

Video question answering (VideoQA) (Zhong et al., 2022; Wu et al., 2024a) is a task to predict the correct answer given a question and a video. Early work (Zeng et al., 2017; Xu et al., 2017; Zhao et al., 2017; Jang et al., 2017) focused on simpler factoid questions with the introduction of datasets like MSVD-QA and TGIF-QA. Techniques during this period primarily relied on attention mechanisms and memory networks to handle the spatial and temporal complexities of video data. Later, more challenging datasets emerged, such as NExT-QA, which emphasized inference and reasoning over merely recognizing visual facts. This shift necessitated the development of more advanced models, including Graph Neural Networks (GNNs) for relational reasoning and Transformers for their powerful sequence modeling capabilities, particularly when enhanced with cross-modal pre-training strategies.

Recently, the focus has increasingly shifted towards models that can handle multi-modal inputs and perform more complex reasoning tasks. Knowledge-based VideoQA datasets and techniques have also attracted more and more attention, pushing the boundaries of what VideoQA systems can achieve. Modular networks and neural-symbolic approaches are being explored to improve flexibility and interpretability, addressing the need for models that can reason about causal and temporal relationships in video content. On the other

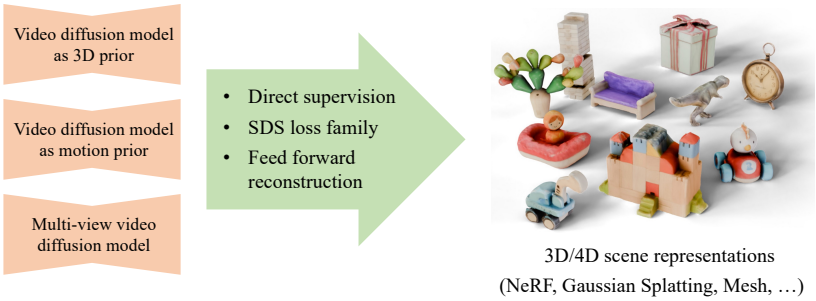

Figure 19: A common paradigm for 3D and 4D generation is by distilling 3D or motion knowledge from video generation models to 3D and 4D scene representation.

side, understanding long videos could be a big challenge to current models as long videos require a more comprehensive understanding among different frames and a long term memory.

In the future, pre-trained models originally designed for video generation can be used to enhance VideoQA by predicting future frames or generating hypothetical scenarios to answer complex questions. Also, text-to-video generation methods can be used for generating diverse VideoQA benchmarks.

5.4 3D and 4D generation

One emerging area of research focuses on generating 3D and 4D scene representations, such as textured meshes, Neural Radiance Fields (NeRF) (Mildenhall et al., 2021), and Gaussian Splatting (GS) (Kerbl et al., 2023). These representations hold significant potential for applications in 3D content creation and immersive virtual reality. However, due to the heterogeneous nature of 3D and 4D representations, and the scarcity of large-scale 3D and 4D datasets, it is difficult to design feed-forward neural networks capable of directly generating such representations.

To address these challenges, a common approach involves distilling knowledge from video generative models to reconstruct multiple viewpoints of a 3D scene. This strategy leverages advancements in video generation to synthesize complex 3D structures effectively. Recent studies have explored the potential of video diffusion models in facilitating 3D and 4D generation, offering promising avenues for bridging the gap between video and high-dimensional scene representation.

5.4.1 Video diffusion for 3D generation

When generating 3D scenes from 2D models using multiple views, a major challenge is to maintain view consistency, which requires capturing inter-frame correlations across the generated views. Video diffusion models provide a general solution to inter-frame correlations. By treating the temporal dimension as different viewpoints, pre-trained video diffusion models can be fine-tuned into multi-view diffusion models. Several methods have been proposed to use a 2D video generation model for 3D scene generation:

V3D (Chen et al., 2024f) leverages the predictions of fine-tuned video diffusion models as direct supervision to generate 3D Gaussian splatting or meshes. SV3D (Voleti et al., 2024) employs the outputs of a fine-tuned Stable Video Diffusion model to supervise a Neural Radiance Field (NeRF) in the coarse stage, then uses SDS loss to refine high-frequency details of DMTet (Shen et al., 2021) initialized from the coarse stage. IM-3D (Melas-Kyriazi et al., 2024) adopts an instructive NeRF-to-NeRF (Haque et al., 2023) pipeline for distillation. This involves iteratively adding noise to rendered results and using a diffusion model to denoise the images, which then serve as targets for updating the 3D representation. VFusion3D (Junlin Han, 2024) demonstrates the potential of fine-tuned video diffusion models as data generators for creating large-scale 3D datasets. These datasets can be used to train feed-forward 3D generation models. Hi3D (Yang et al., 2024c) follows a coarse-to-fine 3D generation pipeline. It first generates low-resolution orbiting videos using a text-to-video model, then refines these into high-resolution orbiting videos with a video-to-video model. Both models are fine-tuned from pre-trained video diffusion models with camera condition extensions. The

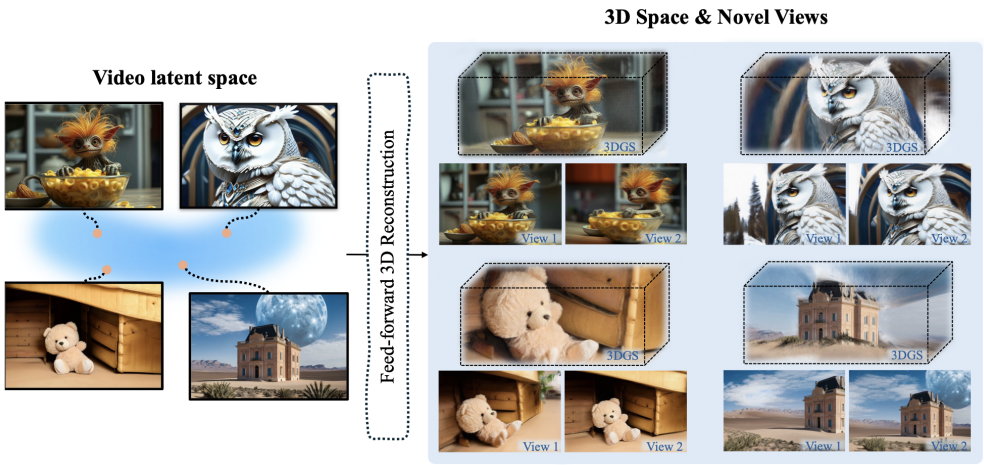

Figure 20: By training a feed-forward reconstruction model from a video generative model, Wonderland Liang et al. (2024b) achieves remarkable 3D scene generation results.

high-resolution orbiting videos are subsequently used to reconstruct 3D meshes. ReconX (Liu et al., 2024a) fine-tunes video diffusion models for sparse-view novel view synthesis, enabling efficient reconstruction of 3D scenes from limited input views. With recent advancements in large reconstruction models (LRMs) (Hong et al., 2023b; Zhang et al., 2024e), Wonderland (Liang et al., 2024b) demonstrates that by training a feed-forward 3D reconstruction model from the latent space of a video generative model, remarkable scene generation results can be achieved. Some examples are shown in Fig. 20.

5.4.2 Video diffusion for 4D generation

The incorporation of the additional time dimension in 4D generation significantly increases the complexity of developing and training feed-forward networks. Video diffusion models, functioning as motion generators, offer a promising solution by enabling the extraction of scene dynamics and motion information for 4D generation.

Several approaches leverage video diffusion models to train dynamic Neural Radiance Fields (NeRFs) or other 4D representations: MAV3D (Singer et al., 2023), 4D-fy (Bahmani et al., 2024c), Dream-in-4D (Zheng et al., 2024b), Align-Your-Gaussians (Ling et al., 2024a), and Animate124 (Zhao et al., 2023e) apply Score Distillation Sampling (SDS) loss along the temporal axis to train dynamic NeRFs using video diffusion models. These methods enable the models to learn motion dynamics directly from video diffusion. Vidu4D (Wang et al., 2024g) and STAG4D (Zeng et al., 2024b) propose robust reconstruction pipelines to reconstruct dynamic Gaussian Surfels or Gaussian splatting with monocular videos generated by video diffusion models. PLA4D (Miao et al., 2024) animates static 3D Gaussian splatting generated by 3D diffusion models, using video diffusion predictions combined with a motion alignment model. TC4D (Bahmani et al., 2024a) uses SDS loss to supervise dynamic NeRFs, incorporating a trajectory-conditioned video model that disentangles global and local motion components, facilitating the generation of large-scale motions.

Dynamic motion knowledge can also be combined with spatial 3D knowledge from multi-view diffusion models: EG4D (Sun et al., 2024) use a combination of SVD and SV3D models to directly generate multi-view videos, which are then used to supervise a 4D Gaussian splatting. 4Real (Yu et al., 2024a) generates 4D videos by using video diffusion model to supervise fixed-viewpoint video and freeze-time video with SDS loss. The use of deformable 3D GS ensures the temporal and view consistency. DreamGaussian4D (Ren et al., 2023) employs a training-free video-to-video pipeline that uses pre-trained video diffusion models to refine the dynamic textures of generated mesh sequences.

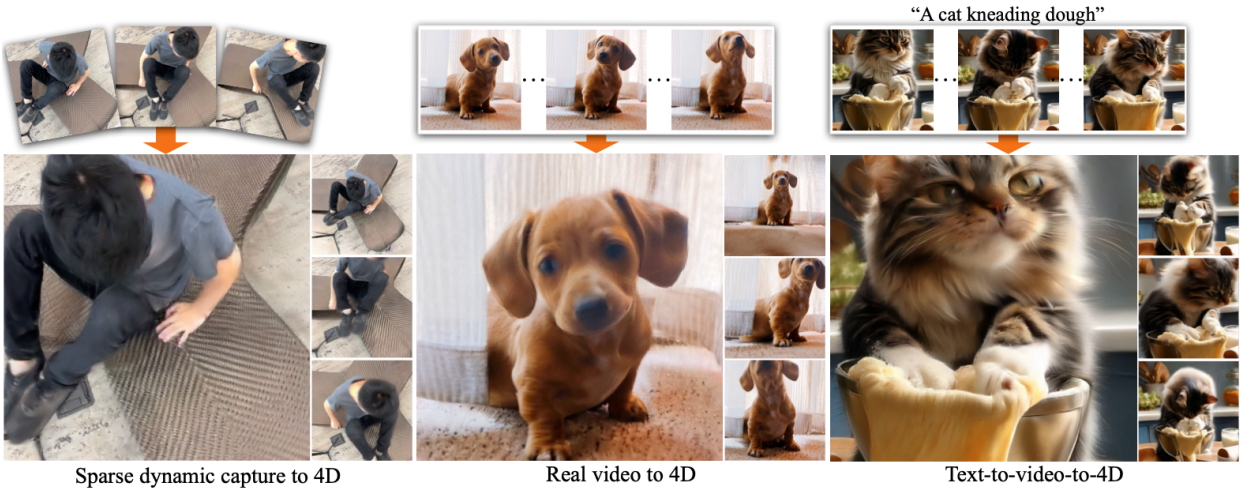

Figure 21: CAT4D (Wu et al., 2024e) trains a multi-view video diffusion model conditioned on a monocular video, which enables 4D view synthesis from casually captured monocular videos.

Several approaches aim to fine-tune video diffusion models into 4D-aware diffusion models, enabling the unified learning of spatial and temporal information. Such a direct 4D generator could be further distilled into a 4D scene representation for better temporal and view consistency or real-time rendering.

Diffusion4D (LIANG et al., 2024) fine-tunes a video diffusion model conditioned on camera pose and timestamps to generate orbiting views of dynamic scenes, which are then used to optimize dynamic Gaussian splatting. 4Diffusion (Zhang et al., 2024c) and Animate3D (Jiang et al., 2024a) train multi-view video diffusion models capable of simultaneously generating videos from different viewpoints, and then train dynamic NeRFs with SDS loss. VideoMV (Zuo et al., 2024) trains a multi-view video diffusion model and a feed-forward Gaussian splatting reconstruction model that directly predicts GS from sparse views generated by the multi-view video diffusion model. Vivid-ZOO (Li et al., 2024a) reuses pre-trained 2D video and multi-view diffusion models to bridge the gap toward 4D generation.

SV4D (Xie et al., 2024b) and CAT4D (Wu et al., 2024e) train multi-view video diffusion models conditioned on monocular reference videos, enabling video-to-4D tasks, as shown in Fig. 21.

6 Conclusion and outlook

This survey presented a comprehensive analysis of diffusion-based video generation, tracing its evolution from traditional GAN-based approaches to current state-of-the-art methodologies. Through our systematic examination, we have highlighted how diffusion models have addressed many historical challenges in video generation while introducing new opportunities and considerations for future research. The field of diffusion-based video generation has demonstrated remarkable progress in generating temporally consistent and visually compelling videos.

Our analysis reveals several key insights: First, the transition from GAN-based methods to diffusion models has significantly improved training stability and output quality, though computational efficiency remains a crucial challenge. Second, the integration of diffusion models with various architectural innovations has enhanced temporal coherence and motion consistency, particularly in long video generation. Third, the application of video generation methods has broadened considerably, from low-level vision tasks to complex video understanding problems.

Despite these advances, several critical challenges remain:

- Computational Efficiency: Future research should focus on reducing the computational demands of both training and inference, particularly for real-time applications.

- Long-Video Generation: While progress has been made in handling long video generation, maintaining consistency and coherence in long videos remains challenging.
- Adhering Physical Rules: Ensuring generated videos adhere to physical laws and maintain realistic object dynamics requires continued attention.
- Ethical Considerations: As these technologies become more powerful, developing robust frameworks for addressing bias and preventing misuse becomes increasingly important.

Corresponding to these challenges, we anticipate several promising research directions: 1) the development of more efficient architectures and training strategies to reduce computational requirements while maintaining generation quality. 2) integration of physical priors and domain knowledge to improve the realism of generated videos. 3) exploration of hybrid approaches that combine the strengths of diffusion models with other generative frameworks. 4) investigation of scalable solutions for real-world applications, particularly in domains such as virtual reality and autonomous systems.

As the field continues to evolve, the relations between diffusion-based video generation and related domains, such as video understanding and 3D generation, will likely drive further innovations. The community's focus on addressing both technical and ethical challenges will be crucial in realizing the full potential of this technology while ensuring its responsible development and deployment.

References

Rameen Abdal, Or Patashnik, Ivan Skorokhodov, Willi Menapace, Aliaksandr Siarohin, Sergey Tulyakov, Daniel Cohen-Or, and Kfir Aberman. Dynamic concepts personalization from single videos, 2025. URL `https://arxiv.org/abs/2502.14844`. 4.3

Luca Savant Aira, Antonio Montanaro, Emanuele Aiello, Diego Valsesia, and Enrico Magli. Motioncraft: Physics-based zero-shot video generation. *arXiv preprint arXiv:2405.13557*, 2024. 4.1.6

Michael S. Albergo, Nicholas M. Boffi, and Eric Vanden-Eijnden. Stochastic interpolants: A unifying framework for flows and diffusions. *arXiv: 2303.08797*, 2023. 2.2.4

Nuha Aldausari, Arcot Sowmya, Nadine Marcus, and Gelareh Mohammadi. Video generative adversarial networks: a review. *ACM Comput. Surv.*, 55(2):1–25, 2022. 1, 2.1.1

Jie An, Songyang Zhang, Harry Yang, Sonal Gupta, Jia-Bin Huang, Jiebo Luo, and Xi Yin. Latent-shift: Latent diffusion with temporal shift for efficient text-to-video generation. *arXiv preprint arXiv:2304.08477*, 2023. 2.5.1

Pierfrancesco Ardino, Marco De Nadai, Bruno Lepri, Elisa Ricci, and Stephane Lathuiliere. Click to move: Controlling video generation with sparse motion. In *ICCV*, pp. 14729–14738, 2021. 2.2.5

Md. Adnan Arefeen, Biplob Debnath, Md. Yusuf Sarwar Uddin, and Srimat Chakradhar. irag: An incremental retrieval augmented generation system for videos. *CoRR*, abs/2404.12309, 2024. 5.2

Dawit Mureja Argaw, Fabian Caba Heilbron, Joon-Young Lee, Markus Woodson, and In So Kweon. The anatomy of video editing: A dataset and benchmark suite for ai-assisted video editing. In Shai Avidan, Gabriel Brostow, Moustapha Cissé, Giovanni Maria Farinella, and Tal Hassner (eds.), *Computer Vision – ECCV 2022*, volume 13668, pp. 201–218, 2022. 3.1

Anurag Arnab, Mostafa Dehghani, Georg Heigold, Chen Sun, Mario Lučić, and Cordelia Schmid. Vivit: A video vision transformer. In *ICCV*, pp. 6836–6846, 2021. 2.5.2

Sherwin Bahmani, Xian Liu, Wang Yifan, Ivan Skorokhodov, Victor Rong, Ziwei Liu, Xihui Liu, Jeong Joon Park, Sergey Tulyakov, Gordon Wetzstein, Andrea Tagliasacchi, and David B. Lindell. Tc4d: Trajectory-conditioned text-to-4d generation. In *ECCV*, pp. 53–72, 2024a. 5.4.2

Sherwin Bahmani, Ivan Skorokhodov, Guocheng Qian, Aliaksandr Siarohin, Willi Menapace, Andrea Tagliasacchi, David B Lindell, and Sergey Tulyakov. Ac3d: Analyzing and improving 3d camera control in video diffusion transformers. *arXiv preprint arXiv:2411.18673*, 2024b. 4.1.3, 4.6.3

Sherwin Bahmani, Ivan Skorokhodov, Victor Rong, Gordon Wetzstein, Leonidas Guibas, Peter Wonka, Sergey Tulyakov, Jeong Joon Park, Andrea Tagliasacchi, and David B. Lindell. 4d-fy: Text-to-4d generation using hybrid score distillation sampling. In *CVPR*, pp. 7996–8006, 2024c. 5.4.2

Sherwin Bahmani, Ivan Skorokhodov, Aliaksandr Siarohin, Willi Menapace, Guocheng Qian, Michael Vasilkovsky, Hsin-Ying Lee, Chaoyang Wang, Jiaxu Zou, Andrea Tagliasacchi, et al. Vd3d: Taming large video diffusion transformers for 3d camera control. *arXiv preprint arXiv:2407.12781*, 2024d. 4.1.3, 4.6.3

Jianhong Bai, Tianyu He, Yuchi Wang, Junliang Guo, Haoji Hu, Zuozhu Liu, and Jiang Bian. Uniedit: A unified tuning-free framework for video motion and appearance editing. *arXiv preprint arXiv:2402.13185*, 2024. 4.1.5

Max Bain, Arsha Nagrani, Gül Varol, and Andrew Zisserman. Frozen in time: A joint video and image encoder for end-to-end retrieval. In *ICCV*, 2021. 1, 3.1, 3.4, 4.6.1

Fan Bao, Shen Nie, Kaiwen Xue, Yue Cao, Chongxuan Li, Hang Su, and Jun Zhu. All are worth words: A vit backbone for diffusion models. In *CVPR*, pp. 22669–22679, 2023a. 2.5.4

Fan Bao, Shen Nie, Kaiwen Xue, Chongxuan Li, Shi Pu, Yaole Wang, Gang Yue, Yue Cao, Hang Su, and Jun Zhu. One transformer fits all distributions in multi-modal diffusion at scale. In *ICML*, pp. 1692–1717, 2023b. 2.5.3

Michael J Black and Padmanabhan Anandan. A framework for the robust estimation of optical flow. In *ICCV*, pp. 231–236, 1993. 2.4.2

Andreas Blattmann, Tim Dockhorn, Sumith Kulal, Daniel Mendelevitch, Maciej Kilian, Dominik Lorenz, Yam Levi, Zion English, Vikram Voleti, Adam Letts, et al. Stable video diffusion: Scaling latent video diffusion models to large datasets. *arXiv preprint arXiv:2311.15127*, 2023a. 3.2, 4.1.1, 4.6.1

Andreas Blattmann, Robin Rombach, Huan Ling, Tim Dockhorn, Seung Wook Kim, Sanja Fidler, and Karsten Kreis. Align your latents: High-resolution video synthesis with latent diffusion models. In *CVPR*, pp. 22563–22575, 2023b. 2.1.3, 2.4.1, 2.4.4, 2.5.3

Nicolas Bonneel, James Tompkin, Kalyan Sunkavalli, Deqing Sun, Sylvain Paris, and Hanspeter Pfister. Blind video temporal consistency. *TOG*, 34(6), 2015. 3.3

Adam Botach, Evgenii Zheltonozhskii, and Chaim Baskin. End-to-end referring video object segmentation with multimodal transformers. In *CVPR*, pp. 4975–4985, 2022. 5.1

Tim Brooks, Janne Hellsten, Miika Aittala, Ting-Chun Wang, Timo Aila, Jaakko Lehtinen, Ming-Yu Liu, Alexei A. Efros, and Tero Karras. Generating long videos of dynamic scenes, 2022. 4.5

Tim Brooks, Aleksander Holynski, and Alexei A. Efros. Instructpix2pix: Learning to follow image editing instructions. In *CVPR*, pp. 18392–18402, 2023. 4.1.1

Tom B. Brown, Benjamin Mann, Nick Ryder, Melanie Subbiah, Jared Kaplan, Prafulla Dhariwal, Arvind Neelakantan, Pranav Shyam, Girish Sastry, Amanda Askell, Sandhini Agarwal, Ariel Herbert-Voss, Gretchen Krueger, Tom Henighan, Rewon Child, Aditya Ramesh, Daniel M. Ziegler, Jeffrey Wu, Clemens Winter, Christopher Hesse, Mark Chen, Eric Sigler, Mateusz Litwin, Scott Gray, Benjamin Chess, Jack Clark, Christopher Berner, Sam McCandlish, Alec Radford, Ilya Sutskever, and Dario Amodei. Language models are few-shot learners. In *NeurIPS*, 2020. 5.2

Andrés Bruhn, Joachim Weickert, and Christoph Schnörr. Lucas/kanade meets horn/schunck: Combining local and global optic flow methods. *Int. J. Comput. Vis.*, 61(3):211–231, 2005. 2.4.2

Ryan Burgert, Yuancheng Xu, Wenqi Xian, Oliver Pilarski, Pascal Clausen, Mingming He, Li Ma, Yitong Deng, Lingxiao Li, Mohsen Mousavi, et al. Go-with-the-flow: Motion-controllable video diffusion models using real-time warped noise. *arXiv preprint arXiv:2501.08331*, 2025. 3, 2.4.2

Shuqiang Cao, Bairui Wang, Wei Zhang, and Lin Ma. Visual consensus modeling for video-text retrieval. In *AAAI*, pp. 167–175, 2022. 5.1, 5.2

Yihan Cao, Siyu Li, Yixin Liu, Zhiling Yan, Yutong Dai, Philip S. Yu, and Lichao Sun. A comprehensive survey of ai-generated content (aigc): A history of generative ai from gan to chatgpt, 2023. (document), 1

Joao Carreira and Andrew Zisserman. Quo vadis, action recognition? a new model and the kinetics dataset. In *CVPR*, 2017. 3.1

Duygu Ceylan, Chun-Hao P. Huang, and Niloy J. Mitra. Pix2video: Video editing using image diffusion. In *ICCV*, pp. 23149–23160, 2023. 4.1.5

Wenhao Chai, Xun Guo, Gaoang Wang, and Yan Lu. Stablevideo: Text-driven consistency-aware diffusion video editing. In *ICCV*, pp. 23040–23050, 2023. 1, 4.1.5, 4.4

Di Chang, Yichun Shi, Quankai Gao, Hongyi Xu, Jessica Fu, Guoxian Song, Qing Yan, Yizhe Zhu, Xiao Yang, and Mohammad Soleymani. Magicpose: Realistic human poses and facial expressions retargeting with identity-aware diffusion. In *ICML*, 2023a. 4.1.5

Pascal Chang, Jingwei Tang, Markus Gross, and Vinicius C Azevedo. How i warped your noise: a temporally-correlated noise prior for diffusion models. In *ICLR*, 2024. 2.4.2, 4.4

Shao-Yu Chang, Hwann-Tzong Chen, and Tyng-Luh Liu. Diffusionatlas: High-fidelity consistent diffusion video editing. *arXiv preprint arXiv:2312.03772*, 2023b. 4.1.5

Ya-Liang Chang, Zhe Yu Liu, Kuan-Ying Lee, and Winston Hsu. Free-form video inpainting with 3d gated convolution and temporal patchgan. In *ICCV*, pp. 9066–9075, 2019. 4.2.2

Hila Chefer, Shiran Zada, Roni Paiss, Ariel Ephrat, Omer Tov, Michael Rubinstein, Lior Wolf, Tali Dekel, Tomer Michaeli, and Inbar Mosseri. Still-moving: Customized video generation without customized video data. *ACM Transactions on Graphics (TOG)*, 43(6):1–11, 2024. 4.3

Haoxin Chen, Menghan Xia, Yingqing He, Yong Zhang, Xiaodong Cun, Shaoshu Yang, Jinbo Xing, Yaofang Liu, Qifeng Chen, Xintao Wang, et al. Videocrafter1: Open diffusion models for high-quality video generation. *arXiv preprint arXiv:2310.19512*, 2023a. 2.4.4, 2.5.3, 3.4, 4.1.1

Haoxin Chen, Yong Zhang, Xiaodong Cun, Menghan Xia, Xintao Wang, Chao Weng, and Ying Shan. Videocrafter2: Overcoming data limitations for high-quality video diffusion models. In *CVPR*, pp. 7310–7320, 2024a. 2.4.4, 3.1, 3.4

Jiahui Chen et al. Internvid: Learning text-to-video generation from web-scale video-text data. *arXiv preprint arXiv:2303.11123*, 2023b. 4.6.1

Junsong Chen, YU Jincheng, GE Chongjian, Lewei Yao, Enze Xie, Zhongdao Wang, James Kwok, Ping Luo, Huchuan Lu, and Zhenguo Li. Pixart-alpha: Fast training of diffusion transformer for photorealistic text-to-image synthesis. In *ICLR*, 2023c. 2.5.3

Long Chen and Jing Sun. Videogen: Generalized text-to-video generation. *arXiv preprint arXiv:2306.05012*, 2023. 2.4.4

Shoufa Chen, Mengmeng Xu, Jiawei Ren, Yuren Cong, Sen He, Yanping Xie, Animesh Sinha, Ping Luo, Tao Xiang, and Juan-Manuel Perez-Rua. Gentron: Diffusion transformers for image and video generation. In *CVPR*, pp. 6441–6451, 2024b. 2.5.2, 5.2

Ting Chen. On the importance of noise scheduling for diffusion models. *arXiv preprint arXiv:2301.10972*, 2023. 2.4.3

Tsai-Shien Chen, Aliaksandr Siarohin, Willi Menapace, Ekaterina Deyneka, Hsiang-Wei Chao, Byung Eun Jeon, Yuwei Fang, Hsin-Ying Lee, Jian Ren, Ming-Hsuan Yang, and Sergey Tulyakov. Panda-70m: Captioning 70m videos with multiple cross-modality teachers. In *CVPR*, pp. 13320–13331, 2024c. 1, 3.1

Tsai-Shien Chen, Aliaksandr Siarohin, Willi Menapace, Yuwei Fang, Kwot Sin Lee, Ivan Skorokhodov, Kfir Aberman, Jun-Yan Zhu, Ming-Hsuan Yang, and Sergey Tulyakov. Multi-subject open-set personalization in video generation. *arXiv preprint arXiv:2501.06187*, 2025. 4.3

Xinyuan Chen, Yaohui Wang, Lingjun Zhang, Shaobin Zhuang, Xin Ma, Jiashuo Yu, Yali Wang, Dahua Lin, Yu Qiao, and Ziwei Liu. Seine: Short-to-long video diffusion model for generative transition and prediction. In *ICLR*, 2024d. 2.4.4, 2.5.3, 3.4, 4.4

Zhikai Chen, Fuchen Long, Zhaofan Qiu, Ting Yao, Wengang Zhou, Jiebo Luo, and Tao Mei. Learning spatial adaptation and temporal coherence in diffusion models for video super-resolution. In *CVPR*, pp. 9232–9241, 2024e. 4.2.4

Zilong Chen, Yikai Wang, Feng Wang, Zhengyi Wang, and Huaping Liu. V3d: Video diffusion models are effective 3d generators, 2024f. 4.6.1, 5.4.1

Jiaxin Cheng, Tianjun Xiao, and Tong He. Consistent video-to-video transfer using synthetic dataset. *arXiv preprint arXiv:2311.00213*, 2023. 4.1.5

Xing Cheng, Hezheng Lin, Xiangyu Wu, Fan Yang, and Dong Shen. Improving video-text retrieval by multi-stream corpus alignment and dual softmax loss. *CoRR*, abs/2109.04290, 2021. 5.2

Xiaowei Chi, Rongyu Zhang, Zhengkai Jiang, Yijiang Liu, Yatian Wang, Xingqun Qi, Wenhan Luo, Peng Gao, Shanghang Zhang, Qifeng Liu, and Yike Guo. M^2chat: Empowering vlm for multimodal llm interleaved text-image generation, 2024. 5.1

Gene Chou, Kai Zhang, Sai Bi, Hao Tan, Zexiang Xu, Fujun Luan, Bharath Hariharan, and Noah Snavely. Generating 3d-consistent videos from unposed internet photos, 2024. 4.6.1, 4.6.2

Ernie Chu, Shuo-Yen Lin, and Jun-Cheng Chen. Video controlnet: Towards temporally consistent synthetic-to-real video translation using conditional image diffusion models. *arXiv preprint arXiv:2305.19193*, 2023. 4.1.5

Hyungjin Chung, Jeongsol Kim, Geon Yeong Park, Hyelin Nam, and Jong Chul Ye. Cfg++: Manifold-constrained classifier free guidance for diffusion models. *arXiv preprint arXiv:2406.08070*, 2024. 2.3.1

Aidan Clark, Jeff Donahue, and Karen Simonyan. Adversarial video generation on complex datasets. *arXiv preprint arXiv:1907.06571*, 2019. 1, 2.1.1

Paul Couairon, Clément Rambour, Jean-Emmanuel Haugeard, and Nicolas Thome. Videdit: Zero-shot and spatially aware text-driven video editing. *TMLR*, 2023. 4.1.5

Ioana Croitoru, Simion-Vlad Bogolin, Marius Leordeanu, Hailin Jin, Andrew Zisserman, Samuel Albanie, and Yang Liu. Teachtext: Crossmodal generalized distillation for text-video retrieval. In *ICCV*, pp. 11563–11573, 2021. 5.2

Zuozhuo Dai, Zhenghao Zhang, Yao Yao, Bingxue Qiu, Siyu Zhu, Long Qin, and Weizhi Wang. Fine-grained open domain image animation with motion guidance, 2023. 4.1.1

Duolikun Danier, Fan Zhang, and David Bull. Ldmvfi: Video frame interpolation with latent diffusion models. In *AAAI*, pp. 1472–1480, 2024. 4.2.3

Tri Dao, Daniel Y. Fu, Stefano Ermon, Atri Rudra, and Christopher Ré. Flashattention: Fast and memory-efficient exact attention with io-awareness. In *NeurIPS*, 2022. 3.2

Aram Davtyan and Paolo Favaro. Controllable video generation through global and local motion dynamics. In *ECCV*, pp. 68–84, 2022. 1

Matt Deitke, Dustin Schwenk, Jordi Salvador, Luca Weihs, Oscar Michel, Eli VanderBilt, Ludwig Schmidt, Kiana Ehsani, Aniruddha Kembhavi, and Ali Farhadi. Objaverse: A universe of annotated 3d objects. *arXiv preprint arXiv:2212.08051*, 2022. 4.6.1

Matt Deitke, Ruoshi Liu, Matthew Wallingford, Huong Ngo, Oscar Michel, Aditya Kusupati, Alan Fan, Christian Laforte, Vikram Voleti, Samir Yitzhak Gadre, Eli VanderBilt, Aniruddha Kembhavi, Carl Vondrick, Georgia Gkioxari, Kiana Ehsani, Ludwig Schmidt, and Ali Farhadi. Objaverse-xl: A universe of 10m+ 3d objects. *arXiv preprint arXiv:2307.05663*, 2023. 4.6.1

Boyang Deng, Richard Tucker, Zhengqi Li, Leonidas Guibas, Noah Snavely, and Gordon Wetzstein. Streetscapes: Large-scale consistent street view generation using autoregressive video diffusion. In *SIGGRAPH*, pp. 1–11, 2024a. 4.1.2, 4.4

Yitong Deng, Winnie Lin, Lingxiao Li, Dmitriy Smirnov, Ryan Burgert, Ning Yu, Vincent Dedun, and Mohammad H. Taghavi. Infinite-resolution integral noise warping for diffusion models, 2024b. 2.4.2

Yufan Deng, Ruida Wang, Yuhao Zhang, Yu-Wing Tai, and Chi-Keung Tang. Dragvideo: Interactive drag-style video editing. *arXiv preprint arXiv:2312.02216*, 2023. 4.1.5

Jacob Devlin, Ming-Wei Chang, Kenton Lee, and Kristina Toutanova. Bert: Pre-training of deep bidirectional transformers for language understanding. In *NAACL*, pp. 4171–4186, 2019. 2.5.4, 5.2

Prafulla Dhariwal and Alexander Nichol. Diffusion models beat gans on image synthesis. In *NeurIPS*, pp. 8780–8794, 2021. 2.3.1, 2.3.1, 1, 2, 2.4.3, 2.5.3

Jianfeng Dong, Xirong Li, Chaoxi Xu, Shouling Ji, Yuan He, Gang Yang, and Xun Wang. Dual encoding for zero-example video retrieval. In *CVPR*, pp. 9346–9355, 2019. 5.2

Alexey Dosovitskiy, Philipp Fischer, Eddy Ilg, Philip Hausser, Caner Hazirbas, Vladimir Golkov, Patrick Van Der Smagt, Daniel Cremers, and Thomas Brox. Flownet: Learning optical flow with convolutional networks. In *ICCV*, pp. 2758–2766, 2015. 2.4.2

Alexey Dosovitskiy, Lucas Beyer, Alexander Kolesnikov, Dirk Weissenborn, Xiaohua Zhai, Thomas Unterthiner, Mostafa Dehghani, Matthias Minderer, Georg Heigold, Sylvain Gelly, et al. An image is worth 16x16 words: Transformers for image recognition at scale. In *ICLR*, 2020. 2.5.1

Laura Downs, Anthony Francis, Nate Koenig, Brandon Kinman, Ryan Hickman, Krista Reymann, Thomas B. McHugh, and Vincent Vanhoucke. Google scanned objects: A high-quality dataset of 3d scanned household items, 2022. 4.6.1

Nikita Drobyshev, Antoni Bigata Casademunt, Konstantinos Vougioukas, Zoe Landgraf, Stavros Petridis, and Maja Pantic. Emoportraits: Emotion-enhanced multimodal one-shot head avatars. In *Proceedings of the IEEE/CVF Conference on Computer Vision and Pattern Recognition*, pp. 8498–8507, 2024. 4.1.4, 4.3

Zhengxiao Du, Yujie Qian, Xiao Liu, Ming Ding, Jiezhong Qiu, Zhilin Yang, and Jie Tang. Glm: General language model pretraining with autoregressive blank infilling. *arXiv preprint arXiv:2103.10360*, 2021. 2.5.4

Titir Dutta, Anurag Singh, and Soma Biswas. Styleguide: Zero-shot sketch-based image retrieval using style-guided image generation. *IEEE Trans. Multim.*, 23:2833–2842, 2021. 5.2

Maksim Dzabraev, Maksim Kalashnikov, Stepan Komkov, and Aleksandr Petiushko. Mdmmt: Multidomain multimodal transformer for video retrieval. In *CVPR Workshops*, pp. 3354–3363, 2021. 5.2

Patrick Esser, Robin Rombach, and Bjorn Ommer. Taming transformers for high-resolution image synthesis. In *CVPR*, pp. 12873–12883, 2021. 2.5.3

Patrick Esser, Johnathan Chiu, Parmida Atighehchian, Jonathan Granskog, and Anastasis Germanidis. Structure and content-guided video synthesis with diffusion models. In *ICCV*, pp. 7346–7356, 2023. 2.4.1, 4.1.5

Patrick Esser, Sumith Kulal, Andreas Blattmann, Rahim Entezari, Jonas Müller, Harry Saini, Yam Levi, Dominik Lorenz, Axel Sauer, Frederic Boesel, et al. Scaling rectified flow transformers for high-resolution image synthesis. In *ICML*, 2024. 2.5.3, 2.5.4

Fanda Fan, Chunjie Luo, Wanling Gao, and Jianfeng Zhan. Aigcbench: Comprehensive evaluation of image-to-video content generated by ai, 2024. URL `https://arxiv.org/abs/2401.01651`. 3.1, 3.3

Ruoyu Feng, Wenming Weng, Yanhui Wang, Yuhui Yuan, Jianmin Bao, Chong Luo, Zhibo Chen, and Baining Guo. Ccedit: Creative and controllable video editing via diffusion models, 2024a. 2.1.3

Wanquan Feng, Jiawei Liu, Pengqi Tu, Tianhao Qi, Mingzhen Sun, Tianxiang Ma, Songtao Zhao, Siyu Zhou, and Qian He. I2vcontrol-camera: Precise video camera control with adjustable motion strength, 2024b. 4.6.3

Weixi Feng, Jiachen Li, Michael Saxon, Tsu-jui Fu, Wenhu Chen, and William Yang Wang. Tc-bench: Benchmarking temporal compositionality in text-to-video and image-to-video generation, June 2024c. 3.3

Rafail Fridman, Amit Abecasis, Yoni Kasten, and Tali Dekel. Scenescape: Text-driven consistent scene generation, 2023. 4.4

Tsu-Jui Fu, Licheng Yu, Ning Zhang, Cheng-Yang Fu, Jong-Chyi Su, William Yang Wang, and Sean Bell. Tell me what happened: Unifying text-guided video completion via multimodal masked video generation. In *CVPR*, pp. 10681–10692, 2023. 4.2.3, 12

Xiao Fu, Xian Liu, Xintao Wang, Sida Peng, Menghan Xia, Xiaoyu Shi, Ziyang Yuan, Pengfei Wan, Di Zhang, and Dahua Lin. 3dtrajmaster: Mastering 3d trajectory for multi-entity motion in video generation. *arXiv preprint arXiv:2412.07759*, 2024. 9, 4.1.3

Hiroki Furuta, Heiga Zen, Dale Schuurmans, Aleksandra Faust, Yutaka Matsuo, Percy Liang, and Sherry Yang. Improving dynamic object interactions in text-to-video generation with ai feedback. *arXiv preprint arXiv:2412.02617*, 2024a. 2.2.5

Hiroki Furuta et al. Learning dynamic object interactions in video generation through ai feedback. *arXiv preprint*, 2024b. 2.2.5

Valentin Gabeur, Chen Sun, Karteek Alahari, and Cordelia Schmid. Multi-modal transformer for video retrieval. In *ECCV*, pp. 214–229, 2020. 5.1, 5.2

Rinon Gal, Yuval Alaluf, Yuval Atzmon, Or Patashnik, Amit H Bermano, Gal Chechik, and Daniel Cohen-Or. An image is worth one word: Personalizing text-to-image generation using textual inversion. *arXiv preprint arXiv:2208.01618*, 2022. 2.2.8

Zhe Gan, Yen-Chun Chen, Linjie Li, Chen Zhu, Yu Cheng, and Jingjing Liu. Large-scale adversarial training for vision-and-language representation learning. In *NeurIPS*, 2020. 5.2

Kaifeng Gao, Jiaxin Shi, Hanwang Zhang, Chunping Wang, and Jun Xiao. Vid-gpt: Introducing gpt-style autoregressive generation in video diffusion models, 2024. 4.5

Zijian Gao, Jingyu Liu, Sheng Chen, Dedan Chang, Hao Zhang, and Jinwei Yuan. Clip2tv: An empirical study on transformer-based methods for video-text retrieval. *CoRR*, abs/2111.05610, 2021. 5.2

Ruiqi Gao∗, Aleksander Holynski∗, Philipp Henzler, Arthur Brussee, Ricardo Martin-Brualla, Pratul P. Srinivasan, Jonathan T. Barron, and Ben Poole∗. Cat3d: Create anything in 3d with multi-view diffusion models. *arXiv*, 2024. 4.6.2, 4.6.3

Songwei Ge, Thomas Hayes, Harry Yang, Xi Yin, Guan Pang, David Jacobs, Jia-Bin Huang, and Devi Parikh. Long video generation with time-agnostic vqgan and time-sensitive transformer. In *ECCV*, pp. 102–118, 2022. 2.1.2, 4.5

Songwei Ge, Seungjun Nah, Guilin Liu, Tyler Poon, Andrew Tao, Bryan Catanzaro, David Jacobs, Jia-Bin Huang, Ming-Yu Liu, and Yogesh Balaji. Preserve your own correlation: A noise prior for video diffusion models. In *ICCV*, pp. 22930–22941, 2023. 2.4.1, 4.4

Daniel Geng, Charles Herrmann, Junhwa Hur, Forrester Cole, Serena Zhang, Tobias Pfaff, Tatiana Lopez-Guevara, Carl Doersch, Yusuf Aytar, Michael Rubinstein, Chen Sun, Oliver Wang, Andrew Owens, and Deqing Sun. Motion prompting: Controlling video generation with motion trajectories. *arXiv preprint arXiv:2412.02700*, 2024a. 3.2, 4.6.3

Daniel Geng, Charles Herrmann, Junhwa Hur, Forrester Cole, Serena Zhang, Tobias Pfaff, Tatiana Lopez-Guevara, Carl Doersch, Yusuf Aytar, Michael Rubinstein, et al. Motion prompting: Controlling video generation with motion trajectories. *arXiv preprint arXiv:2412.02700*, 2024b. 4.1.2

Michal Geyer, Omer Bar-Tal, Shai Bagon, and Tali Dekel. Tokenflow: Consistent diffusion features for consistent video editing. *arXiv preprint arXiv:2307.10373*, 2023. 4.1.5, 4.4

Litong Gong, Yiran Zhu, Weijie Li, Xiaoyang Kang, Biao Wang, Tiezheng Ge, and Bo Zheng. Atomovideo: High fidelity image-to-video generation, 2024. 4.1.1

Ian Goodfellow, Jean Pouget-Abadie, Mehdi Mirza, Bing Xu, David Warde-Farley, Sherjil Ozair, Aaron Courville, and Yoshua Bengio. Generative adversarial nets. In *NeurIPS*, 2014. 1

Satya Krishna Gorti, Noël Vouitsis, Junwei Ma, Keyvan Golestan, Maksims Volkovs, Animesh Garg, and Guangwei Yu. X-pool: Cross-modal language-video attention for text-video retrieval. In *CVPR*, pp. 4996–5005, 2022. 5.2

Dylan Green, William Harvey, Saeid Naderiparizi, Matthew Niedoba, Yunpeng Liu, Xiaoxuan Liang, Jonathan Lavington, Ke Zhang, Vasileios Lioutas, Setareh Dabiri, et al. Semantically consistent video inpainting with conditional diffusion models. *arXiv preprint arXiv:2405.00251*, 2024. 4.2.2

Xianfan Gu, Chuan Wen, Weirui Ye, Jiaming Song, and Yang Gao. Seer: Language instructed video prediction with latent diffusion models. In *ICLR*, 2024a. 4.1.1

Yuchao Gu, Yipin Zhou, Bichen Wu, Licheng Yu, Jia-Wei Liu, Rui Zhao, Jay Zhangjie Wu, David Junhao Zhang, Mike Zheng Shou, and Kevin Tang. Videoswap: Customized video subject swapping with interactive semantic point correspondence. In *CVPR*, pp. 7621–7630, 2024b. 4.1.5

Zekai Gu, Rui Yan, Jiahao Lu, Peng Li, Zhiyang Dou, Chenyang Si, Zhen Dong, Qifeng Liu, Cheng Lin, Ziwei Liu, Wenping Wang, and Yuan Liu. Diffusion as shader: 3d-aware video diffusion for versatile video generation control, 2025. 4.6.2, 4.6.3

Lanqing Guo, Yingqing He, Haoxin Chen, Menghan Xia, Xiaodong Cun, Yufei Wang, Siyu Huang, Yong Zhang, Xintao Wang, Qifeng Chen, et al. Make a cheap scaling: A self-cascade diffusion model for higher-resolution adaptation. In *ECCV*, pp. 39–55, 2025. 4.2.4

Qiushan Guo, Sifei Liu, Yizhou Yu, and Ping Luo. Rethinking the noise schedule of diffusion-based generative models. *N/A*, 2023a. 2.4.3

Xiefan Guo, Jinlin Liu, Miaomiao Cui, and Di Huang. I4vgen: Image as stepping stone for text-to-video generation. *arXiv preprint arXiv:2406.02230*, 2024a. 2.4.4

Xun Guo, Mingwu Zheng, Liang Hou, Yuan Gao, Yufan Deng, Pengfei Wan, Di Zhang, Yufan Liu, Weiming Hu, Zhengjun Zha, Haibin Huang, and Chongyang Ma. I2v-adapter: A general image-to-video adapter for diffusion models, 2023b. 4.1.1

Yuwei Guo, Ceyuan Yang, Anyi Rao, Zhengyang Liang, Yaohui Wang, Yu Qiao, Maneesh Agrawala, Dahua Lin, and Bo Dai. Animatediff: Animate your personalized text-to-image diffusion models without specific tuning. *arXiv preprint arXiv:2307.04725*, 2023c. 2.4.4, 2.5.3

Yuwei Guo, Ceyuan Yang, Anyi Rao, Maneesh Agrawala, Dahua Lin, and Bo Dai. Sparsectrl: Adding sparse controls to text-to-video diffusion models. In *ECCV*, pp. 330–348, 2024b. 4.1.1, 4.1.2

Agrim Gupta, Lijun Yu, Kihyuk Sohn, Xiuye Gu, Meera Hahn, Li Fei-Fei, Irfan Essa, Lu Jiang, and José Lezama. Photorealistic video generation with diffusion models. *arXiv preprint arXiv:2312.06662*, 2023. 2.4.4, 3.4

Yoav HaCohen, Nisan Chiprut, Benny Brazowski, Daniel Shalem, Dudu Moshe, Eitan Richardson, Eran Levin, Guy Shiran, Nir Zabari, Ori Gordon, Poriya Panet, Sapir Weissbuch, Victor Kulikov, Yaki Bitterman, Zeev Melumian, and Ofir Bibi. Ltx-video: Realtime video latent diffusion, 2024. 2.4.4, 3.4

Ayaan Haque, Matthew Tancik, Alexei A. Efros, Aleksander Holynski, and Angjoo Kanazawa. Instruct-nerf2nerf: Editing 3d scenes with instructions. In *ICCV*, pp. 19683–19693, 2023. 5.4.1

William Harvey, Saeid Naderiparizi, Vaden Masrani, Christian Dietrich Weilbach, and Frank Wood. Flexible diffusion modeling of long videos. In *NeurIPS*, 2022. 4.5

Hao He, Yinghao Xu, Yuwei Guo, Gordon Wetzstein, Bo Dai, Hongsheng Li, and Ceyuan Yang. Cameractrl: Enabling camera control for text-to-video generation. *arXiv preprint arXiv:2404.02101*, 2024a. 4.1.3, 4.6.3

Jingwen He, Tianfan Xue, Dongyang Liu, Xinqi Lin, Peng Gao, Dahua Lin, Yu Qiao, Wanli Ouyang, and Ziwei Liu. Venhancer: Generative space-time enhancement for video generation. *arXiv preprint arXiv:2407.07667*, 2024b. 4.2.4, 4.2.5

Kaiming He, Xiangyu Zhang, Shaoqing Ren, and Jian Sun. Deep residual learning for image recognition. In *CVPR*, pp. 770–778, 2016. 5.1

Mingming He, Pascal Clausen, Ahmet Levent Taşel, Li Ma, Oliver Pilarski, Wenqi Xian, Laszlo Rikker, Xueming Yu, Ryan Burgert, Ning Yu, and Paul Debevec. Diffrelight: Diffusion-based facial performance relighting. In *SIGGRAPH Asia*, pp. 1–12, 2024c. 4.1.1

Xuanhua He, Quande Liu, Shengju Qian, Xin Wang, Tao Hu, Ke Cao, Keyu Yan, and Jie Zhang. Id-animator: Zero-shot identity-preserving human video generation, 2024d. 4.1.1

Yingqing He, Tianyu Yang, Yong Zhang, Ying Shan, and Qifeng Chen. Latent video diffusion models for high-fidelity video generation with arbitrary lengths. *arXiv preprint arXiv:2211.13221*, 2022. 2.5.1

Yingqing He, Menghan Xia, Haoxin Chen, Xiaodong Cun, Yuan Gong, Jinbo Xing, Yong Zhang, Xintao Wang, Chao Weng, Ying Shan, and Qifeng Chen. Animate-a-story: Storytelling with retrieval-augmented video generation. *CoRR*, abs/2307.06940, 2023a. 2.2.8, 2.4.4, 5.2

Yingqing He, Shaoshu Yang, Haoxin Chen, Xiaodong Cun, Menghan Xia, Yong Zhang, Xintao Wang, Ran He, Qifeng Chen, and Ying Shan. Scalecrafter: Tuning-free higher-resolution visual generation with diffusion models. In *ICLR*, 2023b. 2.4.1

Fabian Caba Heilbron, Victor Escorcia, Bernard Ghanem, and Juan Carlos Niebles. Activitynet: A large-scale video benchmark for human activity understanding. In *CVPR*, pp. 961–970, 2015. 3.1

Lisa Anne Hendricks, Oliver Wang, Eli Shechtman, Josef Sivic, Trevor Darrell, and Bryan Russell. Localizing moments in video with natural language. In *ICCV*, pp. 5804–5813, 2017. 3.1

Roberto Henschel, Levon Khachatryan, Daniil Hayrapetyan, Hayk Poghosyan, Vahram Tadevosyan, Zhangyang Wang, Shant Navasardyan, and Humphrey Shi. Streamingt2v: Consistent, dynamic, and extendable long video generation from text, 2024. 4.4

Martin Heusel, Hubert Ramsauer, Thomas Unterthiner, Bernhard Nessler, and Sepp Hochreiter. Gans trained by a two time-scale update rule converge to a local nash equilibrium. In *NeurIPS*, pp. 6626–6637, 2017. 3.3

Jonathan Ho and Tim Salimans. Classifier-free diffusion guidance. *arXiv preprint arXiv:2207.12598*, 2022. 2.3.2

Jonathan Ho, Ajay Jain, and Pieter Abbeel. Denoising diffusion probabilistic models. In *NeurIPS*, pp. 6840–6851, 2020. 1, 2, 2.2.1, 2.4.3, 2.5.3

Jonathan Ho, William Chan, Chitwan Saharia, Jay Whang, Ruiqi Gao, Alexey Gritsenko, Diederik P Kingma, Ben Poole, Mohammad Norouzi, David J Fleet, et al. Imagen video: High definition video generation with diffusion models. *arXiv preprint arXiv:2210.02303*, 2022a. 2.1.3, 2.4.4, 2.5.1, 2.5.3, 2.5.4

Jonathan Ho, Chitwan Saharia, William Chan, David J Fleet, Mohammad Norouzi, and Tim Salimans. Cascaded diffusion models for high fidelity image generation. *JMLR*, 23(47):1–33, 2022b. 2.1.3, 2.5.3

Jonathan Ho, Tim Salimans, Alexey Gritsenko, William Chan, Mohammad Norouzi, and David J Fleet. Video diffusion models. *arXiv:2204.03458*, 2022c. 1, 2.1.3, 2.4.1, 2.5.1

Sepp Hochreiter and Jürgen Schmidhuber. Long short-term memory. *Neural Comput.*, 9(8):1735–1780, 1997. 5.1

Fa-Ting Hong and Dan Xu. Implicit identity representation conditioned memory compensation network for talking head video generation. In *Proceedings of the IEEE/CVF International Conference on Computer Vision*, pp. 23062–23072, 2023. 4.3

Fa-Ting Hong, Longhao Zhang, Li Shen, and Dan Xu. Depth-aware generative adversarial network for talking head video generation. In *CVPR*, pp. 3397–3406, 2022. 1

Sirui Hong, Mingchen Zhuge, Jiaqi Chen, Xiawu Zheng, Yuheng Cheng, Ceyao Zhang, Jinlin Wang, Zili Wang, Steven Ka Shing Yau, Zijuan Lin, Liyang Zhou, Chenyu Ran, Lingfeng Xiao, Chenglin Wu, and Jürgen Schmidhuber. Metagpt: Meta programming for a multi-agent collaborative framework, 2024a. 2.4.4

Wenyi Hong, Ming Ding, Wendi Zheng, Xinghan Liu, and Jie Tang. Cogvideo: Large-scale pretraining for text-to-video generation via transformers. In *ICLR*, 2023a. 2.1.2, 2.4.4, 2.5.2, 3.2, 4.5

Wenyi Hong, Weihan Wang, Ming Ding, Wenmeng Yu, Qingsong Lv, Yan Wang, Yean Cheng, Shiyu Huang, Junhui Ji, Zhao Xue, Lei Zhao, Zhuoyi Yang, Xiaotao Gu, Xiaohan Zhang, Guanyu Feng, Da Yin, Zihan Wang, Ji Qi, Xixuan Song, Peng Zhang, Debing Liu, Bin Xu, Juanzi Li, Yuxiao Dong, and Jie Tang. Cogvlm2: Visual language models for image and video understanding. *arxiv preprint arXiv:2408.16500*, 2024b. 3.2

Yicong Hong, Kai Zhang, Jiuxiang Gu, Sai Bi, Yang Zhou, Difan Liu, Feng Liu, Kalyan Sunkavalli, Trung Bui, and Hao Tan. Lrm: Large reconstruction model for single image to 3d, 2023b. 5.4.1

Emiel Hoogeboom, Jonathan Heek, and Tim Salimans. simple diffusion: End-to-end diffusion for high resolution images. In *ICML*, pp. 13213–13232, 2023. 2.4.3

J J Hopfield. Neural networks and physical systems with emergent collective computational abilities. *PNAS*, 79(8):2554–2558, 1982. 5.1

Tobias Höppe, Arash Mehrjou, Stefan Bauer, Didrik Nielsen, and Andrea Dittadi. Diffusion models for video prediction and infilling. *arXiv preprint arXiv:2206.07696*, 2022. 4.2.3

Berthold KP Horn and Brian G Schunck. Determining optical flow. *Artif. Intell.*, 17(1-3):185–203, 1981. 2.4.2

Chen Hou, Guoqiang Wei, Yan Zeng, and Zhibo Chen. Training-free camera control for video generation, 2024. 4.6.4

Hanzhe Hu, Zhizhuo Zhou, Varun Jampani, and Shubham Tulsiani. Mvd-fusion: Single-view 3d via depth-consistent multi-view generation. In *CVPR*, 2024. 4.6.2

Li Hu. Animate anyone: Consistent and controllable image-to-video synthesis for character animation. In *CVPR*, pp. 8153–8163, 2024. 4.1.5

Miao Hu, Xianzhuo Luo, Jiawen Chen, Young Choon Lee, Yipeng Zhou, and Di Wu. Virtual reality: A survey of enabling technologies and its applications in iot. *CoRR*, abs/2103.06472, 2021. 1

Xiaotao Hu, Zhewei Huang, Ailin Huang, Jun Xu, and Shuchang Zhou. A dynamic multi-scale voxel flow network for video prediction. In *CVPR*, pp. 6121–6131, 2023. 2.4.2

Zhihao Hu and Dong Xu. Videocontrolnet: A motion-guided video-to-video translation framework by using diffusion model with controlnet. *arXiv preprint arXiv:2307.14073*, 2023. 4.1.5

Hanzhuo Huang, Yufan Feng, Cheng Shi, Lan Xu, Jingyi Yu, and Sibei Yang. Free-bloom: Zero-shot text-to-video generator with llm director and ldm animator. In *NeurIPS*, 2023a. 2.2.7

Jiahui Huang, Yew Ken Chia, Samson Yu, Kevin Yee, Dennis Küster, Eva G Krumhuber, Dorien Herremans, and Gemma Roig. Single image video prediction with auto-regressive gans. *Sensors*, 22(9):3533, 2022a. 2.1.2

Xinyue Huang et al. Lavie: Latent video encoding for diffusion models. *arXiv preprint arXiv:2309.04512*, 2023b. 1, 2.5.3, 3.4

Yonglong Huang, Cheng Yu, Nannan Li, Fuqin Deng, Ruiquan Ge, and Changmiao Wang. Make an image move: Few-shot based video generation guided by clip. In *ICPR*, pp. 146–161, 2025. 2.2.6

Zehuan Huang, Hao Wen, Junting Dong, Yaohui Wang, Yangguang Li, Xinyuan Chen, Yan-Pei Cao, Ding Liang, Yu Qiao, Bo Dai, et al. Epidiff: Enhancing multi-view synthesis via localized epipolar-constrained diffusion. *arXiv preprint arXiv:2312.06725*, 2023c. 4.6.2

Zhaoyang Huang, Xiaoyu Shi, Chao Zhang, Qiang Wang, Ka Chun Cheung, Hongwei Qin, Jifeng Dai, and Hongsheng Li. Flowformer: A transformer architecture for optical flow. *arXiv preprint arXiv:2203.16194*, 2022b. 2.4.2

Ziqi Huang, Yinan He, Jiashuo Yu, Fan Zhang, Chenyang Si, Yuming Jiang, Yuanhan Zhang, Tianxing Wu, Qingyang Jin, Nattapol Chanpaisit, Yaohui Wang, Xinyuan Chen, Limin Wang, Dahua Lin, Yu Qiao, and Ziwei Liu. Vbench: Comprehensive benchmark suite for video generative models. In *CVPR*, 2024a. 3.1, 3.3

Ziqi Huang, Fan Zhang, Xiaojie Xu, Yinan He, Jiashuo Yu, Ziyue Dong, Qianli Ma, Nattapol Chanpaisit, Chenyang Si, Yuming Jiang, Yaohui Wang, Xinyuan Chen, Ying-Cong Chen, Limin Wang, Dahua Lin, Yu Qiao, and Ziwei Liu. Vbench++: Comprehensive and versatile benchmark suite for video generative models, 2024b. 3.3

Tak-Wai Hui, Xiaoou Tang, and Chen Change Loy. Liteflownet: A lightweight convolutional neural network for optical flow estimation. In *CVPR*, pp. 8981–8989, 2018. 2.4.2

Tak-Wai Hui, Xiaoou Tang, and Chen Change Loy. A lightweight optical flow cnn—revisiting data fidelity and regularization. *IEEE Trans. Pattern Anal. Mach. Intell.*, 43(8):2555–2569, 2020. 2.4.2

Eddy Ilg, Nikolaus Mayer, Tonmoy Saikia, Margret Keuper, Alexey Dosovitskiy, and Thomas Brox. Flownet 2.0: Evolution of optical flow estimation with deep networks. In *CVPR*, pp. 2462–2470, 2017. 2.4.2

Siddhant Jain, Daniel Watson, Eric Tabellion, Ben Poole, Janne Kontkanen, et al. Video interpolation with diffusion models. In *CVPR*, pp. 7341–7351, 2024a. 4.2.3

Yash Jain, Anshul Nasery, Vibhav Vineet, and Harkirat Behl. Peekaboo: Interactive video generation via masked-diffusion. In *CVPR*, pp. 8079–8088, 2024b. 2.2.7

Y. Jang, Y. Song, Y. Yu, Y. Kim, and G. Kim. Tgif-qa: Toward spatio-temporal reasoning in visual question answering. In *CVPR*, pp. 1359–1367, 2017. 5.3

Menglin Jia, Luming Tang, Bor-Chun Chen, Claire Cardie, Serge Belongie, Bharath Hariharan, and Ser-Nam Lim. Visual prompt tuning. In *ECCV*, 2022. 3.2

Yanqin Jiang, Chaohui Yu, Chenjie Cao, Fan Wang, Weiming Hu, and Jin Gao. Animate3d: Animating any 3d model with multi-view video diffusion. In *NeurIPS*, 2024a. 5.4.2

Yifan Jiang, Kevin Yang, et al. Videocomposer: Compositional text-to-video generation with latent diffusion models. *arXiv preprint arXiv:2302.01329*, 2023a. 2.4.4, 4.1.5

Yuming Jiang, Shuai Yang, Tong Liang Koh, Wayne Wu, Chen Change Loy, and Ziwei Liu. Text2performer: Text-driven human video generation. In *ICCV*, pp. 22690–22700, 2023b. 2.5.2

Yuming Jiang, Tianxing Wu, Shuai Yang, Chenyang Si, Dahua Lin, Yu Qiao, Chen Change Loy, and Ziwei Liu. Videobooth: Diffusion-based video generation with image prompts. In *CVPR*, pp. 6689–6700, 2024b. 4.1.1, 4.1.1, 4.4

Yang Jin, Zhicheng Sun, Ningyuan Li, Kun Xu, Hao Jiang, Nan Zhuang, Quzhe Huang, Yang Song, Yadong Mu, and Zhouchen Lin. Pyramidal flow matching for efficient video generative modeling. *arXiv preprint arXiv:2410.05954*, 2024. 2.1.4

Xuan Ju, Yiming Gao, Zhaoyang Zhang, Ziyang Yuan, Xintao Wang, Ailing Zeng, Yu Xiong, Qiang Xu, and Ying Shan. Miradata: A large-scale video dataset with long durations and structured captions. In *NeurIPS*, 2024. 1, 3.1

Philip Torr Junlin Han, Filippos Kokkinos. Vfusion3d: Learning scalable 3d generative models from video diffusion models. *arXiv preprint arXiv:2403.12034*, 2024. 4.6.1, 5.4.1

Nal Kalchbrenner, Aäron Oord, Karen Simonyan, Ivo Danihelka, Oriol Vinyals, Alex Graves, and Koray Kavukcuoglu. Video pixel networks. In *ICML*, pp. 1771–1779, 2017. 2.1.2

Yash Kant, Aliaksandr Siarohin, Ziyi Wu, Michael Vasilkovsky, Guocheng Qian, Jian Ren, Riza Alp Guler, Bernard Ghanem, Sergey Tulyakov, and Igor Gilitschenski. Spad: Spatially aware multi-view diffusers. In *CVPR*, pp. 10026–10038, 2024. 4.6.2

Ozgur Kara, Bariscan Kurtkaya, Hidir Yesiltepe, James M Rehg, and Pinar Yanardag. Rave: Randomized noise shuffling for fast and consistent video editing with diffusion models. In *CVPR*, pp. 6507–6516, 2024. 4.1.5

Johanna Karras, Aleksander Holynski, Ting-Chun Wang, and Ira Kemelmacher-Shlizerman. Dreampose: Fashion image-to-video synthesis via stable diffusion. In *ICCV*, pp. 22623–22633, 2023. 4.1.5

Tero Karras, Samuli Laine, Miika Aittala, Janne Hellsten, Jaakko Lehtinen, and Timo Aila. Analyzing and improving the image quality of stylegan. In *CVPR*, pp. 8110–8119, 2020. 2.1.1

Tero Karras, Miika Aittala, Timo Aila, and Samuli Laine. Elucidating the design space of diffusion-based generative models. In *NeurIPS*, pp. 26565–26577, 2022. 2.2.3, 2.2.3, 2.4.3

Yoni Kasten, Dolev Ofri, Oliver Wang, and Tali Dekel. Layered neural atlases for consistent video editing. *TOG*, 40(6):1–12, 2021. 4.1.5

Bingxin Ke, Anton Obukhov, Shengyu Huang, Nando Metzger, Rodrigo Caye Daudt, and Konrad Schindler. Repurposing diffusion-based image generators for monocular depth estimation. In *CVPR*, 2024. 4.1.1

Bernhard Kerbl, Georgios Kopanas, Thomas Leimkühler, and George Drettakis. 3d gaussian splatting for real-time radiance field rendering. *TOG*, 42(4), 2023. 5.4

Levon Khachatryan, Andranik Movsisyan, Vahram Tadevosyan, Roberto Henschel, Zhangyang Wang, Shant Navasardyan, and Humphrey Shi. Text2video-zero: Text-to-image diffusion models are zero-shot video generators. In *ICCV*, pp. 15954–15964, 2023. 2.2.7, 3.1, 4.1.5

Taekyung Ki and Dongchan Min. Stylelipsync: Style-based personalized lip-sync video generation. In *ICCV*, pp. 22784–22793, 2023. 2.1.1

Gyeongman Kim, Hajin Shim, Hyunsu Kim, Yunjey Choi, Junho Kim, and Eunho Yang. Diffusion video autoencoders: Toward temporally consistent face video editing via disentangled video encoding. In *CVPR*, pp. 6091–6100, 2023a. 4.1.5

Pum Jun Kim, Seojun Kim, and Jaejun Yoo. Stream: Spatio-temporal evaluation and analysis metric for video generative models. In *ICLR*, 2023b. 3.3

Seung Wook Kim, Jonah Philion, Antonio Torralba, and Sanja Fidler. Drivegan: Towards a controllable high-quality neural simulation. In *CVPR*, pp. 5820–5829, 2021. 2.4.4

Diederik P Kingma. Auto-encoding variational bayes. *arXiv preprint arXiv:1312.6114*, 2013. 2.5.3

Dan Kondratyuk, Lijun Yu, Xiuye Gu, José Lezama, Jonathan Huang, Rachel Hornung, Hartwig Adam, Hassan Akbari, Yair Alon, Vighnesh Birodkar, et al. Videopoet: A large language model for zero-shot video generation. *arXiv preprint arXiv:2312.14125*, 2023. 2.5.3

Weijie Kong, Qi Tian, Zijian Zhang, Rox Min, Zuozhuo Dai, Jin Zhou, Jiangfeng Xiong, Xin Li, Bo Wu, Jianwei Zhang, Kathrina Wu, Qin Lin, Junkun Yuan, Yanxin Long, Aladdin Wang, Andong Wang, Changlin Li, Duojun Huang, Fang Yang, Hao Tan, Hongmei Wang, Jacob Song, Jiawang Bai, Jianbing Wu, Jinbao Xue, Joey Wang, Kai Wang, Mengyang Liu, Pengyu Li, Shuai Li, Weiyan Wang, Wenqing Yu, Xinchi Deng, Yang Li, Yi Chen, Yutao Cui, Yuanbo Peng, Zhentao Yu, Zhiyu He, Zhiyong Xu, Zixiang Zhou, Zunnan Xu, Yangyu Tao, Qinglin Lu, Songtao Liu, Dax Zhou, Hongfa Wang, Yong Yang, Di Wang, Yuhong Liu, Jie Jiang, and Caesar Zhong. Hunyuanvideo: A systematic framework for large video generative models, 2025. 2.4.4, 2.5.3, 2.5.4, 3.4

Yu Kong, Zhiqiang Tao, and Yun Fu. Deep sequential context networks for action prediction. In *CVPR*, pp. 3662–3670, 2017. 5.1

Alex Krizhevsky, Ilya Sutskever, and Geoffrey E Hinton. Imagenet classification with deep convolutional neural networks. In *NeurIPS*, 2012. 5.1

Max Ku, Cong Wei, Weiming Ren, Huan Yang, and Wenhu Chen. Anyv2v: A tuning-free framework for any video-to-video editing tasks. *TMLR*, 2024. 2.2.7, 4.1.5

Zhengfei Kuang, Shengqu Cai, Hao He, Yinghao Xu, Hongsheng Li, Leonidas Guibas, and Gordon Wetzstein. Collaborative video diffusion: Consistent multi-video generation with camera control. *arXiv preprint arXiv:2405.17414*, 2024. 4.1.3, 4.6.1, 4.6.3

Jeong-gi Kwak, Erqun Dong, Yuhe Jin, Hanseok Ko, Shweta Mahajan, and Kwang Moo Yi. Vivid-1-to-3: Novel view synthesis with video diffusion models. In *CVPR*, pp. 6775–6785, 2024. 1, 4.6.4

PKU-Yuan Lab and Tuzhan AI etc. Open-sora-plan, 2024. 2.4.4, 2.5.3, 2.5.4

Black Forest Labs. Flux, 2024. 2.5.4

LAION. Laion-coco. `https://laion.ai/blog/laion-coco/`, 2023. 1

Matthew Le, Apoorv Vyas, Bowen Shi, Brian Karrer, Leda Sari, Rashel Moritz, Mary Williamson, Vimal Manohar, Yossi Adi, Jay Mahadeokar, et al. Voicebox: Text-guided multilingual universal speech generation at scale. *arXiv preprint arXiv:2306.15687*, 2023. 2.2.4

Guillaume Le Moing, Jean Ponce, and Cordelia Schmid. Ccvs: Context-aware controllable video synthesis. *Advances in Neural Information Processing Systems*, 34:14042–14055, 2021. 4.1.4

Sangho Lee, Jiwan Chung, Youngjae Yu, Gunhee Kim, Thomas Breuel, Gal Chechik, and Yale Song. Acav100m: Automatic curation of large-scale datasets for audio-visual video representation learning. In *ICCV*, pp. 10254–10264, 2021. 3.1

Yao-Chih Lee, Ji-Ze Genevieve Jang, Yi-Ting Chen, Elizabeth Qiu, and Jia-Bin Huang. Shape-aware text-driven layered video editing. In *CVPR*, pp. 14317–14326, 2023. 4.1.5

Jie Lei, Linjie Li, Luowei Zhou, Zhe Gan, Tamara L. Berg, Mohit Bansal, and Jingjing Liu. Less is more: Clipbert for video-and-language learning via sparse sampling. In *CVPR*, pp. 7331–7341, 2021. 5.1, 5.2

Wentao Lei, Jinting Wang, Fengji Ma, Guanjie Huang, and Li Liu. A comprehensive survey on human video generation: Challenges, methods, and insights, 2024a. (document), 1

Wentao Lei, Jinting Wang, Fengji Ma, Guanjie Huang, and Li Liu. A comprehensive survey on human video generation: Challenges, methods, and insights, 2024b. (document), 1

Bing Li, Cheng Zheng, Wenxuan Zhu, Jinjie Mai, Biao Zhang, Peter Wonka, and Bernard Ghanem. Vivid-zoo: Multi-view video generation with diffusion model. In *NeurIPS*, 2024a. 4.6.2, 5.4.2

Daiqing Li, Aleks Kamko, Ehsan Akhgari, Ali Sabet, Linmiao Xu, and Suhail Doshi. Playground v2. 5: Three insights towards enhancing aesthetic quality in text-to-image generation. *arXiv preprint arXiv:2402.17245*, 2024b. 2.5.3

Dongxu Li, Junnan Li, Hongdong Li, Juan Carlos Niebles, and Steven C. H. Hoi. Align and prompt: Video-and-language pre-training with entity prompts. In *CVPR*, pp. 4943–4953, 2022. 5.1

Feng Li, Renrui Zhang, Hao Zhang, Yuanhan Zhang, Bo Li, Wei Li, Zejun MA, and Chunyuan Li. LLaVA-neXT-interleave: Tackling multi-image, video, and 3d in large multimodal models. In *The Thirteenth International Conference on Learning Representations*, 2025. 3.2

Hengjia Li, Haonan Qiu, Shiwei Zhang, Xiang Wang, Yujie Wei, Zekun Li, Yingya Zhang, Boxi Wu, and Deng Cai. Personalvideo: High id-fidelity video customization without dynamic and semantic degradation. *arXiv preprint arXiv:2411.17048*, 2024c. 4.3

Jiachen Li, Weixi Feng, Tsu-Jui Fu, Xinyi Wang, Sugato Basu, Wenhu Chen, and William Yang Wang. T2v-turbo: Breaking the quality bottleneck of video consistency model with mixed reward feedback. *arXiv preprint arXiv:2405.18750*, 2024d. 2.2.5

Jiachen Li, Qian Long, Jian Zheng, Xiaofeng Gao, Robinson Piramuthu, Wenhu Chen, and William Yang Wang. T2v-turbo-v2: Enhancing video generation model post-training through data, reward, and conditional guidance design. *arXiv preprint arXiv:2410.05677*, 2024e. 2.2.5

Maomao Li, Yu Li, Tianyu Yang, Yunfei Liu, Dongxu Yue, Zhihui Lin, and Dong Xu. A video is worth 256 bases: Spatial-temporal expectation-maximization inversion for zero-shot video editing. In *CVPR*, pp. 7528–7537, 2024f. 4.1.5

Wei Li, Linchao Zhu, Longyin Wen, and Yi Yang. Decap: Decoding clip latents for zero-shot captioning via text-only training. In *ICLR*, 2023. 5.1

Xirui Li, Chao Ma, Xiaokang Yang, and Ming-Hsuan Yang. Vidtome: Video token merging for zero-shot video editing. In *CVPR*, pp. 7486–7495, 2024g. 4.1.5, 4.4

Xiujun Li, Xi Yin, Chunyuan Li, Pengchuan Zhang, Xiaowei Hu, Lei Zhang, Lijuan Wang, Houdong Hu, Li Dong, Furu Wei, Yejin Choi, and Jianfeng Gao. Oscar: Object-semantics aligned pre-training for vision-language tasks. In *ECCV*, pp. 121–137, 2020. 5.2

Xuanyi Li, Daquan Zhou, Chenxu Zhang, Shaodong Wei, Qibin Hou, and Ming-Ming Cheng. Sora generates videos with stunning geometrical consistency. *arXiv preprint arXiv: 2402.17403*, 2024h. 4.6

Zhengqi Li, Richard Tucker, Noah Snavely, and Aleksander Holynski. Generative image dynamics. In *CVPR*, 2024i. 4.1.1

Zhimin Li, Jianwei Zhang, Qin Lin, Jiangfeng Xiong, Yanxin Long, Xinchi Deng, Yingfang Zhang, Xingchao Liu, Minbin Huang, Zedong Xiao, et al. Hunyuan-dit: A powerful multi-resolution diffusion transformer with fine-grained chinese understanding. *arXiv preprint arXiv:2405.08748*, 2024j. 2.5.3, 2.5.4, 3.2

Long Lian, Baifeng Shi, Adam Yala, Trevor Darrell, and Boyi Li. Llm-grounded video diffusion models. In *ICLR*, 2024. 2.3.1

Feng Liang, Bichen Wu, Jialiang Wang, Licheng Yu, Kunpeng Li, Yinan Zhao, Ishan Misra, Jia-Bin Huang, Peizhao Zhang, Peter Vajda, et al. Flowvid: Taming imperfect optical flows for consistent video-to-video synthesis. In *CVPR*, pp. 8207–8216, 2024a. 4.1.5

Hanwen Liang, Junli Cao, Vidit Goel, Guocheng Qian, Sergei Korolev, Demetri Terzopoulos, Konstantinos Plataniotis, Sergey Tulyakov, and Jian Ren. Wonderland: Navigating 3d scenes from a single image. *arXiv preprint arXiv:2412.12091*, 2024b. 4.6.2, 4.6.3, 20, 5.4.1

HANWEN LIANG, Yuyang Yin, Dejia Xu, hanxue liang, Zhangyang Wang, Konstantinos N Plataniotis, Yao Zhao, and Yunchao Wei. Diffusion4d: Fast spatial-temporal consistent 4d generation via video diffusion models. In *NeurIPS*, 2024. 4.6.1, 5.4.2

Jingyun Liang, Yuchen Fan, Kai Zhang, Radu Timofte, Luc Van Gool, and Rakesh Ranjan. Movideo: Motion-aware video generation with diffusion model. In *ECCV*, pp. 56–74, 2025. 2.5.1

Jun Hao Liew, Hanshu Yan, Jianfeng Zhang, Zhongcong Xu, and Jiashi Feng. Magicedit: High-fidelity and temporally coherent video editing. *arXiv preprint arXiv:2308.14749*, 2023. 4.1.5

Gaojie Lin, Jianwen Jiang, Jiaqi Yang, Zerong Zheng, and Chao Liang. Omnihuman-1: Rethinking the scaling-up of one-stage conditioned human animation models. *arXiv preprint arXiv:2502.01061*, 2025. 4.1.4

Han Lin, Abhay Zala, Jaemin Cho, and Mohit Bansal. Videodirectorgpt: Consistent multi-scene video generation via llm-guided planning, 2024a. 2.4.4

Zongyu Lin, Wei Liu, Chen Chen, Jiasen Lu, Wenze Hu, Tsu-Jui Fu, Jesse Allardice, Zhengfeng Lai, Liangchen Song, Bowen Zhang, et al. Stiv: Scalable text and image conditioned video generation. *arXiv preprint arXiv:2412.07730*, 2024b. 2.4.4

Huan Ling, Seung Wook Kim, Antonio Torralba, Sanja Fidler, and Karsten Kreis. Align your gaussians: Text-to-4d with dynamic 3d gaussians and composed diffusion models, 2024a. 5.4.2

Lu Ling, Yichen Sheng, Zhi Tu, Wentian Zhao, Cheng Xin, Kun Wan, Lantao Yu, Qianyu Guo, Zixun Yu, Yawen Lu, Xuanmao Li, Xingpeng Sun, Rohan Ashok, Aniruddha Mukherjee, Hao Kang, Xiangrui Kong, Gang Hua, Tianyi Zhang, Bedrich Benes, and Aniket Bera. Dl3dv-10k: A large-scale scene dataset for deep learning-based 3d vision. In *CVPR*, pp. 22160–22169, 2024b. 4.6.1

Pengyang Ling, Jiazi Bu, Pan Zhang, Xiaoyi Dong, Yuhang Zang, Tong Wu, Huaian Chen, Jiaqi Wang, and Yi Jin. Motionclone: Training-free motion cloning for controllable video generation. *arXiv preprint arXiv:2406.05338*, 2024c. 4.1.5

Yaron Lipman, Ricky TQ Chen, Heli Ben-Hamu, Maximilian Nickel, and Matt Le. Flow matching for generative modeling. In *iclr*, 2023. 2.2.4

Alexander Liu, SouYoung Jin, Cheng-I Lai, Andrew Rouditchenko, Aude Oliva, and James Glass. Cross-modal discrete representation learning. In *ACL*, pp. 3013–3035, 2022a. 5.2

Fangfu Liu, Wenqiang Sun, Hanyang Wang, Yikai Wang, Haowen Sun, Junliang Ye, Jun Zhang, and Yueqi Duan. Reconx: Reconstruct any scene from sparse views with video diffusion model, 2024a. 5.4.1

Fangfu Liu, Hanyang Wang, Weiliang Chen, Haowen Sun, and Yueqi Duan. Make-your-3d: Fast and consistent subject-driven 3d content generation. In *ECCV*, pp. 389–406, 2024b. 4.6.2

Hanyuan Liu, Minshan Xie, Jinbo Xing, Chengze Li, and Tien-Tsin Wong. Video colorization with pre-trained text-to-image diffusion models. *arXiv preprint arXiv:2306.01732*, 2023a. 4.1.5

Haogeng Liu, Tao Wang, Jie Cao, Ran He, and Jianhua Tao. Boosting fast and high-quality speech synthesis with linear diffusion. *arXiv preprint arXiv:2306.05708*, 2023b. 2.2.4

Jun Liu, Amir Shahroudy, Dong Xu, and Gang Wang. Spatio-temporal lstm with trust gates for 3d human action recognition. In *ECCV*, pp. 816–833, 2016. 5.1

Jun Liu, Gang Wang, Ling-Yu Duan, Kamila Abdiyeva, and Alex C. Kot. Skeleton-based human action recognition with global context-aware attention lstm networks. *IEEE Trans. Image Process.*, 27(4):1586–1599, 2018. 5.1

Shaowei Liu, Zhongzheng Ren, Saurabh Gupta, and Shenlong Wang. Physgen: Rigid-body physics-grounded image-to-video generation. In *European Conference on Computer Vision*, pp. 360–378. Springer, 2024c. 4.1.6

Tao Liu, Feilong Chen, Shuai Fan, Chenpeng Du, Qi Chen, Xie Chen, and Kai Yu. Anitalker: Animate vivid and diverse talking faces through identity-decoupled facial motion encoding. *arXiv preprint arXiv:2405.03121*, 2024d. 4.1.4, 4.1.5, 4.3

Tianyi Liu, Kejun Wu, Yi Wang, Wenyang Liu, Kim-Hui Yap, and Lap-Pui Chau. Bitstream-corrupted video recovery: A novel benchmark dataset and method. In *NeurIPS*, 2023c. 3.1

Xian Liu, Qianyi Wu, Hang Zhou, Yuanqi Du, Wayne Wu, Dahua Lin, and Ziwei Liu. Audio-driven co-speech gesture video generation. *Advances in Neural Information Processing Systems*, 35:21386–21399, 2022b. 4.1.4, 4.3

Xingchao Liu, Chengyue Gong, et al. Flow straight and fast: Learning to generate and transfer data with rectified flow. In *ICLR*, 2022c. 2.2.4

Xingchao Liu, Xiwen Zhang, Jianzhu Ma, Jian Peng, et al. Instaflow: One step is enough for high-quality diffusion-based text-to-image generation. In *ICLR*, 2023d. 2.2.4

Yixin Liu, Kai Zhang, Yuan Li, Zhiling Yan, Chujie Gao, Ruoxi Chen, Zhengqing Yuan, Yue Huang, Hanchi Sun, Jianfeng Gao, et al. Sora: A review on background, technology, limitations, and opportunities of large vision models. *arXiv preprint arXiv:2402.17177*, 2024e. 2.5.3

Yuanxin Liu, Lei Li, Shuhuai Ren, Rundong Gao, Shicheng Li, Sishuo Chen, Xu Sun, and Lu Hou. Fetv: A benchmark for fine-grained evaluation of open-domain text-to-video generation. In *NeurIPS*, 2023e. 3.1, 3.3

Yuqi Liu, Pengfei Xiong, Luhui Xu, Shengming Cao, and Qin Jin. Ts2-net: Token shift and selection transformer for text-video retrieval. In *ECCV*, pp. 319–335, 2022d. 5.2

Zexiang Liu, Yangguang Li, Youtian Lin, Xin Yu, Sida Peng, Yan-Pei Cao, Xiaojuan Qi, Xiaoshui Huang, Ding Liang, and Wanli Ouyang. Unidream: Unifying diffusion priors for relightable text-to-3d generation. In *ECCV*, pp. 74–91, 2024f. 4.6.2

Haoyu Lu, Guoxing Yang, Nanyi Fei, Yuqi Huo, Zhiwu Lu, Ping Luo, and Mingyu Ding. Vdt: General-purpose video diffusion transformers via mask modeling. In *ICLR*, 2024a. 2.5.2, 4.1.1

Shilin Lu et al. Vine: Video editing with generative feedback priors. *arXiv preprint*, 2024b. 2.2.5

Zeyu Lu, Zidong Wang, Di Huang, Chengyue Wu, Xihui Liu, Wanli Ouyang, and Lei Bai. Fit: Flexible vision transformer for diffusion model. *arXiv preprint arXiv:2402.12376*, 2024c. 2.5.3, 2.5.4

Andreas Lugmayr, Martin Danelljan, Andres Romero, Fisher Yu, Radu Timofte, and Luc Van Gool. Repaint: Inpainting using denoising diffusion probabilistic models. In *CVPR*, pp. 11461–11471, 2022. 4.2.2

Huaishao Luo, Lei Ji, Ming Zhong, Yang Chen, Wen Lei, Nan Duan, and Tianrui Li. Clip4clip: An empirical study of clip for end to end video clip retrieval and captioning. *Neurocomputing*, 508:293–304, 2022. 5.2

Jiaxi Lv, Yi Huang, Mingfu Yan, Jiancheng Huang, Jianzhuang Liu, Yifan Liu, Yafei Wen, Xiaoxin Chen, and Shifeng Chen. Gpt4motion: Scripting physical motions in text-to-video generation via blender-oriented gpt planning. In *CVPR*, pp. 1430–1440, 2024. 2.2.7

Guoqing Ma, Haoyang Huang, Kun Yan, Liangyu Chen, Nan Duan, Shengming Yin, Changyi Wan, Ranchen Ming, Xiaoniu Song, Xing Chen, Yu Zhou, Deshan Sun, Deyu Zhou, Jian Zhou, Kaijun Tan, Kang An, Mei Chen, Wei Ji, Qiling Wu, Wen Sun, Xin Han, Yanan Wei, Zheng Ge, Aojie Li, Bin Wang, Bizhu Huang, Bo Wang, Brian Li, Changxing Miao, Chen Xu, Chenfei Wu, Chenguang Yu, Dapeng Shi, Dingyuan Hu, Enle Liu, Gang Yu, Ge Yang, Guanzhe Huang, Gulin Yan, Haiyang Feng, Hao Nie, Haonan Jia, Hanpeng Hu, Hanqi Chen, Haolong Yan, Heng Wang, Hongcheng Guo, Huilin Xiong, Huixin Xiong, Jiahao Gong, Jianchang Wu, Jiaoren Wu, Jie Wu, Jie Yang, Jiashuai Liu, Jiashuo Li, Jingyang Zhang, Junjing Guo, Junzhe Lin, Kaixiang Li, Lei Liu, Lei Xia, Liang Zhao, Liguo Tan, Liwen Huang, Liying Shi, Ming Li, Mingliang Li, Muhua Cheng, Na Wang, Qiaohui Chen, Qinglin He, Qiuyan Liang, Quan Sun, Ran Sun, Rui Wang, Shaoliang Pang, Shiliang Yang, Sitong Liu, Siqi Liu, Shuli Gao, Tiancheng Cao, Tianyu Wang, Weipeng Ming, Wenqing He, Xu Zhao, Xuelin Zhang, Xianfang Zeng, Xiaojia Liu, Xuan Yang, Yaqi Dai, Yanbo Yu, Yang Li, Yineng Deng, Yingming Wang, Yilei Wang, Yuanwei Lu, Yu Chen, Yu Luo, Yuchu Luo, Yuhe Yin, Yuheng Feng, Yuxiang Yang, Zecheng Tang, Zekai Zhang, Zidong Yang, Binxing Jiao, Jiansheng Chen, Jing Li, Shuchang Zhou, Xiangyu Zhang, Xinhao Zhang, Yibo Zhu, Heung-Yeung Shum, and Daxin Jiang. Step-video-t2v technical report: The practice, challenges, and future of video foundation model, 2025. 2.4.4, 2.5.3, 2.5.4

Nanye Ma, Mark Goldstein, Michael S Albergo, Nicholas M Boffi, Eric Vanden-Eijnden, and Saining Xie. Sit: Exploring flow and diffusion-based generative models with scalable interpolant transformers. *arXiv preprint arXiv:2401.08740*, 2024a. 2.4.4, 2.5.2, 2.5.3, 2.5.4

Xin Ma, Yaohui Wang, Gengyun Jia, Xinyuan Chen, Yuan-Fang Li, Cunjian Chen, and Yu Qiao. Cinemo: Consistent and controllable image animation with motion diffusion models, 2024b. 4.1.1, 4.4

Xin Ma, Yaohui Wang, Gengyun Jia, Xinyuan Chen, Ziwei Liu, Yuan-Fang Li, Cunjian Chen, and Yu Qiao. Latte: Latent diffusion transformer for video generation. *arXiv preprint arXiv:2401.03048*, 2024c. 2.4.1, 2.5.3, 2.5.4

Yifeng Ma, Shiwei Zhang, Jiayu Wang, Xiang Wang, Yingya Zhang, and Zhidong Deng. Dreamtalk: When expressive talking head generation meets diffusion probabilistic models. *arXiv preprint arXiv:2312.09767*, 2023. 4.1.4, 4.3

Yiwei Ma, Guohai Xu, Xiaoshuai Sun, Ming Yan, Ji Zhang, and Rongrong Ji. X-clip: End-to-end multi-grained contrastive learning for video-text retrieval. In *ACM MM*, pp. 638–647, 2022. 5.2

Yue Ma, Yingqing He, Xiaodong Cun, Xintao Wang, Siran Chen, Xiu Li, and Qifeng Chen. Follow your pose: Pose-guided text-to-video generation using pose-free videos. In *AAAI*, pp. 4117–4125, 2024d. 4.1.5

Ze Ma, Daquan Zhou, Chun-Hsiao Yeh, Xue-She Wang, Xiuyu Li, Huanrui Yang, Zhen Dong, Kurt Keutzer, and Jiashi Feng. Magic-me: Identity-specific video customized diffusion. *arXiv preprint arXiv:2402.09368*, 2024e. 2.2.7

Luke Melas-Kyriazi, Iro Laina, Christian Rupprecht, Natalia Neverova, Andrea Vedaldi, Oran Gafni, and Filippos Kokkinos. Im-3d: Iterative multiview diffusion and reconstruction for high-quality 3d generation, 2024. 4.6.1, 5.4.1

Andrew Melnik, Michal Ljubljanac, Cong Lu, Qi Yan, Weiming Ren, and Helge Ritter. Video diffusion models: A survey, 2024. (document), 1

Willi Menapace, Aliaksandr Siarohin, Ivan Skorokhodov, Ekaterina Deyneka, Tsai-Shien Chen, Anil Kag, Yuwei Fang, Aleksei Stoliar, Elisa Ricci, Jian Ren, et al. Snap video: Scaled spatiotemporal transformers for text-to-video synthesis. In *CVPR*, pp. 7038–7048, 2024. 2.4.4

Qiaowei Miao, JinSheng Quan, Kehan Li, and Yawei Luo. Pla4d: Pixel-level alignments for text-to-4d gaussian splatting, 2024. 5.4.2

Antoine Miech, Dimitri Zhukov, Jean-Baptiste Alayrac, Makarand Tapaswi, Ivan Laptev, and Josef Sivic. Howto100m: Learning a text-video embedding by watching hundred million narrated video clips. In *ICCV*, pp. 2630–2640, 2019. 3.1

Antoine Miech, Jean-Baptiste Alayrac, Lucas Smaira, Ivan Laptev, Josef Sivic, and Andrew Zisserman. End-to-end learning of visual representations from uncurated instructional videos. In *ECCV*, pp. 9876–9886, 2020. 5.2

Ben Mildenhall, Pratul P Srinivasan, Matthew Tancik, Jonathan T Barron, Ravi Ramamoorthi, and Ren Ng. Nerf: Representing scenes as neural radiance fields for view synthesis. *Commun. ACM.*, 65(1):99–106, 2021. 5.4

Chong Mou, Mingdeng Cao, Xintao Wang, Zhaoyang Zhang, Ying Shan, and Jian Zhang. Revideo: Remake a video with motion and content control. *arXiv preprint arXiv:2405.13865*, 2024. 4.1.5

Urwa Muaz, Wondong Jang, Rohun Tripathi, Santhosh Mani, Wenbin Ouyang, Ravi Teja Gadde, Baris Gecer, Sergio Elizondo, Reza Madad, and Naveen Nair. Sidgan: High-resolution dubbed video generation via shift-invariant learning. In *ICCV*, pp. 7833–7842, 2023. 2.1.1, 5.2

Arsha Nagrani, Paul Hongsuck Seo, Bryan Seybold, Anja Hauth, Santiago Manen, Chen Sun, and Cordelia Schmid. Learning audio-video modalities from image captions. In Shai Avidan, Gabriel Brostow, Moustapha Cissé, Giovanni Maria Farinella, and Tal Hassner (eds.), *Computer Vision – ECCV 2022*, volume 13674, pp. 407–426, 2022. ISBN 978-3-031-19780-2 978-3-031-19781-9. 3.1

Koichi Namekata, Sherwin Bahmani, Ziyi Wu, Yash Kant, Igor Gilitschenski, and David B Lindell. Sg-i2v: Self-guided trajectory control in image-to-video generation. *arXiv preprint arXiv:2411.04989*, 2024. 4.1.2

Kepan Nan, Rui Xie, Penghao Zhou, Tiehan Fan, Zhenheng Yang, Zhijie Chen, Xiang Li, Jian Yang, and Ying Tai. Openvid-1m: A large-scale high-quality dataset for text-to-video generation. *arXiv preprint arXiv:2407.02371*, 2024. 4.6.1

Haomiao Ni, Changhao Shi, Kai Li, Sharon X Huang, and Martin Renqiang Min. Conditional image-to-video generation with latent flow diffusion models. In *CVPR*, pp. 18444–18455, 2023. 4.1.1, 4.4

Alex Nichol, Prafulla Dhariwal, Aditya Ramesh, Pranav Shyam, Pamela Mishkin, Bob McGrew, Ilya Sutskever, and Mark Chen. Glide: Towards photorealistic image generation and editing with text-guided diffusion models. *arXiv preprint arXiv:2112.10741*, 2021. 2.5.4

Alexander Quinn Nichol and Prafulla Dhariwal. Improved denoising diffusion probabilistic models. In *ICML*, pp. 8162–8171, 2021. 1, 2.2.1, 2.4.3

Yeongtak Oh, Jooyoung Choi, Yongsung Kim, Minjun Park, Chaehun Shin, and Sungroh Yoon. Controldreamer: Blending geometry and style in text-to-3d, 2023. 4.6.2

Hao Ouyang, Qiuyu Wang, Yuxi Xiao, Qingyan Bai, Juntao Zhang, Kecheng Zheng, Xiaowei Zhou, Qifeng Chen, and Yujun Shen. Codef: Content deformation fields for temporally consistent video processing. In *CVPR*, pp. 8089–8099, 2024a. 4.1.5

Wenqi Ouyang, Yi Dong, Lei Yang, Jianlou Si, and Xingang Pan. I2vedit: First-frame-guided video editing via image-to-video diffusion models. *arXiv preprint arXiv:2405.16537*, 2024b. 4.1.5

Yichen Ouyang, jianhao Yuan, Hao Zhao, Gaoang Wang, and Bo zhao. Flexifilm: Long video generation with flexible conditions, 2024c. 4.4

Junting Pan, Ziyi Lin, Xiatian Zhu, Jing Shao, and Hongsheng Li. St-adapter: Parameter-efficient image-to-video transfer learning for action recognition. *arXiv preprint arXiv:2206.13559*, 2022. 3.2

Junting Pan, Ziyi Lin, Yuying Ge, Xiatian Zhu, Renrui Zhang, Yi Wang, Yu Qiao, and Hongsheng Li. Retrieving-to-answer: Zero-shot video question answering with frozen large language models. In *ICCV*, pp. 272–283, 2023. 5.1

Youxin Pang, Yong Zhang, Weize Quan, Yanbo Fan, Xiaodong Cun, Ying Shan, and Dong-ming Yan. Dpe: Disentanglement of pose and expression for general video portrait editing. In *CVPR*, pp. 427–436, 2023. 4.1.5

Jae Sung Park, Sheng Shen, Ali Farhadi, Trevor Darrell, Yejin Choi, and Anna Rohrbach. Exposing the limits of video-text models through contrast sets. In *NAACL*, pp. 3574–3586, 2022. 5.2

Deepak Pathak, Philipp Krahenbuhl, Jeff Donahue, Trevor Darrell, and Alexei A Efros. Context encoders: Feature learning by inpainting. In *CVPR*, pp. 2536–2544, 2016. 4.2.2

William Peebles and Saining Xie. Scalable diffusion models with transformers. In *ICCV*, 2023. 2.5.2, 2.5.3, 2.5.4

Dustin Podell, Zion English, Kyle Lacey, Andreas Blattmann, Tim Dockhorn, Jonas Müller, Joe Penna, and Robin Rombach. Sdxl: Improving latent diffusion models for high-resolution image synthesis. In *ICLR*, 2023. 2.5.3

Chenyang Qi, Xiaodong Cun, Yong Zhang, Chenyang Lei, Xintao Wang, Ying Shan, and Qifeng Chen. Fatezero: Fusing attentions for zero-shot text-based video editing. In *ICCV*, 2023. 2.2.7

Bosheng Qin, Juncheng Li, Siliang Tang, Tat-Seng Chua, and Yueting Zhuang. Instructvid2vid: Controllable video editing with natural language instructions. In *ICME*, pp. 1–6, 2024. 4.1.5

Zhiwu Qing, Shiwei Zhang, Jiayu Wang, Xiang Wang, Yujie Wei, Yingya Zhang, Changxin Gao, and Nong Sang. Hierarchical spatio-temporal decoupling for text-to-video generation. In *CVPR*, pp. 6635–6645, 2024. 2.4.4

Haonan Qiu, Zhaoxi Chen, Zhouxia Wang, Yingqing He, Menghan Xia, and Ziwei Liu. Freetraj: Tuning-free trajectory control in video diffusion models. *arXiv preprint arXiv:2406.16863*, 2024a. 4.1.2

Haonan Qiu, Menghan Xia, Yong Zhang, Yingqing He, Xintao Wang, Ying Shan, and Ziwei Liu. Freenoise: Tuning-free longer video diffusion via noise rescheduling. In *ICLR*, 2024b. 4.5

Y. Qiu et al. Freescale: High-resolution video generation with cascaded diffusion models. *arXiv preprint*, 2024c. 2.2.5, 4.2.4

Weize Quan, Jiaxi Chen, Yanli Liu, Dong-Ming Yan, and Peter Wonka. Deep learning-based image and video inpainting: A survey. *Int. J. Comput. Vis.*, pp. 1–34, 2024. 4.2.2

Alec Radford, Jeff Wu, Rewon Child, David Luan, Dario Amodei, and Ilya Sutskever. Language models are unsupervised multitask learners, 2019. 5.2

Alec Radford, Jong Wook Kim, Chris Hallacy, Aditya Ramesh, Gabriel Goh, Sandhini Agarwal, Girish Sastry, Amanda Askell, Pamela Mishkin, Jack Clark, et al. Learning transferable visual models from natural language supervision. In *ICML*, pp. 8748–8763, 2021. 2.5.4, 3.3, 5.1

Colin Raffel, Noam Shazeer, Adam Roberts, Katherine Lee, Sharan Narang, Michael Matena, Yanqi Zhou, Wei Li, and Peter J Liu. Exploring the limits of transfer learning with a unified text-to-text transformer. *JMLR*, 21(140):1–67, 2020. 2.5.4

Samyam Rajbhandari, Jeff Rasley, Olatunji Ruwase, and Yuxiong He. Zero: memory optimizations toward training trillion parameter models. In *Proceedings of the International Conference for High Performance Computing, Networking, Storage and Analysis*, pp. 1–16, 2020. 3.2

Ruslan Rakhimov, Denis Volkhonskiy, Alexey Artemov, Denis Zorin, and Evgeny Burnaev. Latent video transformer. *arXiv preprint arXiv:2006.10704*, 2020. 2.1.2

Rustam Rakhimov, Artur Sanakoyeu, et al. Lvdm: Latent video diffusion models. *arXiv preprint arXiv:2301.00203*, 2023. 2.4.4

Aditya Ramesh, Mikhail Pavlov, Gabriel Goh, Scott Gray, Chelsea Voss, Alec Radford, Mark Chen, and Ilya Sutskever. Zero-shot text-to-image generation. In *ICML*, pp. 8821–8831, 2021. 2.5.4

Aditya Ramesh, Prafulla Dhariwal, Alex Nichol, Casey Chu, and Mark Chen. Hierarchical text-conditional image generation with clip latents. *arXiv preprint arXiv:2204.06125*, 2022. 2.5.3, 2.5.4

Anurag Ranjan and Michael J Black. Optical flow estimation using a spatial pyramid network. In *CVPR*, pp. 4161–4170, 2017. 2.4.2

Elham Ravanbakhsh, Yongqing Liang, J. Ramanujam, and Xin Li. Deep video representation learning: a survey, 2024. 5.1

Nikhila Ravi, Valentin Gabeur, Yuan-Ting Hu, Ronghang Hu, Chaitanya Ryali, Tengyu Ma, Haitham Khedr, Roman Rädle, Chloe Rolland, Laura Gustafson, Eric Mintun, Junting Pan, Kalyan Vasudev Alwala, Nicolas Carion, Chao-Yuan Wu, Ross Girshick, Piotr Dollár, and Christoph Feichtenhofer. Sam 2: Segment anything in images and videos. *arXiv preprint arXiv:2408.00714*, 2024. URL `https://arxiv.org/abs/2408.00714`. 4.6.1

Nikhila Ravi, Valentin Gabeur, Yuan-Ting Hu, Ronghang Hu, Chaitanya Ryali, Tengyu Ma, Haitham Khedr, Roman Rädle, Chloe Rolland, Laura Gustafson, Eric Mintun, Junting Pan, Kalyan Vasudev Alwala, Nicolas Carion, Chao-Yuan Wu, Ross Girshick, Piotr Dollar, and Christoph Feichtenhofer. SAM 2: Segment anything in images and videos. In *ICLR*, 2025. 3.2

Scott Reed, Aäron Oord, Nal Kalchbrenner, Sergio Gómez Colmenarejo, Ziyu Wang, Yutian Chen, Dan Belov, and Nando Freitas. Parallel multiscale autoregressive density estimation. In *ICML*, pp. 2912–2921, 2017. 2.1.2

Jeremy Reizenstein, Roman Shapovalov, Philipp Henzler, Luca Sbordone, Patrick Labatut, and David Novotny. Common objects in 3d: Large-scale learning and evaluation of real-life 3d category reconstruction. In *ICCV*, 2021. 4.6.1

Jiawei Ren, Liang Pan, Jiaxiang Tang, Chi Zhang, Ang Cao, Gang Zeng, and Ziwei Liu. Dreamgaussian4d: Generative 4d gaussian splatting, 2023. 5.4.2

Weiming Ren, Huan Yang, Ge Zhang, Cong Wei, Xinrun Du, Wenhao Huang, and Wenhu Chen. Consisti2v: Enhancing visual consistency for image-to-video generation, 2024. 1, 4.1.1, 4.4

Anna Rohrbach, Marcus Rohrbach, Niket Tandon, and Bernt Schiele. A dataset for movie description. In *CVPR*, pp. 3202–3212, 2015. 3.1

Robin Rombach, Andreas Blattmann, Dominik Lorenz, Patrick Esser, and Björn Ommer. High-resolution image synthesis with latent diffusion models. In *CVPR*, pp. 10684–10695, 2022. 2.1.3, 2.5.1, 2.5.3, 2.5.4

Olaf Ronneberger, Philipp Fischer, and Thomas Brox. U-net: Convolutional networks for biomedical image segmentation. In *MICCAI*, pp. 234–241, 2015. 2.5.1

Kevin Dela Rosa. Video enriched retrieval augmented generation using aligned video captions. *CoRR*, abs/2405.17706, 2024. 5.2

Andreas Rössler, Davide Cozzolino, Luisa Verdoliva, Christian Riess, Justus Thies, and Matthias Nießner. Faceforensics: A large-scale video dataset for forgery detection in human faces. In *CVPR*, 2018. 1

Claudio Rota, Marco Buzzelli, Simone Bianco, and Raimondo Schettini. Video restoration based on deep learning: a comprehensive survey. *Artif. Intell. Rev.*, 56(6):5317–5364, 2023. 4.2.1

Chitwan Saharia, William Chan, Saurabh Saxena, Lala Li, Jay Whang, Emily L Denton, Kamyar Ghasemipour, Raphael Gontijo Lopes, Burcu Karagol Ayan, Tim Salimans, et al. Photorealistic text-to-image diffusion models with deep language understanding. In *NeurIPS*, pp. 36479–36494, 2022. 2.5.1, 2.5.3, 3.1

Masaki Saito, Eiichi Matsumoto, and Shunta Saito. Temporal generative adversarial nets with singular value clipping. In *ICCV*, pp. 2830–2839, 2017. 2.1.1

Masaki Saito, Shunta Saito, Masanori Koyama, and Sosuke Kobayashi. Train sparsely, generate densely: Memory-efficient unsupervised training of high-resolution temporal gan. *Int. J. Comput. Vis.*, 128(10): 2586–2606, 2020. 2.1.1

Ramon Sanabria, Ozan Caglayan, Shruti Palaskar, Desmond Elliott, Loïc Barrault, Lucia Specia, and Florian Metze. How2: A large-scale dataset for multimodal language understanding, 2018. 3.1

Seonguk Seo, Joon-Young Lee, and Bohyung Han. Urvos: Unified referring video object segmentation network with a large-scale benchmark. In *ECCV*, pp. 208–223, 2020. 5.1

Younggyo Seo, Kimin Lee, Fangchen Liu, Stephen James, and Pieter Abbeel. Harp: Autoregressive latent video prediction with high-fidelity image generator. In *ICIP*, pp. 3943–3947, 2022. 2.1.2

Tianchang Shen, Jun Gao, Kangxue Yin, Ming-Yu Liu, and Sanja Fidler. Deep marching tetrahedra: a hybrid representation for high-resolution 3d shape synthesis. In *NeurIPS*, 2021. 5.4.1

Xiaoqian Shen, Xiang Li, and Mohamed Elhoseiny. Mostgan-v: Video generation with temporal motion styles. In *CVPR*, pp. 5652–5661, 2023. 4.4

Changhao Shi, Haomiao Ni, Kai Li, Shaobo Han, Mingfu Liang, and Martin Renqiang Min. Exploring compositional visual generation with latent classifier guidance. In *CVPR*, pp. 853–862, 2023a. 2.3.1

Xiaoyu Shi, Zhaoyang Huang, Weikang Bian, Dasong Li, Manyuan Zhang, Ka Chun Cheung, Simon See, Hongwei Qin, Jifeng Dai, and Hongsheng Li. Videoflow: Exploiting temporal cues for multi-frame optical flow estimation. *arXiv preprint arXiv:2303.08340*, 2023b. 2.4.2

Xiaoyu Shi, Zhaoyang Huang, Dasong Li, Manyuan Zhang, Ka Chun Cheung, Simon See, Hongwei Qin, Jifeng Dai, and Hongsheng Li. Flowformer++: Masked cost volume autoencoding for pretraining optical flow estimation. *arXiv preprint arXiv:2303.01237*, 2023c. 2.4.2

Xiaoyu Shi, Zhaoyang Huang, Fu-Yun Wang, Weikang Bian, Dasong Li, Yi Zhang, Manyuan Zhang, Ka Chun Cheung, Simon See, Hongwei Qin, et al. Motion-i2v: Consistent and controllable image-to-video generation with explicit motion modeling. In *SIGGRAPH*, pp. 1–11, 2024. 2.4.2, 4.1.1, 4.1.2, 4.4

Yichun Shi, Peng Wang, Jianglong Ye, Long Mai, Kejie Li, and Xiao Yang. Mvdream: Multi-view diffusion for 3d generation. In *ICLR*, 2023d. 4.6.2

Chaehun Shin, Heeseung Kim, Che Hyun Lee, Sang-gil Lee, and Sungroh Yoon. Edit-a-video: Single video editing with object-aware consistency. In *ACML*, pp. 1215–1230, 2024. 4.1.5

Chenyang Si, Weichen Fan, Zhengyao Lv, Ziqi Huang, Yu Qiao, and Ziwei Liu. Repvideo: Rethinking cross-layer representation for video generation. *arXiv preprint arXiv:2501.08994*, 2025. 2.4.4

Aliaksandr Siarohin, Stéphane Lathuilière, Sergey Tulyakov, Elisa Ricci, and Nicu Sebe. First order motion model for image animation. In *NeurIPS*, 2019. 1

Uri Singer, Adam Polyak, et al. Make-a-video: Text-to-video generation without text-video data. *arXiv preprint arXiv:2209.14792*, 2022. 2.1.3, 2.4.4, 2.5.3

Uriel Singer, Shelly Sheynin, Adam Polyak, Oron Ashual, Iurii Makarov, Filippos Kokkinos, Naman Goyal, Andrea Vedaldi, Devi Parikh, Justin Johnson, et al. Text-to-4d dynamic scene generation. *arXiv preprint arXiv:2301.11280*, 2023. 2.4.1, 5.4.2

Amanpreet Singh, Ronghang Hu, Vedanuj Goswami, Guillaume Couairon, Wojciech Galuba, Marcus Rohrbach, and Douwe Kiela. Flava: A foundational language and vision alignment model. In *CVPR*, pp. 15617–15629, 2022. 5.2

Ivan Skorokhodov, Sergey Tulyakov, and Mohamed Elhoseiny. Stylegan-v: A continuous video generator with the price, image quality and perks of stylegan2. In *CVPR*, pp. 3616–3626, 2022. 2.1.1, 4.4, 4.5

SkyReels-AI. Skyreels v1: Human-centric video foundation model. `https://github.com/SkyworkAI/SkyReels-V1`, 2025. 2.4.4, 2.5.3, 2.5.4

Jascha Sohl-Dickstein, Eric Weiss, Niru Maheswaranathan, and Surya Ganguli. Deep unsupervised learning using nonequilibrium thermodynamics. In *ICML*, pp. 2256–2265, 2015. 1, 2.2.1

Jiaming Song, Chenlin Meng, and Stefano Ermon. Denoising diffusion implicit models. *arXiv preprint arXiv:2010.02502*, 2020a. 2.2.3

Yang Song, Jascha Sohl-Dickstein, Diederik P Kingma, Abhishek Kumar, Stefano Ermon, and Ben Poole. Score-based generative modeling through stochastic differential equations. In *ICLR*, 2020b. 2.4.3

Yeji Song, Wonsik Shin, Junsoo Lee, Jeesoo Kim, and Nojun Kwak. Save: Protagonist diversification with structure agnostic video editing. *arXiv preprint arXiv:2312.02503*, 2023. 4.1.5

Achint Soni, Sreyas Venkataraman, Abhranil Chandra, Sebastian Fischmeister, Percy Liang, Bo Dai, and Sherry Yang. Videoagent: Self-improving video generation. *arXiv preprint arXiv:2410.10076*, 2024a. 4.1.6

Achint Soni, Sreyas Venkataraman, Abhranil Chandra, Sebastian Fischmeister, Percy Liang, Bo Dai, and Sherry Yang. Videoagent: Self-improving video generation, 2024b. 2.4.4

Khurram Soomro, Amir Roshan Zamir, and Mubarak Shah. Ucf101: A dataset of 101 human actions classes from videos in the wild, 2012. 1, 3.1

Alexandros Stergiou and Ronald Poppe. Adapool: Exponential adaptive pooling for information-retaining downsampling. *IEEE Trans. Image Process.*, 32:251–266, 2023. 1, 3.1

Jonathan C. Stroud, Zhichao Lu, Chen Sun, Jia Deng, Rahul Sukthankar, Cordelia Schmid, and David A. Ross. Learning video representations from textual web supervision, 2021. 3.1

Deqing Sun, Stefan Roth, and Michael J Black. A quantitative analysis of current practices in optical flow estimation and the principles behind them. *Int. J. Comput. Vis.*, 106(2):115–137, 2014. 2.4.2

Deqing Sun, Xiaodong Yang, Ming-Yu Liu, and Jan Kautz. Pwc-net: Cnns for optical flow using pyramid, warping, and cost volume. In *CVPR*, pp. 8934–8943, 2018. 2.4.2

Jiaming Sun, Zehong Shen, Yuang Wang, Hujun Bao, and Xiaowei Zhou. Loftr: Detector-free local feature matching with transformers. In *CVPR*, pp. 8922–8931, 2021. 2.4.2

Mingzhen Sun, Weining Wang, Zihan Qin, Jiahui Sun, Sihan Chen, and Jing Liu. Glober: Coherent non-autoregressive video generation via global guided video decoder. In *NeurIPS*, 2023a. 4.4

Mingzhen Sun, Weining Wang, Xinxin Zhu, and Jing Liu. Moso: Decomposing motion, scene and object for video prediction. In *CVPR*, pp. 18727–18737, 2023b. 4.4

Qi Sun, Zhiyang Guo, Ziyu Wan, Jing Nathan Yan, Shengming Yin, Wengang Zhou, Jing Liao, and Houqiang Li. Eg4d: Explicit generation of 4d object without score distillation, 2024. 5.4.2

Yuqing Sun, Yifan Xu, et al. Latent-shift: Exploring latent shifts for video generation. *arXiv preprint arXiv:2302.02016*, 2023c. 2.4.4

Ryan Szeto and Jason J. Corso. The devil is in the details: A diagnostic evaluation benchmark for video inpainting. In *CVPR*, pp. 21022–21031, 2022. 3.1

Shuai Tan, Bin Ji, and Ye Pan. Flowvqtalker: High-quality emotional talking face generation through normalizing flow and quantization. In *Proceedings of the IEEE/CVF Conference on Computer Vision and Pattern Recognition*, pp. 26317–26327, 2024a. 10, 4.1.4, 4.3

Zhenxiong Tan, Xingyi Yang, Songhua Liu, and Xinchao Wang. Video-infinity: Distributed long video generation, 2024b. 4.5

Zhiyu Tan, Mengping Yang, Luozheng Qin, Hao Yang, Ye Qian, Qiang Zhou, Cheng Zhang, and Hao Li. An empirical study and analysis of text-to-image generation using large language model-powered textual representation. *arXiv preprint arXiv:2405.12914*, 2024c. 2.5.4

Shitao Tang, Fuyang Zhang, Jiacheng Chen, Peng Wang, and Yasutaka Furukawa. Mvdiffusion: Enabling holistic multi-view image generation with correspondence-aware diffusion. *arXiv preprint*, 2023. 4.6.2

Shitao Tang, Jiacheng Chen, Dilin Wang, Chengzhou Tang, Fuyang Zhang, Yuchen Fan, Vikas Chandra, Yasutaka Furukawa, and Rakesh Ranjan. Mvdiffusion++: A dense high-resolution multi-view diffusion model for single or sparse-view 3d object reconstruction. *arXiv preprint arXiv:2402.12712*, 2024. 4.6.2

Genmo Team. Mochi 1. `https://github.com/genmoai/models`, 2024a. 2.4.4, 2.5.3, 3.4

Kolors Team. Kolors: Effective training of diffusion model for photorealistic text-to-image synthesis. *arXiv preprint*, 2024b. 2.5.3, 2.5.4

The Movie Gen teamMeta. Movie gen: A cast of media foundation models, 2024. 2.5.3

Zachary Teed and Jia Deng. Raft: Recurrent all-pairs field transforms for optical flow. In *ECCV*, pp. 402–419, 2020. 2.4.2, 3.3

Yao Teng, Enze Xie, Yue Wu, Haoyu Han, Zhenguo Li, and Xihui Liu. Drag-a-video: Non-rigid video editing with point-based interaction. *arXiv preprint arXiv:2312.02936*, 2023. 4.1.5

Yannis Tevissen, Khalil Guetari, and Frédéric Petitpont. Towards retrieval augmented generation over large video libraries. *CoRR*, abs/2406.14938, 2024. 5.2

Linrui Tian, Qi Wang, Bang Zhang, and Liefeng Bo. Emo: Emote portrait alive-generating expressive portrait videos with audio2video diffusion model under weak conditions. *arXiv preprint arXiv:2402.17485*, 2024. 4.1.1, 4.1.4, 4.3, 4.4

Yu Tian, Jian Ren, Menglei Chai, Kyle Olszewski, Xi Peng, Dimitris N Metaxas, and Sergey Tulyakov. A good image generator is what you need for high-resolution video synthesis. In *ICLR*, 2020. 2.1.1

Alexander Tong, Nikolay Malkin, Guillaume Huguet, Yanlei Zhang, Jarrid Rector-Brooks, Kilian FATRAS, Guy Wolf, and Yoshua Bengio. Improving and generalizing flow-based generative models with minibatch optimal transport. In *ICML Workshop*, 2023. 2.2.4

Hugo Touvron, Thibaut Lavril, Gautier Izacard, Xavier Martinet, Marie-Anne Lachaux, Timothée Lacroix, Baptiste Rozière, Naman Goyal, Eric Hambro, Faisal Azhar, et al. Llama: Open and efficient foundation language models. *arXiv preprint arXiv:2302.13971*, 2023a. 2.5.4, 3.2

Hugo Touvron, Louis Martin, Kevin Stone, Peter Albert, Amjad Almahairi, Yasmine Babaei, Nikolay Bashlykov, Soumya Batra, Prajjwal Bhargava, Shruti Bhosale, et al. Llama 2: Open foundation and fine-tuned chat models. *arXiv preprint arXiv:2307.09288*, 2023b. 2.5.4, 3.2

Du Tran, Lubomir D. Bourdev, Rob Fergus, Lorenzo Torresani, and Manohar Paluri. Learning spatiotemporal features with 3d convolutional networks. In *ICCV*, pp. 4489–4497, 2015. 5.1

Shuyuan Tu, Qi Dai, Zhi-Qi Cheng, Han Hu, Xintong Han, Zuxuan Wu, and Yu-Gang Jiang. Motioneditor: Editing video motion via content-aware diffusion. In *CVPR*, pp. 7882–7891, 2024. 4.1.5

Sergey Tulyakov, Ming-Yu Liu, Xiaodong Yang, and Jan Kautz. Mocogan: Decomposing motion and content for video generation. In *CVPR*, pp. 1526–1535, 2018. 2.1.1

Thomas Unterthiner, Sjoerd van Steenkiste, Karol Kurach, Raphaël Marinier, Marcin Michalski, and Sylvain Gelly. Fvd: A new metric for video generation. In *ICLR Workshop*, 2019. 3.3

Aaron Van Den Oord, Oriol Vinyals, et al. Neural discrete representation learning. In *NeurIPS*, 2017. 2.5.3

Basile Van Hoorick, Rundi Wu, Ege Ozguroglu, Kyle Sargent, Ruoshi Liu, Pavel Tokmakov, Achal Dave, Changxi Zheng, and Carl Vondrick. Generative camera dolly: Extreme monocular dynamic novel view synthesis. In *ECCV*, pp. 313–331, 2024. 4.6.1, 4.6.3

Ashish Vaswani, Noam Shazeer, Niki Parmar, Jakob Uszkoreit, Llion Jones, Aidan N Gomez, Ł ukasz Kaiser, and Illia Polosukhin. Attention is all you need. In *NeurIPS*, 2017. 5.1

Ruben Villegas, Mohammad Babaeizadeh, Pieter-Jan Kindermans, Hernan Moraldo, Han Zhang, Mohammad Taghi Saffar, Santiago Castro, Julius Kunze, and Dumitru Erhan. Phenaki: Variable length video generation from open domain textual descriptions. In *ICLR*, 2022. 2.4.4, 2.5.3, 3.4

Vikram Voleti, Alexia Jolicoeur-Martineau, and Christopher Pal. Mcvd - masked conditional video diffusion for prediction, generation, and interpolation. In *NeurIPS*, 2022. 4.2.3, 4.2.5

Vikram Voleti, Chun-Han Yao, Mark Boss, Adam Letts, David Pankratz, Dmitry Tochilkin, Christian Laforte, Robin Rombach, and Varun Jampani. Sv3d: Novel multi-view synthesis and 3d generation from a single image using latent video diffusion. *arXiv preprint arXiv:2403.12008*, 2024. 4.6.3, 5.4.1

Zhen Wan, Yue Ma, Chenyang Qi, Zhiheng Liu, and Tao Gui. Unipaint: Unified space-time video inpainting via mixture-of-experts. *arXiv preprint arXiv:2412.06340*, 2024. 4.2.2, 4.2.5

Cong Wang, Jiaxi Gu, Panwen Hu, Songcen Xu, Hang Xu, and Xiaodan Liang. Dreamvideo: High-fidelity image-to-video generation with image retention and text guidance, 2023a. 4.1.1

Fu-Yun Wang, Wenshuo Chen, Guanglu Song, Han-Jia Ye, Yu Liu, and Hongsheng Li. Gen-l-video: Multi-text to long video generation via temporal co-denoising, 2023b. 4.5

Fu-Yun Wang, Zhaoyang Huang, Weikang Bian, Xiaoyu Shi, Keqiang Sun, Guanglu Song, Yu Liu, and Hongsheng Li. Animatelcm: Computation-efficient personalized style video generation without personalized video data, 2024a. 2.4.4

Haoran Wang, Di Xu, Dongliang He, Fu Li, Zhong Ji, Jungong Han, and Errui Ding. Boosting video-text retrieval with explicit high-level semantics. In *ACM MM*, pp. 4887–4898, 2022a. 5.2

Jiamian Wang, Guohao Sun, Pichao Wang, Dongfang Liu, Sohail A. Dianat, Majid Rabbani, Raghuveer Rao, and Zhiqiang Tao. Text is mass: Modeling as stochastic embedding for text-video retrieval. *CoRR*, abs/2403.17998, 2024b. 5.1

Jianyi Wang, Zongsheng Yue, Shangchen Zhou, Kelvin CK Chan, and Chen Change Loy. Exploiting diffusion prior for real-world image super-resolution. *Int. J. Comput. Vis.*, pp. 1–21, 2024c. 13, 4.2.4

Jiawei Wang, Yuchen Zhang, Jiaxin Zou, Yan Zeng, Guoqiang Wei, Liping Yuan, and Hang Li. Boximator: Generating rich and controllable motions for video synthesis. *arXiv preprint arXiv:2402.01566*, 2024d. 4.1.2

Jiuniu Wang, Hangjie Yuan, Dayou Chen, Yingya Zhang, Xiang Wang, and Shiwei Zhang. Modelscope text-to-video technical report. *arXiv preprint arXiv:2308.06571*, 2023c. 2.4.1, 2.4.4, 2.5.1

Qinghe Wang, Yawen Luo, Xiaoyu Shi, Xu Jia, Huchuan Lu, Tianfan Xue, Xintao Wang, Pengfei Wan, Di Zhang, and Kun Gai. Cinemaster: A 3d-aware and controllable framework for cinematic text-to-video generation, 2025. URL `https://arxiv.org/abs/2502.08639`. 4.1.2, 4.1.3, 4.6.1, 4.6.2, 4.6.3

Tan Wang, Linjie Li, Kevin Lin, Yuanhao Zhai, Chung-Ching Lin, Zhengyuan Yang, Hanwang Zhang, Zicheng Liu, and Lijuan Wang. Disco: Disentangled control for realistic human dance generation. In *CVPR*, pp. 9326–9336, 2024e. 4.1.5

Wen Wang, Yan Jiang, Kangyang Xie, Zide Liu, Hao Chen, Yue Cao, Xinlong Wang, and Chunhua Shen. Zero-shot video editing using off-the-shelf image diffusion models. *arXiv preprint arXiv:2303.17599*, 2023d. 4.1.5

Wenhao Wang and Yi Yang. Vidprom: A million-scale real prompt-gallery dataset for text-to-video diffusion models. In *NeurIPS*, 2024. 1, 3.1

Wenjing Wang, Huan Yang, Zixi Tuo, Huiguo He, Junchen Zhu, Jianlong Fu, and Jiaying Liu. Swap attention in spatiotemporal diffusions for text-to-video generation, 2024f. 3.1

Xiang Wang, Hangjie Yuan, Shiwei Zhang, Dayou Chen, Jiuniu Wang, Yingya Zhang, Yujun Shen, Deli Zhao, and Jingren Zhou. Videocomposer: Compositional video synthesis with motion controllability. *arXiv preprint arXiv:2306.02018*, 2023e. 4.1.1, 4.1.1

Xiang Wang, Hangjie Yuan, Shiwei Zhang, Dayou Chen, Jiuniu Wang, Yingya Zhang, Yujun Shen, Deli Zhao, and Jingren Zhou. Videocomposer: Compositional video synthesis with motion controllability. In *NeurIPS*, 2023f. 4.4

Xiaohan Wang, Linchao Zhu, Zhedong Zheng, Mingliang Xu, and Yi Yang. Align and tell: Boosting text-video retrieval with local alignment and fine-grained supervision. *IEEE Trans. Multimedia.*, pp. 1–11, 2022b. 5.2

Xin Wang, Jiawei Wu, Junkun Chen, Lei Li, Yuan-Fang Wang, and William Yang Wang. Vatex: A large-scale, high-quality multilingual dataset for video-and-language research. In *ICCV*, pp. 4580–4590, 2019. 3.1

Yaohui Wang, Xinyuan Chen, Xin Ma, Shangchen Zhou, Ziqi Huang, Yi Wang, Ceyuan Yang, Yinan He, Jiashuo Yu, Peiqing Yang, et al. Lavie: High-quality video generation with cascaded latent diffusion models. *arXiv preprint arXiv:2309.15103*, 2023g. 2.4.4, 3.4

Yi Wang, Yinan He, Yizhuo Li, Kunchang Li, Jiashuo Yu, Xin Ma, Xinhao Li, Guo Chen, Xinyuan Chen, Yaohui Wang, Ping Luo, Ziwei Liu, Yali Wang, Limin Wang, and Yu Qiao. Internvid: A large-scale video-text dataset for multimodal understanding and generation. In *ICLR*, 2023h. 3.1

Yikai Wang, Xinzhou Wang, Zilong Chen, Zhengyi Wang, Fuchun Sun, and Jun Zhu. Vidu4d: Single generated video to high-fidelity 4d reconstruction with dynamic gaussian surfels. In *NeurIPS*, 2024g. 5.4.2

Yimu Wang and Peng Shi. Video-text retrieval by supervised sparse multi-grained learning. In *EMNLP*, 2023. 1

Yimu Wang, Shiyin Lu, and Lijun Zhang. Searching privately by imperceptible lying: A novel private hashing method with differential privacy. In *ACM MM*, pp. 2700–2709, 2020a. 5.2

Yimu Wang, Xiu-Shen Wei, Bo Xue, and Lijun Zhang. Piecewise hashing: A deep hashing method for large-scale fine-grained search. In *PRCV*, pp. 432–444, 2020b. 5.2

Yimu Wang, Bo Xue, Quan Cheng, Yuhui Chen, and Lijun Zhang. Deep unified cross-modality hashing by pairwise data alignment. In *IJCAI*, pp. 1129–1135, 2021. 5.2

Yuhan Wang, Liming Jiang, and Chen Change Loy. Styleinv: A temporal style modulated inversion network for unconditional video generation. In *ICCV*, pp. 22851–22861, 2023i. 2.1.1

Zhen Wang, Yunhao Ba, Pradyumna Chari, Oyku Deniz Bozkurt, Gianna Brown, Parth Patwa, Niranjan Vaddi, Laleh Jalilian, and Achuta Kadambi. Synthetic generation of face videos with plethysmograph physiology. In *Proceedings of the IEEE/CVF conference on computer vision and pattern recognition*, pp. 20587–20596, 2022c. 4.1.6

Zhenzhi Wang, Yixuan Li, Yanhong Zeng, Youqing Fang, Yuwei Guo, Wenran Liu, Jing Tan, Kai Chen, Tianfan Xue, Bo Dai, and Dahua Lin. Humanvid: Demystifying training data for camera-controllable human image animation, 2024h. 4.6.1, 4.6.3

Zhouxia Wang, Yushi Lan, Shangchen Zhou, and Chen Change Loy. Objctrl-2.5 d: Training-free object control with camera poses. *arXiv preprint arXiv:2412.07721*, 2024i. 4.1.2

Zhouxia Wang, Ziyang Yuan, Xintao Wang, Yaowei Li, Tianshui Chen, Menghan Xia, Ping Luo, and Ying Shan. Motionctrl: A unified and flexible motion controller for video generation. In *ACM SIGGRAPH 2024 Conference Papers*, pp. 1–11, 2024j. 4.1.3

Zhouxia Wang, Ziyang Yuan, Xintao Wang, Yaowei Li, Tianshui Chen, Menghan Xia, Ping Luo, and Ying Shan. Motionctrl: A unified and flexible motion controller for video generation. In *SIGGRAPH*, 2024k. 4.6.3

Daniel Watson, Saurabh Saxena, Lala Li, Andrea Tagliasacchi, and David J. Fleet. Controlling space and time with diffusion models, 2024. 4.6.3

Huawei Wei, Zejun Yang, and Zhisheng Wang. Aniportrait: Audio-driven synthesis of photorealistic portrait animation. *arXiv preprint arXiv:2403.17694*, 2024a. 4.1.4, 4.3

Yujie Wei, Shiwei Zhang, Hangjie Yuan, Xiang Wang, Haonan Qiu, Rui Zhao, Yutong Feng, Feng Liu, Zhizhong Huang, Jiaxin Ye, Yingya Zhang, and Hongming Shan. Dreamvideo-2: Zero-shot subject-driven video customization with precise motion control, 2024b. 2.2.7, 14, 4.3

Yujie Wei, Shiwei Zhang, Hangjie Yuan, Xiang Wang, Haonan Qiu, Rui Zhao, Yutong Feng, Feng Liu, Zhizhong Huang, Jiaxin Ye, et al. Dreamvideo-2: Zero-shot subject-driven video customization with precise motion control. *arXiv preprint arXiv:2410.13830*, 2024c. 2.2.8, 4.1.1, 4.1.2, 4.3, 14

Wenming Weng, Ruoyu Feng, Yanhui Wang, Qi Dai, Chunyu Wang, Dacheng Yin, Zhiyuan Zhao, Kai Qiu, Jianmin Bao, Yuhui Yuan, et al. Art-v: Auto-regressive text-to-video generation with diffusion models. In *CVPR*, pp. 7395–7405, 2024. 2.1.4

Dongming Wu, Xingping Dong, Ling Shao, and Jianbing Shen. Multi-level representation learning with semantic alignment for referring video object segmentation. In *CVPR*, pp. 4986–4995, 2022a. 5.1

Haoning Wu, Erli Zhang, Liang Liao, Chaofeng Chen, Jingwen Hou, Annan Wang, Wenxiu Sun, Qiong Yan, and Weisi Lin. Exploring video quality assessment on user generated contents from aesthetic and technical perspectives. In *ICCV*, pp. 20087–20097, 2023a. 3.3

Haoning Wu, Dongxu Li, Bei Chen, and Junnan Li. Longvideobench: A benchmark for long-context interleaved video-language understanding. In *NeurIPS*, 2024a. 5.3

Hongjia Wu, Özgü Alay, Anna Brunstrom, Simone Ferlin, and Giuseppe Caso. Peekaboo: Learning-based multipath scheduling for dynamic heterogeneous environments. *IEEE Journal on Selected Areas in Communications*, 38(10):2295–2310, 2020. 4.1.2

Jay Zhangjie Wu, Yixiao Ge, Xintao Wang, Stan Weixian Lei, Yuchao Gu, Yufei Shi, Wynne Hsu, Ying Shan, Xiaohu Qie, and Mike Zheng Shou. Tune-a-video: One-shot tuning of image diffusion models for text-to-video generation. In *ICCV*, pp. 7623–7633, 2023b. 2.2.6, 4.1.5

Jiannan Wu, Yi Jiang, Peize Sun, Zehuan Yuan, and Ping Luo. Language as queries for referring video object segmentation. In *CVPR*, pp. 4964–4974, 2022b. 5.1

Jianzong Wu, Xiangtai Li, Chenyang Si, Shangchen Zhou, Jingkang Yang, Jiangning Zhang, Yining Li, Kai Chen, Yunhai Tong, Ziwei Liu, et al. Towards language-driven video inpainting via multimodal large language models. In *CVPR*, pp. 12501–12511, 2024b. 4.2.2

Jianzong Wu, Xiangtai Li, Yanhong Zeng, Jiangning Zhang, Qianyu Zhou, Yining Li, Yunhai Tong, and Kai Chen. Motionbooth: Motion-aware customized text-to-video generation. *arXiv preprint arXiv:2406.17758*, 2024c. 4.1.2, 4.1.3

Qingyun Wu, Gagan Bansal, Jieyu Zhang, Yiran Wu, Beibin Li, Erkang Zhu, Li Jiang, Xiaoyun Zhang, Shaokun Zhang, Jiale Liu, et al. Autogen: Enabling next-gen llm applications via multi-agent conversations. In *COLM*, 2024d. 2.4.4

Ruiqi Wu, Liangyu Chen, Tong Yang, Chunle Guo, Chongyi Li, and Xiangyu Zhang. Lamp: Learn a motion pattern for few-shot-based video generation. *arXiv preprint arXiv:2310.10769*, 2023c. 2.2.6

Rundi Wu, Ruiqi Gao, Ben Poole, Alex Trevithick, Changxi Zheng, Jonathan T. Barron, and Aleksander Holynski. Cat4d: Create anything in 4d with multi-view video diffusion models. *arXiv:2411.18613*, 2024e. 4.6.3, 21, 5.4.2

Tong Wu, Jiarui Zhang, Xiao Fu, Yuxin Wang, Liang Pan Jiawei Ren, Wayne Wu, Lei Yang, Jiaqi Wang, Chen Qian, Dahua Lin, and Ziwei Liu. Omniobject3d: Large-vocabulary 3d object dataset for realistic perception, reconstruction and generation. In *CVPR*, 2023d. 4.6.1

Weijia Wu, Zhuang Li, Yuchao Gu, Rui Zhao, Yefei He, David Junhao Zhang, Mike Zheng Shou, Yan Li, Tingting Gao, and Di Zhang. Draganything: Motion control for anything using entity representation. In *European Conference on Computer Vision*, pp. 331–348. Springer, 2024f. 4.1.2

X. Wu et al. Videoprefer: A comprehensive video preference dataset and reward model. *arXiv preprint*, 2024g. 2.2.5

Xiuzhe Wu, Pengfei Hu, Yang Wu, Xiaoyang Lyu, Yan-Pei Cao, Ying Shan, Wenming Yang, Zhongqian Sun, and Xiaojuan Qi. Speech2lip: High-fidelity speech to lip generation by learning from a short video. In *Proceedings of the IEEE/CVF International Conference on Computer Vision*, pp. 22168–22177, 2023e. 4.1.4

Yue Wu, Yu Deng, Jiaolong Yang, Fangyun Wei, Qifeng Chen, and Xin Tong. Anifacegan: Animatable 3d-aware face image generation for video avatars. In *NeurIPS*, 2022c. 2.1.1

Ziyi Wu, Aliaksandr Siarohin, Willi Menapace, Ivan Skorokhodov, Yuwei Fang, Varnith Chordia, Igor Gilitschenski, and Sergey Tulyakov. Mind the time: Temporally-controlled multi-event video generation. *arXiv preprint arXiv:2412.05263*, 2024h. 4.1.6

Hongchi Xia, Yang Fu, Sifei Liu, and Xiaolong Wang. Rgbd objects in the wild: Scaling real-world 3d object learning from rgb-d videos. In *CVPR*, pp. 22378–22389, 2024. 4.6.1

Jinxi Xiang, Ricong Huang, Jun Zhang, Guanbin Li, Xiao Han, and Yang Wei. Versvideo: Leveraging enhanced temporal diffusion models for versatile video generation. In *ICLR*, 2023. 2.5.2

Desai Xie, Zhan Xu, Yicong Hong, Hao Tan, Difan Liu, Feng Liu, Arie Kaufman, and Yang Zhou. Progressive autoregressive video diffusion models. *arXiv preprint arXiv:2410.08151*, 2024a. 2.1.4, 4.5

Liangbin Xie, Xintao Wang, Honglun Zhang, Chao Dong, and Ying Shan. Vfhq: A high-quality dataset and benchmark for video face super-resolution. In *CVPR Workshops*, pp. 656–665, 2022. 3.1

Shaoan Xie, Zhifei Zhang, Zhe Lin, Tobias Hinz, and Kun Zhang. Smartbrush: Text and shape guided object inpainting with diffusion model. In *CVPR*, pp. 22428–22437, 2023. 4.2.2

Yiming Xie, Chun-Han Yao, Vikram Voleti, Huaizu Jiang, and Varun Jampani. Sv4d: Dynamic 3d content generation with multi-frame and multi-view consistency, 2024b. 4.6.2, 5.4.2

Jinbo Xing, Menghan Xia, Yong Zhang, Haoxin Chen, Wangbo Yu, Hanyuan Liu, Xintao Wang, Tien-Tsin Wong, and Ying Shan. Dynamicrafter: Animating open-domain images with video diffusion priors, 2023. 3.2, 4.1.1, 4.1.1

Jinbo Xing, Hanyuan Liu, Menghan Xia, Yong Zhang, Xintao Wang, Ying Shan, and Tien-Tsin Wong. Tooncrafter: Generative cartoon interpolation. *arXiv preprint arXiv:2405.17933*, 2024a. 4.2.3

Zhen Xing, Qi Dai, Han Hu, Zuxuan Wu, and Yu-Gang Jiang. Simda: Simple diffusion adapter for efficient video generation. In *CVPR*, pp. 7827–7839, 2024b. 2.4.4, 2.5.4, 3.2, 4.1.5

Zhen Xing, Qijun Feng, Haoran Chen, Qi Dai, Han Hu, Hang Xu, Zuxuan Wu, and Yu-Gang Jiang. A survey on video diffusion models, 2024c. (document), 1

Yi Xiong, Ayan Chakrabarti, Ronen Basri, Steven J Gortler, David W Jacobs, and Todd Zickler. Learning from synthetic data for sky replacement in images. In *ECCV*, 2018. 1

Dejia Xu, Yifan Jiang, Chen Huang, Liangchen Song, Thorsten Gernoth, Liangliang Cao, Zhangyang Wang, and Hao Tang. Cavia: Camera-controllable multi-view video diffusion with view-integrated attention. *arXiv preprint arXiv:2410.10774*, 2024a. 4.1.3, 18, 4.6.1, 4.6.2, 4.6.3

Dejia Xu, Weili Nie, Chao Liu, Sifei Liu, Jan Kautz, Zhangyang Wang, and Arash Vahdat. Camco: Camera-controllable 3d-consistent image-to-video generation. *arXiv preprint arXiv:2406.02509*, 2024b. 4.1.1, 4.1.1, 4.1.3, 4.6.1, 4.6.2, 4.6.3

Dejing Xu, Zhou Zhao, Jun Xiao, Fei Wu, Hanwang Zhang, Xiangnan He, and Yueting Zhuang. Video question answering via gradually refined attention over appearance and motion. In *ACM MM*, 2017. 5.3

Jiaqi Xu, Xinyi Zou, Kunzhe Huang, Yunkuo Chen, Bo Liu, MengLi Cheng, Xing Shi, and Jun Huang. Easyanimate: A high-performance long video generation method based on transformer architecture. *arXiv preprint arXiv:2405.18991*, 2024c. 2.4.4, 2.5.3, 3.4

Jun Xu, Tao Mei, Ting Yao, and Yong Rui. Msr-vtt: A large video description dataset for bridging video and language. In *CVPR*, pp. 5288–5296, 2016. 1, 3.1

Lin Xu, Yilin Zhao, Daquan Zhou, Zhijie Lin, See-Kiong Ng, and Jiashi Feng. Pllava : Parameter-free llava extension from images to videos for video dense captioning. *arxiv preprint arXiv:2404.16994*, 2024d. 3.2

Sicheng Xu, Guojun Chen, Yu-Xiao Guo, Jiaolong Yang, Chong Li, Zhenyu Zang, Yizhong Zhang, Xin Tong, and Baining Guo. Vasa-1: Lifelike audio-driven talking faces generated in real time. *arXiv preprint arXiv:2404.10667*, 2024e. 4.1.4, 4.3

Hongwei Xue, Tiankai Hang, Yanhong Zeng, Yuchong Sun, Bei Liu, Huan Yang, Jianlong Fu, and Baining Guo. Advancing high-resolution video-language representation with large-scale video transcriptions. In *CVPR*, pp. 5026–5035, 2022a. 3.1

L Xue. mt5: A massively multilingual pre-trained text-to-text transformer. *arXiv preprint arXiv:2010.11934*, 2020. 1

Linting Xue, Aditya Barua, Noah Constant, Rami Al-Rfou, Sharan Narang, Mihir Kale, Adam Roberts, and Colin Raffel. Byt5: Towards a token-free future with pre-trained byte-to-byte models. *TACL*, 10:291–306, 2022b. 2.5.4

Liqi Yan, Qifan Wang, Yiming Cui, Fuli Feng, Xiaojun Quan, Xiangyu Zhang, and Dongfang Liu. Gl-rg: Global-local representation granularity for video captioning. In *IJCAI*, pp. 2769–2775, 2022. 5.1

Wilson Yan, Yunzhi Zhang, Pieter Abbeel, and Aravind Srinivas. Videogpt: Video generation using vq-vae and transformers. *arXiv preprint arXiv:2104.10157*, 2021. 2.1.2, 2.4.4, 2.5.3

Wilson Yan, Andrew Brown, Pieter Abbeel, Rohit Girdhar, and Samaneh Azadi. Motion-conditioned image animation for video editing. *arXiv preprint arXiv:2311.18827*, 2023a. 4.1.5

Wilson Yan, Danijar Hafner, Stephen James, and Pieter Abbeel. Temporally consistent transformers for video generation. In *ICML*, pp. 39062–39098, 2023b. 3.1

Aiyuan Yang, Bin Xiao, Bingning Wang, Borong Zhang, Ce Bian, Chao Yin, Chenxu Lv, Da Pan, Dian Wang, Dong Yan, et al. Baichuan 2: Open large-scale language models. *arXiv preprint arXiv:2309.10305*, 2023a. 2.5.4

Dongjie Yang, Suyuan Huang, Chengqiang Lu, Xiaodong Han, Haoxin Zhang, Yan Gao, Yao Hu, and Hai Zhao. Vript: A video is worth thousands of words. In *NeurIPS*, 2024a. 1, 3.1

Fan Yang, Jianfeng Zhang, Yichun Shi, Bowen Chen, Chenxu Zhang, Huichao Zhang, Xiaofeng Yang, Jiashi Feng, and Guosheng Lin. Magic-boost: Boost 3d generation with mutli-view conditioned diffusion, 2024b. 4.6.2

Gengshan Yang and Deva Ramanan. Volumetric correspondence networks for optical flow. In *NeurIPS*, pp. 794–805, 2019. 2.4.2

Haibo Yang, Yang Chen, Yingwei Pan, Ting Yao, Zhineng Chen, Chong-Wah Ngo, and Tao Mei. Hi3d: Pursuing high-resolution image-to-3d generation with video diffusion models. In *ACM MM*, 2024c. 4.6.3, 5.4.1

Hao Yang, Chunfeng Yuan, Bing Li, Yang Du, Junliang Xing, Weiming Hu, and Stephen J. Maybank. Asymmetric 3d convolutional neural networks for action recognition. *Pattern Recognit.*, 85:1–12, 2019. 5.1

Jiayu Yang, Ziang Cheng, Yunfei Duan, Pan Ji, and Hongdong Li. Consistnet: Enforcing 3d consistency for multi-view images diffusion. In *CVPR*, pp. 7079–7088, 2024d. 4.6.2

Lihe Yang, Bingyi Kang, Zilong Huang, Xiaogang Xu, Jiashi Feng, and Hengshuang Zhao. Depth anything: Unleashing the power of large-scale unlabeled data. In *CVPR*, 2024e. 4.6.1

Lihe Yang, Bingyi Kang, Zilong Huang, Zhen Zhao, Xiaogang Xu, Jiashi Feng, and Hengshuang Zhao. Depth anything v2. *arXiv:2406.09414*, 2024f. 4.6.1

Sherry Yang, Yilun Du, Seyed Kamyar Seyed Ghasemipour, Jonathan Tompson, Leslie Pack Kaelbling, Dale Schuurmans, and Pieter Abbeel. Learning interactive real-world simulators. In *ICLR*, 2024g. 2.4.4

Shiyuan Yang, Liang Hou, Haibin Huang, Chongyang Ma, Pengfei Wan, Di Zhang, Xiaodong Chen, and Jing Liao. Direct-a-video: Customized video generation with user-directed camera movement and object motion. In *Special Interest Group on Computer Graphics and Interactive Techniques Conference Conference Papers '24*, pp. 1–12, 2024h. 4.6.3

Shiyuan Yang, Liang Hou, Haibin Huang, Chongyang Ma, Pengfei Wan, Di Zhang, Xiaodong Chen, and Jing Liao. Direct-a-video: Customized video generation with user-directed camera movement and object motion. In *ACM SIGGRAPH 2024 Conference Papers*, pp. 1–12, 2024i. 4.1.3

Shuai Yang, Yifan Zhou, Ziwei Liu, and Chen Change Loy. Rerender a video: Zero-shot text-guided video-to-video translation. In *SIGGRAPH Asia*, pp. 1–11, 2023b. 4.1.5

Zhuoyi Yang, Jiayan Teng, Wendi Zheng, Ming Ding, Shiyu Huang, Jiazheng Xu, Yuanming Yang, Wenyi Hong, Xiaohan Zhang, Guanyu Feng, et al. Cogvideox: Text-to-video diffusion models with an expert transformer. *arXiv preprint arXiv:2408.06072*, 2024j. 2.4.4, 2.5.3, 2.5.4, 3.2, 4.1.1

Yining Yao, Xi Guo, Chenjing Ding, and Wei Wu. Mygo: Consistent and controllable multi-view driving video generation with camera control, 2024. 4.6.3

Qinghao Ye, Guohai Xu, Ming Yan, Haiyang Xu, Qi Qian, Ji Zhang, and Fei Huang. Hitea: Hierarchical temporal-aware video-language pre-training. In *ICCV*, pp. 15359–15370, 2023. 5.1

Chen Yeh, You-Ming Chang, Wei-Chen Chiu, and Ning Yu. T2vs meet vlms: A scalable multimodal dataset for visual harmfulness recognition, 2024. 5.1

Hongwei Yi, Shitong Shao, Tian Ye, Jiantong Zhao, Qingyu Yin, Michael Lingelbach, Li Yuan, Yonghong Tian, Enze Xie, and Daquan Zhou. Magic 1-for-1: Generating one minute video clips within one minute, 2025. 2.4.4, 2.5.3, 2.5.4

Shengming Yin, Chenfei Wu, Jian Liang, Jie Shi, Houqiang Li, Gong Ming, and Nan Duan. Dragnuwa: Fine-grained control in video generation by integrating text, image, and trajectory. *arXiv preprint arXiv:2308.08089*, 2023a. 4.1.2

Shengming Yin, Chenfei Wu, Huan Yang, Jianfeng Wang, Xiaodong Wang, Minheng Ni, Zhengyuan Yang, Linjie Li, Shuguang Liu, Fan Yang, Jianlong Fu, Ming Gong, Lijuan Wang, Zicheng Liu, Houqiang Li, and Nan Duan. Nuwa-xl: Diffusion over diffusion for extremely long video generation. In *ACL*, pp. 1309–1320, 2023b. 4.5

Tianwei Yin, Qiang Zhang, Richard Zhang, William T Freeman, Fredo Durand, Eli Shechtman, and Xun Huang. From slow bidirectional to fast causal video generators. *arXiv preprint arXiv:2412.07772*, 2024. 2.1.4, 2.4.4, 2.5.2

Meng You, Zhiyu Zhu, Hui Liu, and Junhui Hou. Nvs-solver: Video diffusion model as zero-shot novel view synthesizer, 2024. 4.6.4

Heng Yu, Chaoyang Wang, Peiye Zhuang, Willi Menapace, Aliaksandr Siarohin, Junli Cao, Laszlo Attila Jeni, Sergey Tulyakov, and Hsin-Ying Lee. 4real: Towards photorealistic 4d scene generation via video diffusion models. In *NeurIPS*, 2024a. 5.4.2

Jiahui Yu, Zhe Lin, Jimei Yang, Xiaohui Shen, Xin Lu, and Thomas S Huang. Generative image inpainting with contextual attention. In *CVPR*, pp. 5505–5514, 2018. 4.2.2

Jiahui Yu, Zirui Wang, Vijay Vasudevan, Legg Yeung, Mojtaba Seyedhosseini, and Yonghui Wu. Coca: Contrastive captioners are image-text foundation models. *TMLR*, 2022a. 3.2

Jiahui Yu, Yuanzhong Xu, Jing Yu Koh, Thang Luong, Gunjan Baid, Zirui Wang, Vijay Vasudevan, Alexander Ku, Yinfei Yang, Burcu Karagol Ayan, et al. Scaling autoregressive models for content-rich text-to-image generation. *arXiv preprint arXiv:2206.10789*, 2022b. 3.1

Lijun Yu, Yong Cheng, Kihyuk Sohn, José Lezama, Han Zhang, Huiwen Chang, Alexander G. Hauptmann, Ming-Hsuan Yang, Yuan Hao, Irfan Essa, and Lu Jiang. Magvit: Masked generative video transformer. In *CVPR*, pp. 10459–10469, 2023a. 2.4.4, 2.5.3

Lijun Yu, Jose Lezama, Nitesh Bharadwaj Gundavarapu, Luca Versari, Kihyuk Sohn, David Minnen, Yong Cheng, Agrim Gupta, Xiuye Gu, Alexander G. Hauptmann, Boqing Gong, Ming-Hsuan Yang, Irfan Essa, David A. Ross, and Lu Jiang. Language model beats diffusion - tokenizer is key to visual generation. In *ICLR*, 2024b. 2.4.4, 2.5.3

Qiying Yu, Yang Liu, Yimu Wang, Ke Xu, and Jingjing Liu. Multimodal federated learning via contrastive representation ensemble. In *ICLR*, 2023b. 5.2

Sihyun Yu, Jihoon Tack, Sangwoo Mo, Hyunsu Kim, Junho Kim, Jung-Woo Ha, and Jinwoo Shin. Generating videos with dynamics-aware implicit generative adversarial networks. In *ICLR*, 2021. 2.1.1, 4.4

Xianggang Yu, Mutian Xu, Yidan Zhang, Haolin Liu, Chongjie Ye, Yushuang Wu, Zizheng Yan, Chenming Zhu, Zhangyang Xiong, Tianyou Liang, Guanying Chen, Shuguang Cui, and Xiaoguang Han. Mvimgnet: A large-scale dataset of multi-view images. In *CVPR*, pp. 9150–9161, 2023c. 4.6.1

Youngjae Yu, Hyungjin Ko, Jongwook Choi, and Gunhee Kim. End-to-end concept word detection for video captioning, retrieval, and question answering. In *CVPR*, pp. 3261–3269, 2017. 5.2

Lu Yuan et al. Instructvideo: Instructing video diffusion models with human feedback. *arXiv preprint*, 2023. 2.2.5, 2.4.4

Shenghai Yuan, Jinfa Huang, Xianyi He, Yunyuan Ge, Yujun Shi, Liuhan Chen, Jiebo Luo, and Li Yuan. Identity-preserving text-to-video generation by frequency decomposition. *arXiv preprint arXiv:2411.17440*, 2024a. 4.3

Xin Yuan, Jinoo Baek, Keyang Xu, Omer Tov, and Hongliang Fei. Inflation with diffusion: Efficient temporal adaptation for text-to-video super-resolution. In *WACV*, pp. 489–496, 2024b. 4.2.4

Zhengqing Yuan, Ruoxi Chen, Zhaoxu Li, Haolong Jia, Lifang He, Chi Wang, and Lichao Sun. Mora: Enabling generalist video generation via a multi-agent framework. *arXiv preprint arXiv:2403.13248*, 2024c. 2.4.4

Rowan Zellers, Ximing Lu, Jack Hessel, Youngjae Yu, Jae Sung Park, Jize Cao, Ali Farhadi, and Yejin Choi. Merlot: Multimodal neural script knowledge models. In *NeurIPS*, pp. 23634–23651, 2021. 3.1

Kuo-Hao Zeng, Tseng-Hung Chen, Ching-Yao Chuang, Yuan-Hong Liao, Juan Carlos Niebles, and Min Sun. Leveraging video descriptions to learn video question answering. In *AAAI*, pp. 4334–4340, 2017. 5.3

Yan Zeng, Guoqiang Wei, Jiani Zheng, Jiaxin Zou, Yang Wei, Yuchen Zhang, and Hang Li. Make pixels dance: High-dynamic video generation. In *CVPR*, pp. 8850–8860, 2024a. 8, 4.1.1

Yifei Zeng, Yanqin Jiang, Siyu Zhu, Yuanxun Lu, Youtian Lin, Hao Zhu, Weiming Hu, Xun Cao, and Yao Yao. Stag4d: Spatial-temporal anchored generative 4d gaussians. In *ECCV*, pp. 163–179, 2024b. 5.4.2

Zheng Zeng, Valentin Deschaintre, Iliyan Georgiev, Yannick Hold-Geoffroy, Yiwei Hu, Fujun Luan, Ling-Qi Yan, and Miloš Hašan. Rgb-x: Image decomposition and synthesis using material- and lighting-aware diffusion models. In *Special Interest Group on Computer Graphics and Interactive Techniques Conference Conference Papers '24*, pp. 1–11, 2024c. 4.1.1

Bowen Zhang, Xiaofei Xie, Haotian Lu, Na Ma, Tianlin Li, and Qing Guo. Mavin: Multi-action video generation with diffusion models via transition video infilling, 2024a. 4.5

David Junhao Zhang, Jay Zhangjie Wu, Jia-Wei Liu, Rui Zhao, Lingmin Ran, Yuchao Gu, Difei Gao, and Mike Zheng Shou. Show-1: Marrying pixel and latent diffusion models for text-to-video generation. *arXiv preprint arXiv:2309.15818*, 2023a. 2.4.1, 2.5.3

Guiwei Zhang, Tianyu Zhang, Guanglin Niu, Zichang Tan, Yalong Bai, and Qing Yang. Camel: Causal motion enhancement tailored for lifting text-driven video editing. In *CVPR*, pp. 9079–9088, 2024b. 4.4

Haiyu Zhang, Xinyuan Chen, Yaohui Wang, Xihui Liu, Yunhong Wang, and Yu Qiao. 4diffusion: Multi-view video diffusion model for 4d generation, 2024c. 5.4.2

Junyi Zhang, Charles Herrmann, Junhwa Hur, Varun Jampani, Trevor Darrell, Forrester Cole, Deqing Sun, and Ming-Hsuan Yang. Monst3r: A simple approach for estimating geometry in the presence of motion. *arXiv preprint arxiv:2410.03825*, 2024d. 4.6.1

Kai Zhang, Sai Bi, Hao Tan, Yuanbo Xiangli, Nanxuan Zhao, Kalyan Sunkavalli, and Zexiang Xu. Gs-lrm: Large reconstruction model for 3d gaussian splatting, 2024e. 5.4.1

Lvmin Zhang, Anyi Rao, and Maneesh Agrawala. Adding conditional control to text-to-image diffusion models. In *ICCV*, pp. 3813–3824, 2023b. 4.1.1

Qihang Zhang, Ceyuan Yang, Yujun Shen, Yinghao Xu, and Bolei Zhou. Towards smooth video composition. In *ICLR*, 2023c. 4.4, 4.5

Shiwei Zhang, Jiayu Wang, Yingya Zhang, Kang Zhao, Hangjie Yuan, Zhiwu Qin, Xiang Wang, Deli Zhao, and Jingren Zhou. I2vgen-xl: High-quality image-to-video synthesis via cascaded diffusion models, 2023d. 4.1.1, 4.1.1

Yabo Zhang, Yuxiang Wei, Dongsheng Jiang, Xiaopeng Zhang, Wangmeng Zuo, and Qi Tian. Controlvideo: Training-free controllable text-to-video generation. *arXiv preprint arXiv:2305.13077*, 2023e. 2.2.7, 4.1.5

Yabo Zhang, Yuxiang Wei, Xianhui Lin, Zheng Hui, Peiran Ren, Xuansong Xie, Xiangyang Ji, and Wangmeng Zuo. Videoelevator: Elevating video generation quality with versatile text-to-image diffusion models. *arXiv preprint arXiv:2403.05438*, 2024f. 2.2.7

Yiming Zhang, Zhening Xing, Yanhong Zeng, Youqing Fang, and Kai Chen. Pia: Your personalized image animator via plug-and-play modules in text-to-image models, 2023f. 4.1.1

Zhenghao Zhang, Junchao Liao, Menghao Li, Zuozhuo Dai, Bingxue Qiu, Siyu Zhu, Long Qin, and Weizhi Wang. Tora: Trajectory-oriented diffusion transformer for video generation. *arXiv preprint arXiv:2407.21705*, 2024g. 4.1.2

Zhixing Zhang, Bichen Wu, Xiaoyan Wang, Yaqiao Luo, Luxin Zhang, Yinan Zhao, Peter Vajda, Dimitris Metaxas, and Licheng Yu. Avid: Any-length video inpainting with diffusion model. In *CVPR*, pp. 7162–7172, 2024h. 11, 4.2.2

Zhongwei Zhang, Fuchen Long, Yingwei Pan, Zhaofan Qiu, Ting Yao, Yang Cao, and Tao Mei. Trip: Temporal residual learning with image noise prior for image-to-video diffusion models. In *CVPR*, pp. 8671–8681, 2024i. 4.1.1, 4.4

Zicheng Zhang, Bonan Li, Xuecheng Nie, Congying Han, Tiande Guo, and Luoqi Liu. Towards consistent video editing with text-to-image diffusion models. In *NeurIPS*, 2024j. 4.1.5

Canyu Zhao, Mingyu Liu, Wen Wang, Weihua Chen, Fan Wang, Hao Chen, Bo Zhang, and Chunhua Shen. Moviedreamer: Hierarchical generation for coherent long visual sequences. In *ICLR*, 2025. 4.5

Haoyu Zhao, Tianyi Lu, Jiaxi Gu, Xing Zhang, Qingping Zheng, Zuxuan Wu, Hang Xu, and Yu-Gang Jiang. *MagDiff: Multi-alignment Diffusion for High-Fidelity Video Generation and Editing*, pp. 205–221. Springer Nature Switzerland, September 2024a. ISBN 9783031726491. doi: 10.1007/978-3-031-72649-1_12. URL `http://dx.doi.org/10.1007/978-3-031-72649-1_12`. 4.1.1, 4.1.1

Kai Zhao, Xiaoli Lin, et al. Dysen-vdm: Dynamic style enhanced video diffusion models. *arXiv preprint arXiv:2305.01012*, 2023a. 2.4.4

Nanxuan Zhao, Jianbo Jiao, Weidi Xie, and Dahua Lin. Cali-nce: Boosting cross-modal video representation learning with calibrated alignment. In *CVPR*, pp. 6317–6327, 2023b. 5.1

Rui Zhao, Yuchao Gu, Jay Zhangjie Wu, David Junhao Zhang, Jiawei Liu, Weijia Wu, Jussi Keppo, and Mike Zheng Shou. Motiondirector: Motion customization of text-to-video diffusion models. *arXiv preprint arXiv:2310.08465*, 2023c. 4.1.5

Ruoyu Zhao et al. Videofactory: Efficient video generation with fine-grained control. *arXiv preprint arXiv:2305.01893*, 2023d. 1

Shuai Zhao, Linchao Zhu, Xiaohan Wang, and Yi Yang. Centerclip: Token clustering for efficient text-video retrieval. In *SIGIR*, pp. 970–981, 2022. 5.1, 5.2

Sijie Zhao, Yong Zhang, Xiaodong Cun, Shaoshu Yang, Muyao Niu, Xiaoyu Li, Wenbo Hu, and Ying Shan. Cv-vae: A compatible video vae for latent generative video models. *arXiv preprint arXiv:2405.20279*, 2024b. 2.5.3

Yuyang Zhao, Zhiwen Yan, Enze Xie, Lanqing Hong, Zhenguo Li, and Gim Hee Lee. Animate124: Animating one image to 4d dynamic scene, 2023e. 5.4.2

Zhou Zhao, Jinghao Lin, Xinghua Jiang, Deng Cai, Xiaofei He, and Yueting Zhuang. Video question answering via hierarchical dual-level attention network learning. In *ACM MM*, pp. 1050–1058, 2017. 5.3

Guangcong Zheng, Teng Li, Rui Jiang, Yehao Lu, Tao Wu, and Xi Li. Cami2v: Camera-controlled image-to-video diffusion model, 2024a. 4.6.2, 4.6.3

Yufeng Zheng, Xueting Li, Koki Nagano, Sifei Liu, Otmar Hilliges, and Shalini De Mello. A unified approach for text-and image-guided 4d scene generation. In *CVPR*, pp. 7300–7309, 2024b. 5.4.2

Zangwei Zheng, Xiangyu Peng, Tianji Yang, Chenhui Shen, Shenggui Li, Hongxin Liu, Yukun Zhou, Tianyi Li, and Yang You. Open-sora: Democratizing efficient video production for all, 2024c. 1, 2.4.4, 2.5.2, 2.5.3, 2.5.4, 3.1, 3.2, 5

Yaoyao Zhong, Wei Ji, Junbin Xiao, Yicong Li, Weihong Deng, and Tat-Seng Chua. Video question answering: Datasets, algorithms and challenges. In *EMNLP*, pp. 6439–6455, 2022. 5.3

Jia Zhou, Yang Dong, et al. Magicvideo: Efficient video generation with latent diffusion models. *arXiv preprint arXiv:2211.11018*, 2022. 2.1.3, 2.4.1, 2.4.4, 1, 2.5.1, 2.5.3

Luowei Zhou, Chenliang Xu, and Jason Corso. Towards automatic learning of procedures from web instructional videos. In *AAAI*, 2018a. 3.1

Qiang Zhou, Shaofeng Zhang, Nianzu Yang, Ye Qian, and Hao Li. Motion control for enhanced complex action video generation. *arXiv preprint arXiv:2411.08328*, 2024a. 4.1.2

Shangchen Zhou, Peiqing Yang, Jianyi Wang, Yihang Luo, and Chen Change Loy. Upscale-a-video: Temporal-consistent diffusion model for real-world video super-resolution. In *CVPR*, pp. 2535–2545, 2024b. 4.2.4

Tinghui Zhou, Richard Tucker, John Flynn, Graham Fyffe, and Noah Snavely. Stereo magnification: Learning view synthesis using multiplane images. *arXiv preprint arXiv:1805.09817*, 2018b. 4.6.1

Xingcheng Zhou, Mingyu Liu, Ekim Yurtsever, Bare Luka Zagar, Walter Zimmer, Hu Cao, and Alois C. Knoll. Vision language models in autonomous driving: A survey and outlook. *IEEE Trans. Intell. Veh.*, pp. 1–20, 2024c. 1

Yiwen Zhou, Xiaoyu Lin, et al. Videofusion: Diffusion-based text-to-video generation. *arXiv preprint arXiv:2302.05798*, 2023. 2.4.4

Yupeng Zhou, Daquan Zhou, Ming-Ming Cheng, Jiashi Feng, and Qibin Hou. Storydiffusion: Consistent self-attention for long-range image and video generation. In *NeurIPS*, 2024d. 4.4

Zhongliang Zhou, Jielu Zhang, Zihan Guan, Mengxuan Hu, Ni Lao, Lan Mu, Sheng Li, and Gengchen Mai. Img2loc: Revisiting image geolocalization using multi-modality foundation models and image-based retrieval-augmented generation. In *SIGIR*, pp. 2749–2754, 2024e. 5.2

Linchao Zhu and Yi Yang. Actbert: Learning global-local video-text representations. In *CVPR*, pp. 8743–8752, 2020. 5.2

Shaobin Zhuang, Kunchang Li, Xinyuan Chen, Yaohui Wang, Ziwei Liu, Yu Qiao, and Yali Wang. Vlogger: Make your dream a vlog. *arXiv preprint arXiv:2401.09414*, 2024. 2.4.4, 3.4

Bojia Zi, Shihao Zhao, Xianbiao Qi, Jianan Wang, Yukai Shi, Qianyu Chen, Bin Liang, Kam-Fai Wong, and Lei Zhang. Cococo: Improving text-guided video inpainting for better consistency, controllability and compatibility. *arXiv preprint arXiv:2403.12035*, 2024. 4.2.2

Qi Zuo, Xiaodong Gu, Lingteng Qiu, Yuan Dong, Zhengyi Zhao, Weihao Yuan, Rui Peng, Siyu Zhu, Zilong Dong, Liefeng Bo, and Qixing Huang. Videomv: Consistent multi-view generation based on large video generative model, 2024. 5.4.2